THE UNIVERSITY
of EDINBURGH

The Role of the Chromatin Remodeller LSH in Oligodendrocyte Differentiation and CNS Myelination

Christian Alexander Belton

Thesis presented for the degree of Doctor of Philosophy

University of Edinburgh

2019

Contents

Declaration

I declare that this thesis is an original report of my research, has been written by me and has not been submitted for any previous degree. The experimental work is almost entirely my own work; the collaborative contributions have been indicated clearly and acknowledged. Due references have been provided on all supporting literatures and resources.

Signed: …….. Date:……

Christian Alexander Belton (2019)

Acknowledgements

I'd like to start by acknowledging my former supervisor Dr. Irina Stancheva whose guidance in the initial stages of my PhD was crucial to my development as an independent scientist and whose intellectual conception of this project led to generation of the *Lsh* conditionally reversible knock-out mouse line by Chao Li, who I would also like to thank. I would like to thank the other former members of the Stancheva lab namely Natalia Torrea, who performed experiments that were essential to verifying the reversibility of the *Lsh* knock-out, Tuo Zhang, who provided initial training in animal handling and dissection, Burak Ozkan, Simon Varzandeh, Ilaria Amendola and Dani Wicaksono whose criticism and support provided valuable insights into my work and motivation to complete my PhD. I'm also grateful to all members of the Voigt, Bird, ffrench-Constant and Buonomo labs who generously allowed me to attend lab meetings and listened to presentation of my own work throughout. I'd like to thank my second supervisor Charles ffrench-Constants personally for generously providing reagents, advice and his time securing funding for my continued research following Irina's dismissal, Andrew Jarjour who provided essential advice and training in performing myelin TEM and animal perfusion in general and Adrian Bird, my primary supervisor, who was instrumental in providing further advice, reagents and lab space in the final stages of my project . From my personal life I'd like to thank my parents, Rosy and Brian Belton who reared me to become the correct levels of resilient and sceptical to survive a career in science and provided me with love and support throughout my PhD. I would also like to thank my partner Sarah McLean who provided both a companion in my joy and sympathetic ear for my woes during the final year of the PhD. Finally, I'd like to thank the School of Biological Sciences who provided funding for both research costs and my stipend in the essential final period following the termination of Irina's grant.

Lay Summary

How the single cell of the fertilised egg becomes the wide variety of cell types present in mammals, for example nerve cells, gut cells and skin cells, while still possessing the same blueprint for construction of components (DNA) is a central question in biology. If all cells have the same blueprint, why don't they all make the same components? The difference between cell types is routed in differences in how they utilise DNA. In the last 50 years it has become apparent that the scaffolding that DNA interacts with is essential in deciding how it is utilised. In my project, I seek to work out the function of a cell component (LSH) that alters the arrangement of that scaffold, allowing machinery of the cell greater or lesser access to certain parts of the DNA blueprint and altering how much certain components are made by the cell. To do this I use a genetically modified mouse that can remove LSH and replace it at different points in the animal's life. By doing this I have been able to show that LSH in early life is essential to produce insulating cells that wrap around nerve cells and allow them to act as efficient electrical circuits controlling movement. These same insulating cells are destroyed in diseases such as multiple sclerosis, causing patients to lose control of movement to varying extents. For some patients, the disease is made more severe as they are not able to produce more insulating cells after the initial ones are destroyed. Understanding why my genetically engineered mice are unable to produce insulating cells, and how alterations in the DNA scaffold cause this problem, could therefor provide insights into why some patients are also unable to do so, and how it might be best to help them.

Abstract

Previous work in embryonic cell lines has implicated LSH in the deposition of DNA methylation, a key regulatory epigenetic modification during mammalian development. We have generated a conditionally reversible knock-out of *Lsh* (*Lsh*^{off}) to investigate its role *in vivo*. *Lsh*$^{off/off}$ mice survive to adulthood but develop a tremor and ataxia phenotype. Transmission election microscopy of nervous tissue shows this phenotype is concurrent with central nervous system (CNS) hypomyelination. *Lsh*$^{off/off}$ animals also have a reduction in mature oligodendrocyte (mOL) cell numbers, but similar number of oligodendrocyte (OL) lineage cells in total, indicating the presence of an OL differentiation defect. Conversion to *Lsh*$^{on/on}$ in OPCs leads to complete rescue of the phenotype, suggesting LSH expression in the OL lineage is necessary for terminal differentiation. OPC specific knock-out of *Lsh* however produces no phenotype. Sequencing of *Lsh*$^{off/off}$ adult optic nerve RNA reveals under-expression of genes associated with mOLs, the myelinating cells of the CNS, but no cognate upregulation of oligodendrocyte precursor cell (OPC) markers. Interrogation of DNA methylation in rescued OPCs however reveals scant to no rescue in the hypomethylation present in *Lsh*$^{off/off}$ OPCs. Taken together these results show an essential role for LSH in OL differentiation and that LSH dependent DNA methylation patterns are not required prior to differentiation to mOLs. We hypothesize that early life LSH expression instead establishes a DNA methylation independent chromatin state required for differentiation and this is maintained in the absence of LSH expression following OPC cell cycle exit.

Introduction- Chapter One

Large eukaryotic genomes present cells with the requirement to compact their DNA compliment within a nucleus of limited size. An additional requirement, for organisms that produce specialised cell types, is to utilise their identical genomes in different ways to produce these cell types. Both of these requirements have long been proposed to be met by spatial organisation, protein interaction with, and chemical modification of DNA in chromatin, the large nucleoprotein complex in which the genome of eukaryotic cells is contained (Kornberg 1974, Holliday and Pugh 1975, Stedman and Stedman 1950).

1.1 Chromatin and Genome Function

The fundamental repeating component of chromatin comprises of ~147bp of DNA wrapped around two copies of each core histone protein variant H2A, H2B, H3 and H4, termed the core nucleosome (Luger et al. 1997, Richmond and Davey 2003, Kornberg 1974). These nucleosomes exhibit non-random spacing across DNA in both yeast and metazoans, leading to consistent amounts of DNA exposed between consecutive wrapping nucleosomes at certain loci in cells (Schones et al. 2008, Mavrich et al. 2008, Lee et al. 2007). The composition of histone variants within nucleosomes and their N-terminal tail post-translational modifications (PTMs) are distributed unevenly across the genome (Kundaje et al. 2012, Chen and Dent 2014, Pokholok et al. 2005).

A non-nucleosomal aspect of chromatin is the covalent attachment of a methyl group to the carbon five of cytosine or DNA methylation. This also has a non-even distribution in the genome. In vertebrates, DNA methylation is most prevalent in a CpG sequence context, though it can occur in different contexts at a frequency dependent on cell-type (Gautier et al. 1977, Ramsahoye et al. 2000). The extent of CpG methylation preference is such that the genome is relatively depleted of CpG dinucleotides due to the frequent spontaneous deamination of 5'methyl-cytosines into thymidines across evolution (Bird 1980, Coulondre et

al. 1978). However, at particular regions, termed CpG islands (CGIs), this CpG methylation bias is reversed (Bird et al. 1985).

The non-random spacing of all these chromatin components has led to them being subject to investigation hypothesising a potential function.Historically however, evidence for a functional role of chromatin appeared long before the molecular characterisation. Chromatin can be classified on a cytogenetic basis into heterochromatin and euchromatin (Heitz 1928). Early work in *Drosophila* found that few phenotypes of mutation mapped genetically to deeply staining heterochromatic regions of chromosomes (Weiler and Wakimoto 1995). This has been found to correspond to a lack of protein coding genes by subsequent sequencing and annotation of the *Drosophila* genome (Smith et al. 2007). In addition, observations that chromosomal rearrangements positioning euchromatic genes proximal to heterochromatic loci led to mosaic inactivation of gene expression within tissues, a phenomenon termed position effect variegation (PEV), hinted at a functional role for heterochromatin in gene silencing (Muller 1930). In the many years since these initial observations, there has been much work into the molecular mechanisms of chromatin's association with gene activity and this has been enabled by increased understanding of the components of repressive and active chromatin at the DNA and protein level. In order to provide context for the work carried out in this thesis, I will give a brief overview of some of this work in this introduction.

1.1.1 Histone PTMs

Genetic screens defining factors modulating PEV uncovered a variety of enzymes and structural DNA binding proteins (Wallrath 1998). These include histone methyltransferase and deacetylase enzymes which catalyse, for example, trimethylation of histone 3 lysine 9 (H3K9me3) and removal of histone acetylation, along with a variety of other PTMs (De Rubertis et al. 1996, Rea et al. 2000, Jenuwein and Allis 2001). These PTMs are often conserved across evolution, indicating functional relevance. Chromatin immunoprecipitation experiments (ChIP) using antibodies specific to histone PTMs enables purification of the

DNA associated with specifically modified nucleosomes. Using this technique for interrogation of the PTMs at both specific loci and genome wide reveal an evolutionarily conserved correlation between presence of certain PTMs at a locus, such as a promoter or enhancer regions, and transcriptional state of the associated gene (Noma et al. 2001, Heintzman et al. 2007, Boyer et al. 2006). This has enabled association of certain histone PTMs to poorly transcribed regions, such as H3K9me3 and histone 3 lysine 27 trimethylation (H3K27me3) and to more well transcribed regions, such as histone 3 lysine 4 tri-methylation (H3K4me3), histone 3 acetylation and, in gene bodies, histone 3 lysine 36 tri-methylation (H3K36me3) (Allis and Jenuwein 2016). Further work has also characterised how the presence of certain modifications excludes or enables associated binding of proteins essential for transcriptional activation, depending on precise context (Xin and Rohs 2018).

1.1.2 Nucleosome Positioning

The correlation between chromatin state and transcriptional activity is also apparent at the level of nucleosome positioning. The promoters of active genes are characterized by a nucleosome-depleted region (NDR), flanked by a downstream nucleosome a canonical distance from the transcription start site (TSS), termed the +1 nucleosome followed by nucleosomes arrayed with gradually decreasing regularity of spacing within a population further downstream from the locus (Pokholok et al. 2005, Barski et al. 2007). Generally there is an inverse correlation between nucleosome occupancy in promoter regions and gene expression and a positive correlation between stringency of phasing and +1 nucleosome positioning relative to the TSS and expression (Weiner et al. 2010, Chereji et al. 2016, Schones et al. 2008). *In vitro* transcription assays on reconstituted chromatin reveal the precise position of the +1 nucleosome is required for efficient transcription and recruitment of transcriptional activators (Stunkel et al. 1997, Zhao et al. 2001). However, this is dependent on the histone composition of the +1 nucleosome, with *in vivo* studies in yeast suggesting the creation of a barrier to RNA polymerase II translocation in yeast, the effectiveness of which varies depending on subnucleosomal content (Weber et al. 2014). The effect this

nucleosome patterning on transcription is thought to mediated by alteration in accessibility of DNA and thus its ability to act as an enzyme substrate.

1.1.3 DNA Methylation

DNA methylation has also long been associated with gene silencing. This originates from the observation that it precludes binding of certain restriction enzymes to DNA, and thus could potentially alter other protein interactions with the DNA substrate (Mann and Smith 1977, Holliday and Pugh 1975). Approximately 60% of annotated gene promoters contain CpG islands, hinting again at a functional relevance for these unmethylated regions (Antequera and Bird 1993, Larsen et al. 1992, Saxonov et al. 2006). More recently, an ability to interrogate DNA methylation and histone PTMs genome wide has revealed correlation between the presence of DNA methylation at certain regions and heterochromatin (Meissner et al. 2008). Further evidence for DNA methylation's role as a repressive chromatin mark comes from observation that treatment with 5-aza-2'deoxycytodine, an inhibitor of DNA methyltransferase enzymes, leads inhibition of cellular differentiation as well as large scale depression of genes (Jones and Taylor 1980, Yang et al. 2012). However, the relationship between DNA-methylation and gene expression is far from simplistic. For example, promoters associated with CGIs remain largely unmethylated despite expression status altering during development and when silenced are more typically marked with H3K27me3 (Brinkman et al. 2012). With the presence of DNA methylation at the flanks of CGIs being posited to be important for prevention of spreading of the repressive H3K27me3 to proximal regions (Lindroth et al. 2008) (Brinkman et al. 2012). For a subset of promoters, reduction in gene expression following developmental transitions is co-occurrent on CpG methylation (Epsztejn-Litman et al. 2008). Locus specific interrogation of the *Oct4* gene promoter show that H3K9 methylation precedes DNA methylation establishment during *in vitro* differentiation of mouse embryonic stem cells and that both the histone methyltransferase G9a and *de novo* DNA methyltransferases DNMT3a and 3b are required for stable silencing of the *Oct4* expression during differentiation (Feldman et al. 2006). Cells with genetic ablation of the

catalytic SET domain of G9a can still deposit DNA methylation at G9a dependent promoters and these promoters are still marked by H3K9me3 (Dong et al. 2008), making the cause consequence relationship between histone PTMs and DNA methylation unclear. DNA methylation has also been associated with the silencing of transcriptional features with reduced CpG density regulatory regions. These features are often found in more repetitive genomic regions. Pericentromeric repeats comprise of major and minor satellite sequences which extend from centromeres of chromosomes in tens of thousands of tandem repeats (Lehnertz et al. 2003). Silencing of these regions is essential for normal development and requires DNA methylation, with missense mutations in the DNA methyltransferase gene *Dnmt3b* causing immunodeficiency, centromeric instability and facial abnormality (ICF) syndrome (Xu et al. 1999). Deposition of H3K9me3 at these regions, while upstream of DNA methylation, is also insufficient for stable silencing (Lehnertz et al. 2003).

Transposable elements also require DNA methylation for silencing. These elements comprise around 40% of mammalian genomes and can be classified into 3 major classes long interspersed nuclear elements (LINEs), short interspersed nuclear elements (SINEs) and long terminal repeat retrotransposons (LTRs) (Waterston et al. 2002). Full-length LTRs, intracisternal A particle (IAP) retroviruses, which are controlled by LTR promoters, and LINEs, require promoter hypermethylation to remain transcriptionally silent,(Yoder et al. 1997) (Walsh et al. 1998, Liang et al. 2002). Again, this silencing via DNA methylation occurs downstream of H3K9me3 establishment at promoters but is required for stable silencing despite the presence of H3K9me3 at a subset, but not all elements (Karimi et al. 2011).

DNA methylation's function is also highly divergent depending on the precise genomic feature it resides in. Gene bodies for example, often display high levels of DNA methylation, within highly transcribed regions, which has been hypothesised to function in preventing aberrant transcription initiation within the gene body or aid in mRNA splicing (Laurent et al.

2010). Analysis of differential expression in RNA-sequencing of *Dnmt3b* (DNA methyl transferase 3B) knock-out in embryonic stem cells has linked reduction in specifically gene body methylation to aberrant transcription initiation (Neri et al. 2017). The role for gene body methylation in transcription initiation site specification and mRNA splicing has also been evidenced by transcriptional and chromatin state profiling of B-cells derived from ICF patients mutated for *DNMT3B* (Gatto et al. 2017).

Recently, a role for DNA methylation in the regulation of enhancer activity has been evidenced through studies into the function of TET enzymes, which facilitate the removal of 5mC by catalysing conversion to the intermediate 5'-hydroxymethyl cytosine (Hon et al. 2014, Wang et al. 2018). This in conjunction with studies looking at lineage specific enhancer activation during cell differentiation transitions add another layer of complexity to DNA methylation's correlation with transcription (Rasmussen et al. 2015).

1.1.4 Chromatin State

As hinted in the previous section, there is often associations and crosstalk between patterns in nucleosome spacing, variant composition, histone PTMs and DNA methylation. It is useful therefor to define the combinations of components that often co-occur (such as repressive histone PTMs and DNA methylation) into "chromatin states" on the basis of what functions they are associated with in the genome (Allis and Jenuwein 2016). Although correlation is apparent across multiple domains of life, unravelling the causative relationship between chromatin state and gene expression however factors has proven difficult.

One aspect required for a causative role of chromatin state in transcriptional output is the correlation between them remaining in response to change. Indeed, following stimuli that lead to changes in cell-lineage commitment, chromatin state alters in conjunction with change in transcriptional output (Mikkelsen et al. 2007). This is also observable through changes in nucleosome positioning at TSSs in response to cellular stimuli that alter transcription (Shivaswamy et al. 2008). Further to this, profiling of chromatin state at distinct

stages in lineage progression also shows changes in chromatin state at certain regulatory elements prior to transcriptional upregulation (Lara-Astiaso et al. 2014). In addition, targeting of chromatin remodelling proteins, that shift nucleosomes relative to each other, to specific genomic loci, causes an increased nucleosome density and results in decreased transcription of associated genes (McKnight et al. 2016). Further evidence for a causal relationship at some loci can be found by similar targeting experiments using enzymes that catalysed DNA methylation (Maeder et al. 2013, Vojta et al. 2016, Amabile et al. 2016, Liu et al. 2016, Stepper et al. 2017). There are examples to the contrary however, with changes in expression occurring prior to chromatin state change (Scruggs et al. 2015, Cirillo et al. 2002, Hsu et al. 2015) or gene expression not being impacted by change in chromatin state (Maeder et al. 2013, Lea et al. 2018).

Taken together, the overview of the chromatin biology presented here supports the notion that transcriptional output of the cell is dynamically regulated by and can be reinforced following modification at the level of histone PTMs, DNA methylation and nucleosome position. Study of this effect complicated by impact transcription itself has on chromatin state, and there is evidence for both chromatin state changes being a cause and a consequence of change in transcription, depending on the precise context.

1.2 Chromatin Remodelling ATPases

Not discussed in any depth in the previous sections is the effects of chromatin state are thought to be mediated at the level of protein recruitment to functional genomic features either through interaction between chromatin “readers” with their associated marks, or increased access of enzymes to their DNA substrate (Musselman et al. 2012). In addition, chromatin modifying enzymes such as those which catalyse histone PTMs or DNA methylation, require accessibility to their substrates for chromatin state to change. Enzymes that can influence the accessibility of chromatin are therefore essential in enabling chromatin to perform its dynamic function.

Enzymes that alter nucleosome position relative to DNA, dependent on ATP hydrolysis, are termed ATP dependent chromatin remodellers. Recognition of the broad spectrum of chromatin remodellers present in cells came from inference of function through phylogenetic characterisation. As more protein sequences became available through the advent of widespread molecular cloning, a large group of proteins sharing a common set of sequence motifs present in the *Escherichia coli* helicases rep, uvrD, recB and recD was identified (Gorbalenya et al. 1988, Gorbalenya and Koonin 1993). Within the sf2 superfamily of this helicase motif group, further families were defined based on helicase motif composition, one such family contains the yeast transcriptional activator SNF2 (Bork and Koonin 1993). SNF2 was first linked to chromatin modifying activity by suppressor screens identifying histone protein mutations were capable of alleviating *SNF*2 mutation phenotypes (Hirschhorn et al. 1992). It was later demonstrated *in vitro* that the products of *SNF* and the closely related *SWI* genes formed a complex with a number of other protein subunits, capable of moving nucleosomes relative to each other (Côté et al. 1994, Kwon et al. 1994). Subsequently multiple other such complexes were isolated and characterised containing unique subunit compositions and distinct ATPases (Tsukiyama and Wu 1995, Tran et al. 2000, Shen et al. 2000).

Early phylogenetic analysis based on sequence identity between the conserved ATPase domains of sf2 family members placed chromatin remodellers into 4 distinct sub–families that also contain common domains outside the core ATPase (Eisen et al. 1995). However, following rapid expansion of sequencing data available at the beginning of the 21st century, new analysis revealed many genes, despite having ATPase similarity, do not fit all the classical features of the previously defined subfamilies, especially outside of the core ATPase domain (Flaus et al. 2006). One such family is that of LSH (Lymphoid Specific Helicase), a name which describes the origin tissue for initial isolation and domain exploited for isolation, rather than an accurate description of its expression pattern or function, is the

mouse homologue of the plant chromatin remodeller DDM1 (Jarvis et al. 1996)(Deficient in DNA Methylation 1) (Brzeski and Jerzmanowski 2003).

Well studied chromatin remodeller sub-families, including those originally distinguished phylogenetically (SWI/SNF, ISW1, CHD and INO80) have been functionally stereotyped in the ways they often manipulate their nucleosome substrate, though there is a wide range of diversity in function within subtypes, and no one subtype is exclusively linked to a function.

1.2.1 SWI/SNF Chromatin Remodellers

LSH is most closely related to the SWI/SNF subfamily on the basis of routed comparison of helicase domain similarity (Flaus et al. 2006). The core ATPase containing subunit of this class of remodelling complex is structurally defined by two RecA like lobes flanking a helicase domain that binds actin related proteins with subfamily members also containing a bromodomain at the C-terminal (Eisen et al. 1995, Schubert et al. 2013). SWI/SNF complexes in mammals and other higher eukaryotes are various, with subunit and core ATPase containing composition often unique to different developmental contexts. For example, mice have an embryonic specific complex conformation of the BRG1 core ATPase subunit containing BAF complex (esBAF) that is required for maintaining pluripotency genes expression (Ho et al. 2009). By contrast when cells differentiate to neurones this complex switches from npBAF, expressed in neural progenitor cells (NPCs) to nBAF on differentiation, which has characterised roles in dendritic outgrowth, neuronal cell fate determination and cell cycle exit (Wu et al. 2007, Lessard et al. 2007).

This subunit composition complexity also leads to an increase in functional complexity in higher eukaryotes. Yeast SWI/SNF containing remodelling complexes are well characterised to be recruited by transcription factors (TFs) to promoters and then remodel nucleosomes to allow access to the underlying DNA (Burns and Peterson 1997, Cosma et al. 1999). However in mammalian T-cell differentiation, the BAF complex is capable of modulating long range interactions between regulatory elements of the lineage specific *Cd4* gene, and either

promotes activation or repression depending on developmental stage (Wan et al. 2009, Chi et al. 2003, Chi et al. 2002). Despite this increased functional flexibility in mammals, conserved functions in gene regulation through regulation of access, either facilitating or preventing, SWI/SNF modellers can be stereotyped as controllers of chromatin access to accessory factors (Clapier et al. 2017).

1.2.2 The Chromatin Remodelling ATPase LSH

Based on this homology to SWI/SNF, it could be speculated that LSH may have a similar role in regulating DNA accessibility. However, early characterisation linking LSH-subfamily proteins to a role in genomic CpG methylation hints at a more complex mechanism of action for the proteins than alteration of accessibility to transcription factors.

The gene for the plant homologue of LSH, *DDM1* was identified in two independent genetic screens for mutations that alter DNA methylation and heterochromatin in plants (Vongs et al. 1993, Mittelsten Scheid et al. 1998). This effect on DNA methylation was also shown to be independent of metabolite levels by experiments showing unaltered levels of the important substrate donor required for DNA methylation, S-adenosylmethionine (SAM) (Kakutani et al. 1995). DDM1 was also identified as a chromatin remodelling protein by sequence homology following its cloning, with all DNA methylation impacting mutations found to be present in or deleting through frameshift the ATPase domain, indicating remodelling activity essential for DNA methylation (Jeddeloh et al. 1999). DDM1 remodelling activity has subsequently been demonstrated *in vitro* (Brzeski and Jerzmanowski 2003). And it's physiological importance demonstrated with characterisation of mutant phenotypes revealing morphological abnormalities, including defects in leaf structure, flowering time, and flower structure (Kakutani et al. 1996).

A human homologue for LSH/DDM1 was cloned (Geiman et al. 1998) and genetic perturbation of mammalian LSH revealed similar functional properties to DDM1, though with a supposedly more severe developmental phenotype. Initial homologous recombination

mediated knock-out in mouse (hereby termed *Lsh*$^{-/-}$), deleting exons 6-7 of the gene and abolishing full-length protein expression causes perinatal lethality, but otherwise grossly normal embryonic development (Geiman et al. 2001). *Lsh*$^{-/-}$ embryos also lack genome wide DNA methylation (Dennis et al. 2001). Other studies which generated hypomorphic mutations to LSH via removal of the ATPase domain also reveal genome wide hypomethylation, with mice surviving postnatally, albeit with a severe growth retardation phenotype (Sun et al. 2004). DNA methylation deficit in *Lsh*$^{-/-}$ is localised to various repetitive sequences, including major and minor satellite repeats and large chromosomal domains associated with the nuclear lamina (Muegge 2005) (Yu et al. 2014).

The DNA methylation loss in the absence of LSH is associated with over expression of developmentally regulated genes in mouse embryonic fibroblasts derived from *Lsh*$^{-/-}$ embryos and renewed silencing of these elements requires the G9a histone methyl transferase, much like previously discussed DNA methylation related silencing (Myant et al. 2011). The cell autonomous role for LSH in this genome wide DNA methylation was underlined in studies rescuing expression in MEFs using lenti-viral transduction, crucially demonstrating that LSH's capacity to induce *de novo* methylation is not dependent on the extrinsic factors and signalling that occur during the developmental stage at which DNA methylation is normally established, and so could be important in subsequent somatic cell differentiation (Termanis et al. 2016, Smith et al. 2012). The extensive subcloning required for purification of MEF lines rescued for LSH in this experiment does not allow for interrogation of the sequence of events required for LSH mediated methylation. It also doesn't address whether under physiological conditions, methylation or silencing would be restored in somatic cells that have had LSH expression rescued.

It has been postulated that LSH allows methylation of certain inaccessible regions of chromatin via remodelling to allow access of these regions to DNA methyltransferases (Meehan et al. 2001). Supporting this hypothesis, LSH interacts with the *de novo* methyl

transferase DNMT3B and histone deacetylases HDACs 1 and 2 (Myant and Stancheva 2008). This idea has also received support from recent studies that integrated chromatin state profiling in *DDM1* and *Lsh* mutants (Lyons and Zilberman 2017). Importantly, LSH's remodelling activity has also been demonstrated *in vitro* only when interacting with the protein CDCA7 (Jenness et al. 2018). Recent identification of mutations in both *HELLS* (human LSH coding gene) and *CDCA7* in the previously mentioned ICF syndrome (Thijssen et al. 2016). This study confirms the functional relevance of LSH and CDCA7 in human disease and development. The postnatal viability of humans with null mutations in *HELLs* also indicates that LSH may not be required for post-natal mammalian development and $Lsh^{-/-}$ perinatal lethality may be a specific to mouse, strain genetic background, or an artefact of the gene targeting strategy.

The perinatal lethality of $Lsh^{-/-}$ conceivably supports the conclusion of previous mouse knock-out studies for DNA methyltransferase genes that genome-wide hypomethylation of DNA is incompatible with development (Walsh and Bestor 1999, Li et al. 1992, Okano et al. 1999). The apparent progression of $Lsh^{-/-}$ mice beyond the developmental stages of the DNMT knock-outs and the ability of similarly hypomethylated *Lsh* hypomorph mutants to survive postnatally, albeit with a debilitating phenotype, suggests the primarily heterochromatic regions which LSH is responsible for silencing may not be as deleterious to normal development as all regions dependent on the DNMTs.

Dnmt1 knock-out leads to rapid global hypomethylation of 90% of CpGs in any dividing cell type and thus causes lethality due to upregulation of apoptotic gene expression and X chromosome inactivation in all but embryonic stem cells (Jackson-Grusby et al. 2001, Panning and Jaenisch 1996, T. Chen et al. 2007, Unterberger et al. 2006). Thus, study of the cell type specific, less severe, effects of LSH ablation could provide previously missed insights on the effect of more subtle changes in DNA methylation in cellular maintenance and differentiation.

1.3 The Oligodendrocyte Lineage

A lineage where LSH may play an unknown role in DNA methylation and wider chromatin state transitions is that of the myelinating cells of the central nervous system (CNS), OLs. Study of the OL lineage benefits from well characterised physiological function and gene expression changes that occur in a relatively well-defined lineage progression (Swiss et al. 2011). This enables relation of mouse phenotypes to specific stages of this progress through histological and gene expression profiling experiments. There are also methods for isolating the specific cell types and lineage stages that are required for study of chromatin in gene regulation (Ho and Crabtree 2010).

1.3.1 Myelin Function

To understand how the OL lineage can be studied, and why it should be, it's important to address the physiological function and features of myelin. The correct physiological function of the mammalian nervous system is dependent on the correct formation of a myelinated axon. Unmyelinated axon membranes (axolemma) contain diffusely distributed voltage-gated Na^+ and K^+ channels, which are capable of propagating electrical impulses or action potentials in a continuous manner along the axon (Ritchie 1984).The axolemma of myelinated axons is dramatically different to unmyelinated counterparts. Voltage-gated Na^+ channels concentrate in the nodes of Ranvier, short nonmyelinated areas of approximately 1µm and are positioned between myelin sheaths along one axon (Salzer 1997), with K^+ channels in the juxtaparanode, the axon area adjacent to the node (Poliak and Peles 2003).The area of depolarization therefore is restricted to the nodes allowing action potentials can jump from node to node. This saltatory conduction allows much faster impulse propagation compared to an unmyelinated axon of the same calibre(Tasaki 1982). Therefore when axons become demylinated and the distinctive clustering of the voltage-gated ion channels at the node of Ranvier is lost, there is decrease in nerve conduction and neurological impairment (Lappe-Siefke et al. 2003). Indeed, mice lacking myelin due to

genetic knock-out of key components present a severe ataxic phenotype (Orian et al. 1994). Myelinating OLs also produce trophic factors that promote neuronal survival, such as the brain-derived neurotrophic factor (BDNF), glial cell-derived neurotrophic factor (GDNF) and insulin-like growth factor (IGF) (Dougherty et al. 2000, Wilkins et al. 2001, Wilkins et al. 2003). In addition, OLs have also been shown to offer metabolic support to neurons (Fünfschilling et al. 2012, Lee et al. 2012).

Interestingly there is also an increased extent of myelination of certain axons following exposure to social experience in rodents during development (Makinodan et al. 2012, Mount and Monje 2017). Thus, processes that regulate myelination and OPC differentiation are conceivably connected to memory and learning. This brief overview of the physiological function of myelin, underlines the importance of its study, and sheds light on the possible phenotypes that a myelin deficiency may present.

1.3.2 Oligodendrocyte Differentiation During Development

OL lineage cells undergo multiple stages of differentiation during development. OPCs are specified from neural progenitor cells (NPCs) and subsequently differentiate into immature, non-myelinating OLs and finally mature into myelinating OLs (Boulanger and Messier 2014).

1.3.2.1 Anatomy and Timing

NPCs of the ventricular neuroepithelium of the embryonic neural tube give rise to neurons, astrocytes and oligodendrocytes (Miller 2002, Martinez et al. 2013). The neural tube is patterned by concentration gradients of different signalling molecules that define domains within it, such as the pre-motor domain (pMN) and the p0-p2 domains, each of which give rise to distinct cell types (Briscoe et al. 2000) (Rowitch 2004). Motor neurons and OPCs are derived from this pMN, which is demarcated by the expression of the transcription factors OLIG1 and OLIG2 (Zhou et al. 2000, Lu et al. 2000). The precise timing of specification and cellular origin of OL is however controversial. There are conflicting results as to whether

OPCs arise from the same progenitors as motor neurons (MNs), or the lineage is specified earlier in development. Studies of *in vitro* differentiated clonally derived progenitor populations showed that NPCs in the SVZ can produce both OPCs and MNs (Kalyani et al. 1997, Qian et al. 2000) (Menn et al. 2006). The dependency for both MN and OPC lineages on OLIG1/2 expression, whereas knock-out of previously expressed bHLH transcription factors (TFs) perturbed either glial or neuronal differentiation (Vetter 2001), also hinted towards a multipotent progenitor origin (Zhou and Anderson 2002). However, derivation of some clonal NPC populations resulted in exclusively glial or neuronal cells arising (Qian et al. 1998). Moreover, retroviral transduction experiments tracing cell lineage revealed most clonally derived lines *in vivo* were composed mainly of distinct cell types (Luskin et al. 1993). Transplantation experiments of mouse cells into chick embryos showed that embryonic day 13.5 (E13.5) NPCs do not retain capacity to differentiate into MNs *in vivo*, whereas earlier timepoint (E9.5) progenitors do (Mukouyama et al. 2006). Genetic ablation of *Olig1* expressing cells, including NPCs that go on to make MNs, showed a remaining population of OLIG2 expressing cells which persist despite complete ablation of NMs in these mice (Wu et al. 2006). This taken together with time-lapse imaging of sequential OPC and MN specification in zebrafish (Ravanelli and Appel 2015), strongly supports that while progenitors may be multipotent *in vitro*, *in vivo* OL lineage specification occurs earlier than when OPCs arise.

None the less, OPCs, defined on the basis of PDGFRα expression arise at approximately E12.5 in mice (Nishiyama et al. 2009, Levine et al. 1993, Richardson et al. 2006). Though multiple waves of OPC specification occur during normal development at embryonic and post-natal timepoints (Kessaris et al. 2006). See Fig1.1-1 for an overview of gene expression changes and timing of OL lineage differentiation. Following specification OPCs proliferate and migrate to form an evenly dispersed population throughout the grey and white matter in the CNS (Rowitch 2004). Close to birth, OPCs begin ceasing to proliferation and differentiate to pre-myelinating OLs (Zhu et al. 2008). Initial myelination starts from birth and MBP

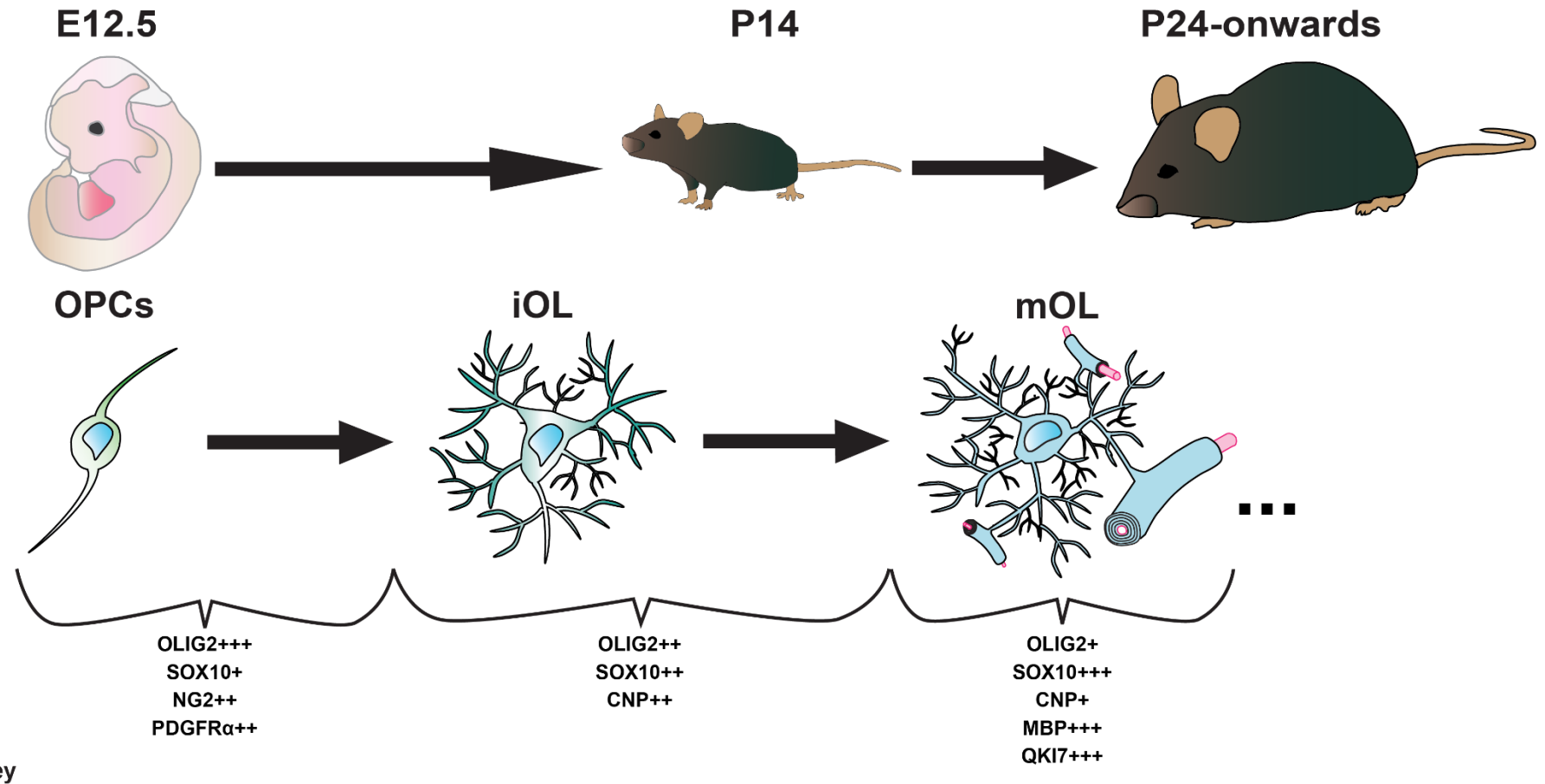

Figure 1-1 Progression through the oligodendrocyte lineage throughout developmental timepoints

Schematic of oligodendrocyte lineage progression at different developmental stages in mouse and gene expression typical to different lineage stages that will be used as marker genes in the analysis in chapter 4. Gene expression is based on the evidence discussed in chapter 1.3.2.1 , 1.3.2.2, (Swiss et al. 2011), for Pdgfrα (Li et al. 2017) and QKI7 (Bin et al. 2016).

expression declines below detectable levels by LacZ assay at around post-natal day 24 (Foran and Peterson, 1992). More recent evidence for continued myelination following this timepoint and throughout adult life comes from label free fluorescent imaging of myelin itself (Hill et al. 2018). However, this study does not postulate that this is the result of continued major waves of OL differentiation from OPCs. A subset of OPCs do indeed remain undifferentiated into adult life (Dawson et al. 2003) and continue to proliferate (Nishiyama et al. 2002). These adult OPCs act to fill vacant spaces missing in adulthood, using self-sensing to distribute evenly, and can proliferate in response to injury (Hughes et al. 2013). Myelinating OLs continue to emerge from this OPC population throughout development (Young et al. 2013). Although this continued differentiation throughout life exists, the relatively well characterised timepoints that large amounts of differentiation occur, informs developmental timepoints to interrogate in suspected OPC differentiation phenotypes.

1.3.2.2 Transcription Factor Requirements

OLIG1 and OLIG2 continue to be expressed in OL lineage cells throughout migration through the CNS following differentiation from NPCs and in myelinating OLs (Lu et al. 2002) (Zhou et al. 2001). OLIG2 does not work in isolation however, with TFs such as ASCL1, OLIG1, NKX2.2, and SOX10 are also subsequently required for OPC differentiation to myelinating OLs(Nakatani et al. 2013) (Xin et al. 2005) (Qi et al. 2001) (Stolt et al. 2002).

OLIG1 and SOX10 bind synergistically to myelin gene promoters, underling their importance in activation of the differentiation program (Li et al. 2007). OLIG2 has been shown to regulate SOX10 expression by binding to its U2 enhancer in reporter gene activation assays (Küspert et al. 2011). The TF MYRF is expressed exclusively in mOLs, both within the OL lineage and other CNS cell types (Cahoy et al. 2008, Emery et al. 2009). MYRF binds directly to myelin protein component genes, such as MAG, PLP and MBP, stimulates their expression (Bujalka et al. 2013). In addition to positive regulators, factors inhibiting differentiation play an important role in preventing improper myelin gene transcription. For

example, control of OLIG2 DNA binding is conveyed by the inhibitors of differentiation, ID2 and ID4, which sequester OLIG2 preventing its activity (Samanta and Kessler 2004). Of course, more examples of the TF contribution to OL differentiation exist, with work in recent years becoming increasingly focused on dissection of the interaction with these key TFs with chromatin.

1.3.3 Epigenetics in Oligodendrocyte Differentiation

One feature of chromatin biology is that it provides a conceptual framework as to how genetic information contained in cells can be utilised differently between cell types, in a manner that is heritable between cell divisions. The field exploring this concept has broadly been termed epigenetics, with an epigenetic trait being a stably heritable phenotype resulting from changes in a chromosome without alterations in the DNA sequence (Berger et al. 2009). The evidence for this potential heritability of chromatin state is present at several levels among the chromatin state components discussed previously (Bird 2002, Margueron and Reinberg 2010).

Epigenetic mechanisms, including recruitment of HDACs and DNA methylation, are also strongly implicated in neuronal lineage differentiation (Hsieh and Gage 2004). Treatment of mice with HDAC inhibitors reveals the proteins catalytic functions are essential for an efficient remyelination response and resultant remyelination defects correlate with perturbation of OPC differentiation to mOLs (Shen et al. 2005). This also provides an intriguing explanation for inefficient remyelination observed in ageing mice (Shen et al. 2008). Use of HDAC1 and HDAC2 conditionally deficient mutants shows that depletion of the proteins leads to reduced nuclear localization of β-catenin and repression of OLIG2 expression (Ye et al. 2009). HDACs are also recruited by the transcriptional repressor and OPC expressed protein, HES5, to the *Mbp* promoter (Liu et al. 2006). However, it's hard to pin down the effects of mutations in proteins that cause such wide-reaching perturbation to

both chromatin state and cytosolic protein PTMs, that are specifically required for OL differentiation.

Dynamic changes in chromatin state have also been implicated in OPC differentiation. The earlier discussed chromatin remodelling ATPase, BRG1 is suggested to be instrumental in the OL differentiation process, with expression increasing following differentiation and the conditional knock-out, driven by the early expression *Olig1* promoter driven CRE, leading to decreased expression of differentiation-associate genes such as *Sox10* and *Mbp*. This is co-occurrent with targeting of BRG1 to promoters by OLIG2, indicated by analysis of concordant BRG1 and OLIG2 binding sites by ChIP-seq experiments and coimmunoprecipitation of the proteins (Yu et al. 2013). However other recent experiments, which used CRE expression under control of a *Cnp* promoter to facilitate later differentiation stage ablation (as the *Cnp* promoter is active in immature oligodendrocytes) of BRG1 and OLIG2, observed an increase rather than decrease in myelination, complicating the picture significantly (Bischof et al. 2015) (Mei et al. 2013). An explanation to reconcile these results is the role of BRG1 is early in OPC specification, where it conceivably primes loci for activation in later maturation, this priming is heritable following subsequent expansion of OPCs, and if absent perturbs their differentiation. Knock-out later in the differentiation pathway however does not prevent this early priming, and so it can be inherited somatically in the absence of BRG1 and differentiation is unperturbed. Other chromatin remodellers have also recently been implicated in OL survival and differentiation. *Olig1* driven CRE expression to generate conditional knock-out of the chromatin remodeller *Chd7* revealed a requirement for OL differentiation, and ChIP-seq again showed OLIG2 and BRG1 mediated targeting to enhancers of maturation essential genes (He et al. 2016). However, again when knocked out at a later stage, using a neonatal tamoxifen induced, *Pdgfrα* driven, ER-CRE, CHD7 showed impact on stage progression from OPCs to more mature OLs once differentiation was initiated, but did cause a reduction in mOL numbers due to a reduction

due to reduced entry into differentiation from OPCs, independent of a co-occurrent survival phenotype (Marie et al. 2018).

These chromatin remodeller studies have all led to focus on genes that are activated in OL differentiation, but also the repression of inhibitors of differentiation has been linked to epigenetic regulation. Characterization of repressive chromatin marks through the OL lineage progression identified H3K9me3 and not H3K27me3 persisting through to mOLs in genes related to neuronal differentiation and this was dependent on the activity of the *Ehmt1* and *Ehmt2* genes coding the GLP and G9a histone methyltransferases respectively (Liu et al. 2015). In addition, there have been attempts to link DNA methylation patterns to proper OL differentiation. Though these convincingly show that *de novo* DNA methylation is not required fpr differentiation from OPCs to mOLs, it sheds no light on the methylation patterns required to be established before this transition, beyond showing that *Dnmt1* knock-out prevents differentiation, which as mentioned previously is easily explainable through knock-out being largely incompatible with life (Moyon et al. 2016).

1.4 Aims and Approach

Due to the earlier discussed unconditional knock-out resulting in early life lethality of *Lsh*$^{-/-}$ and possible residual activity in hypomorphic mutations, the function of LSH in mammalian development *in vivo*, any possible importance in regulation of transcription, and developmental transitions remains unclear. To shed light on this and provide a tool more suitable for investigating time resolved effects of LSH ablation on methylation and gene silencing, Chao Li, a post-doc in the Stancheva lab, produced a conditionally reversible knock-out of *Lsh*. The allele comprises of an inserted stop cassette flanked by successive inverted Frt and loxP sites into intron 3 of *Lsh* gene (Fig. 1.1). The theoretical abolition of LSH protein in the *Lsh*^{off} conformation of the allele and ability to restore expression by conversion to *Lsh*^{on} by tissue specific/inducible recombinase induction provides a system to investigate the following questions, which will form the aims of my thesis:

- **Is *Lsh*$^{off/off}$ a complete knock-out of LSH expression? What phenotypic defect(s) is/are present in the *Lsh*$^{off/off}$ mouse?**

I will address the first part of this aim in chapters 3 and 4, using experiments to interrogate any residual expression of *Lsh* at the RNA and protein level in *Lsh*$^{off/off}$. I will investigate the second part by analysis of mouse growth and survival and by histopathological analysis of any affected tissue also in chapters 3 and 4.

- **In what cell type(s) and at what stage in development is LSH required?**

I will address this in chapter 3 by molecular verification of the conditionally reversible nature of the *Lsh*^{off} allele and chapter 5 by analysis of tissue specific manipulations of LSH expression.

- **What is the molecular mechanism of any *Lsh*$^{off/off}$ phenotype?**

I will address this by looking into changes in expression of genes related to the cellular defect uncovered in aim 2 in chapter 6. I will also attempt to dissect the chromatin defects present in defective cell types following removal of LSH, starting with interrogation of changes in DNA methylation, LSH's most well characterised function during development.

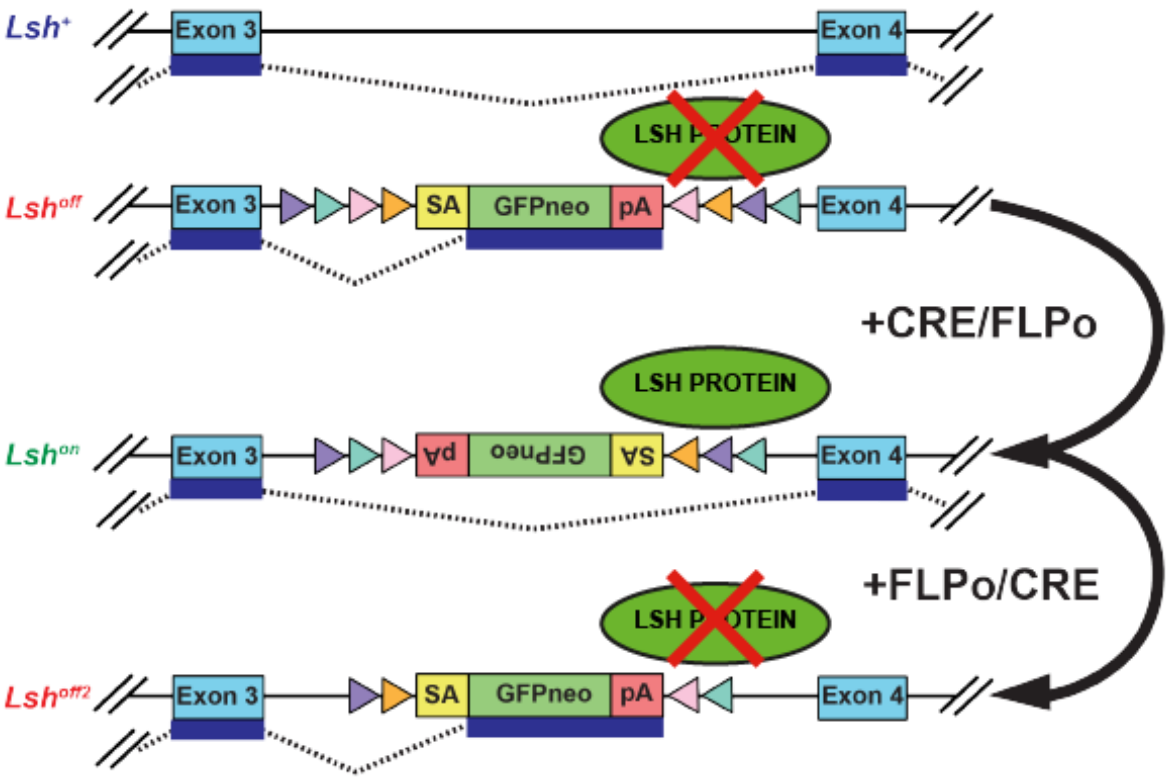

Figure 1-2 *Lsh* conditionally reversible knock-out allele

Schematic representation of *Lsh* allele generated previously in the Stancheva lab. A neomycin resistance gene fused to GFP with a 5' splice acceptor (SA) site and 3' polyadenylation signal (pA) flanked by FRT and F3 sites (purple and turquois triangles respectively), heterotypic targets for FLP recombinase and LoxP and Lox511 (pink and orange triangles respectively) heterotypic targets for CRE recombinase. Transcripts initiated from *Lsh* promoter are spliced from exon 3 to SA, causing transcription and translation of neomycin-GFP fusion gene fused to exons 2 and 3 of LSH. On expression of CRE, the cassette recombines and is inverted either on the LoxP or Lox511 sites to the antisense strand .The recombined target site is place between the 2 sites which were not targeted initially, these are then targeted by CRE and recombined resulting in excision of the initially recombined target site and one of the sites in the second recombination. The effect of this is that the allele is locked as Lsh^{on} and as such splicing occurs as normal and the protein is expressed. This can then be reversed in the same sequence of steps by expressing the FLPo recombinase, however once the excision has occurred the allele is permanently the Lsh^{off2}.

Chapter Two- Materials and Methods

2.1 Materials

2.1.1 Animals

Two *Lsh*$^{+/off}$ strains of mice were generated by injection of 2 independent E14 (129/Ola) ES cell lines, heterozygous for the targeted *Lsh*^{off} allele, into 2 C57Bl6 blastocysts by the Scottish Centre for Regenerative Medicine service unit. Chimeric mice with germline mutations were identified by presences of the allele in offspring and *Lsh*$^{+/off}$ mice were subsequently were maintained on a mixed 129/Ola/C57Bl/6 background. The weight of homozygous *Lsh*$^{off/off}$ and heterozygous *Lsh*$^{+/off}$ littermate controls was monitored and recorded weekly. To generate homozygous *Lsh*$^{on/on}$ animals, the *Lsh*$^{+/off}$ mice were crossed with a FLPo transgene expressing strain, C57BL/6-Tg(CAG-Flpo)1Afst/Ieg, which was purchased from the European Mouse Mutant Archive. *Lsh*$^{+/off}$ mice were also crossed into strain C57BL/6 x CBA Tg(CAG-cre/Esr1*)5Amc for testing of Cre mediated conversion of the allele obtained from the Jackson laboratory. To convert the allele specifically in OPCs *Lsh*$^{+/off}$ and *Lsh*$^{on/on}$ mice were crossed with PDGFRα-Cre strain, C57BL/6-Tg(Pdgfra-cre)1Clc/J, also obtained from the Jackson laboratory. All animals were housed and bred at the School of Biological Sciences animal facility and experimental procedures were conducted in compliance with the Home Office Animals (Scientific Procedures) Act 1986 under license number PPL60/4538.

2.1.2 Buffers (alphabetical order)

NE1: 20 mM Hepes pH 7.0, 10 mM KCl, 1 mM MgCl2, 0.1% (v/v) Triton X-100, 20 % (v/v) glycerol. 0.5 mM DTT and complete protease inhibitors (Sigma) were added at time of use.

NE2: 20 mM Hepes pH 7.0, 420 mM NaCl, 10 mM KCl, 1 mM MgCl2, 0.1 % (v/v) Triton X-100, 20 % (v/v) glycerol. 0.5 mM DTT and complete protease inhibitors (Sigma) were added at time of use.

Panning buffer: 5µg/ml Insulin, 0.2% BSA in PBS

Phosphate buffer (PB) (19 parts 0.2M NaH_2PO_4, 81 parts 0.2M Na_2HPO_4, 100 parts H_2O, pH 7.4 Sigma)

Ponceau S staining solution: 1 % (v/v) glacial acetic acid, 0.5 % (w/v) Ponceau S

SDS PAGE loading buffer (5×): 225 mM Tris-HCl pH 6.8, 50 % glycerol, 5 % SDS, 0.05 % bromophenol blue. 250 mM DTT was added at time of use.

SDS Separating gel: 0.1 % SDS, 0.05 % ammonium persulfate, desired concentration of acrylamide and 375 mM Tris pH 8.8 and made up to 10 ml with dH2O.

SDS Stacking gel: 0.1 % SDS, 0.05 % ammonium persulfate, 4 % Acrylamide, 125 mM Tris pH 6.8 and made up to 10 ml with dH2O. Transfer buffer: 25 mM Tris, 250 mM Glycine.

Tris-EDTA (TE): 10 mM Tris-HCl pH 7.5, 1 mM EDTA pH 8.0

Quantitative PCR reaction mix: 10 ul SYBR qPCR mix, 0.25 uM primers were added to 2 ul diluted cDNA and added up to a total volume of 20 ul.

2.1.3 Primers

All primers were ordered from MWG Eurofins. Lyophilised primers were resuspended in dH2O to 100 uM stock concentration and stored at -20 degrees.

Name	**Sequence**
Mbp F	TTCCAAAATCTTTAAGCTGGGAGG
Mbp R	AGAGAGGGTCTGCTCTAACTAGC
Plp F	ACCTATGCCCTGACTGTTGTATG
Plp R	CCATGGGAGAACACCATACATTCT
Cnp F	AGAGCTTCGACACTTTATTTCTGG
Cnp R	CTTGCCATACGATCTCTTCACCA
Pdgfrα F	CATGCAGGAAGGCTACTGTTTAAG
Pdgfrα R	AGTCAAGATGTTTGCTTTCTCAGC
Id2 F	AGCACGTCATCGATTACATCTTGG
Id2 R	ATTCAGATGCCTGCAAGGACAG
Olig2 F	CCGAAAGGTGTGGATGCTTATTAC
Olig2 R	ATGGCCCCAGGGATGATCTAAG
Hes1 F	CCAAAAATAAAATTCTCTGGGGACTG
Hes1 R	GCTTTGATGACTTTCTGTGCTC
Cspg4 F	GGAGGATCATTCTCAAGATGGGAG
Cspg4 R	ATTAACAGGAAGGATGGTGATCGT
Gapdh F	GGCTCATGACCACAGTCCATGCC
Gapdh R	CACGGAAGGCCATGCCAGTGAG
Mag F	GGGGCACCTGATAAGTATGAGTC
Mag R	CCAGGTCTGAGTGGGAATAACTG
Sox10 F	TCTGGAGGTTGCTGAACGAAAG
Sox10 R	GTAGTGAGCCTGAATAGCAG
on off R	CTTCAGGCTAAGTCCTTCTAAGTCC
on F	GTATGACATCATCAAGGAAACCCTG
off F	CTTCTAGTTGCCAGCCATCTGTT
Gfpneo F	CGCCGACCACTACCAGCAGAACA
Gfpneo R	GCCGGAGAACCTGCGTGCAATC
Lsh WT F	CCTCCCCAAATAAGCAAATAAAAACT
Lsh WT R	CGAAGGTTGCCAGGTTTTGAGATC
Cre F	GACCGTACACCAAAATTTGCCTGC
Cre R	TTACGTATATCCTGGCAGCGATC
Flpo F	GCACCTGATGACCAGCTTTCTGA
Flpo R	CTGTTGATGTAGCTGCTCAGGTAGT

2.1.4 Antibodies and other affinity reagents

Reagent	Dilution	Application	Manufacturer	Catalogue number
H4 mouse anti-LSH	1:1000	WB	Santa cruz biotechnology	sc-46665
Rabbit polyclonal anti-n-terminal LSH	1:1000	WB	Merck Millipore	ABD41
Rabbit polyclonal anti-c-terminal LSH	1:500	WB	Cell signalling technology	7998S
Rabbit polyclonal anti-OLIG2	1:1000	IF	Merck Millipore	AB9610
Mouse monoclonal anti-OLIG2	1:200	IF	Merck Millipore	MABN50
Goat polyclonal anti-OLIG2	1:500	IF	R&D systems	AF2418
Mouse monoclonal anti-QKI7	1:200	IF	UC Davis/NIH NeuroMab Facility	73-200
Rabbit polyclonal to anti-NG2	1:500	IF	Merck Millipore	AB5320
Rat anti-Mouse CD140a	1:666	OPC Iso.	Biolegend	135902
Anti-BSC1 Griffonia Simplicifolia Lectin (BSL1)	1:500	OPC Iso.	Vector Labs	L-1100
AffiniPure Goat Anti-Rat IgG (H+L)	1:333	OPC Iso.	Dianova GmbH	112-005-003

2.1.5 Cell lines

2.1.5.1 $Lsh^{-/-}$ Mouse embryonic fibroblasts (MEFs)

Isolated from *$Lsh^{-/-}$* embryos derived from crosses of heterozygous animals and immortalised by a spontaneous immortalisation (Kathrin Muegge).

2.1.5.2 $Lsh^{+/+}$, $Lsh^{+/off}$ and $Lsh^{off/off}$ MEFs

Isolated from embryos of the appropriate genotype derived from crosses of heterozygous *$Lsh^{+/off}$* animals, expanded to P3 and frozen (Natalia Torrea).

2.1.5.3 $Lsh^{on/on}$ MEFs

Isolated from embryos of the appropriate genotype derived from crosses of heterozygous *$Lsh^{+/on}$* animals, expanded to P3 and frozen (Natalia Torrea).

2.1.5.4 $Lsh^{+/+}$, $Lsh^{+/off}$ and $Lsh^{off/off}$ Embryonic stem cells (ESCs)

The original E14 mouse embryonic stem cells (ATTC) *($Lsh^{+/+}$)* generated by either a single round (*$Lsh^{+/off}$*) of targeting or double round (*$Lsh^{off/off}$)* and subsequent clonal selection by Chao Li.

2.1.5.5 $Lsh^{+/off}$ and $Lsh^{off/off}$ OPCs

Isolated according to methods protocol from P6-P9 brains from mice of the appropriate genotype derived from crosses of heterozygous *$Lsh^{+/off}$* animals.

2.2 Methods

2.2.1 Animal Scoring

Animals were scored blind weekly according to the following simple scheme:

Weight	**Tremor**	**Ataxia**
No loss =0	None =0	None =0
10% =1	Mild =1	Mild =1
10-20% =3	Moderate =2	Moderate =2
>20% =4		Severe =3

- A score of 4 or more and the animal will be euthanized.
- A score of 3 and the PIL/PPL holder will be notified and the animals scored daily.

Weights were taken at the same time as observations for scores. Video examples for different levels of Ataxia are included in appendix videos 1-4

2.2.2 Mammalian Cell Culture

2.2.2.1 MEFs

Cultured in DMEM + 10 % Fetal bovine serum (Sigma) and 5ml 100x penicillin streptomycin glutamine (PSG)(Gibco) 37ºC 5% CO_2

2.2.2.2 ESCs:

Cultured on gelatinized culture flasks (1% in PBS, Sigma) in MEM (Sigma), 10 % FBS, 500µl 1000x 2- mercaptoethanol, (Gibco) 100x 5 ml sodium pyruvate (Gibco), 5 ml PSG, 5ml non-essential amino acids (Gibco) and 1:1000 dilution of LIF (Produced in Stancheva Lab, batch dependent) at 37ºC 5% CO_2.

2.2.2.3 OPCs:

Following primary isolation OPCs were cultured at 37ºC 10% CO_2 in the following medium:

Media Component	**Concentration**	**Manufacturer**
DMEM (high glucose with Glutamax)	1x	Invitrogen
B27 Supplement 50x	1x	Invitrogen
OPC-Sato stock 100x	1x	See below.
PSG 100x	1x	Gibco
N-acetyl cysteine (NAC)	0.3678mM	Sigma
Insulin	5µg/ml	Sigma
Trace Element B	1x	Cellgro; Mediatech
Biotin	4.093nM	Sigma
Forskolin	5nM	Sigma
PDGF-AA	10 ng/ml	Peprotech
NT3	5 ng/ml	Peprotech

OPC Sato Component	**Concentration**	**Manufacturer**
DMEM	1x	Invitrogen
Apo transferin	10mg/ml	Sigma
BSA	1%	Sigma
Progesterone	6.25µg/ml	Sigma
Putrescine	1.6mg/ml	Sigma
Sodium selenite	4µg/ml	Sigma

Plates or coverslips were coated in 1µg/ml Poly-L-lysine (Sigma) dissolved in PBS, washed with ddH2O and left to dry thoroughly before plating of cells.

2.2.3 gDNA extraction

Tissue samples (HPLC and OPC DNA) were resuspended in 2 ml TE buffer. Proteinase K (Sigma) was added to final concentration of 200 µg/ml and SDS (Sigma) added to a final concentration of 1 % overnight at 55ºC. 100 µg/ml RNAse cocktail (Ambion) was added for overnight (HPLC) at 37°C. The salt concentration was subsequently adjusted to 200 mM with NaCl. Digested peptides were removed through one phenol:chloroform:isoamyl alcohol (Sigma, Merck and Merck respectively) and one chloroform extraction. DNA was precipitated in 1 volume isopropanol (Merck) and 1/10- 1/5 volume Sodium Acetate (3 M, pH 5.3 Sigma). DNA was pelleted, washed in ethanol and resuspended in a suitable volume of TE buffer or water. For isolation of gDNA from ear clippings for genotyping, volume of TE was reduced to 200µl and others adjusted accordingly, RNase was not used.

2.2.4 Mouse genotyping PCR (all primers)

Final concentration in reaction: Primers- each at 0.25pmol/ul, 30mM $MgCl_2$ (Sigma), 1x PCR buffer IV (75mM Tris-HCL pH8.8, 20mM (NH4)2SO4, 0.01% tween 20 all produced by Sigma), 200uM dNTPs, 2.5U Taq Pol (made in the Stancheva lab), 0.2-2ng/ul gDNA.

Cycling conditions: 95ºC 5mins, 95ºC 30s, 58ºC 30s, 72ºC 40s, steps 2-3 x35, 72ºC 10mins.

2.2.5 Protein quantification

Bicinchoninic Acid Protein Assay Kit (Sigma) was used for protein quantification. 0.04 absorbance units are approximately equivalent to 1ug protein. Quantified protein extracts were stored at -80°C.

2.2.6 Western Blotting

Nuclei from MEFs or ESCs was disrupted with Dounce homogeniser in NE1 buffer and nuclei were pelleted for 5 min at 3000 rpm at 4ºC. The nuclei were resuspended in NE2 buffer, treated with Benzonase (thermo scientific) for 30 min on ice and the NaCl concentration adjusted to 500 mM. The nuclei were incubated in this high salt buffer on rotating wheel for 45 min and the supernatants containing nuclear proteins were collected following centrifugation for 15 min at 13000 rpm at 4ºC. 40-60µg of each nuclear extract were resolved on 8.5% SDS-PAGE gel, transferred to nitrocellulose membrane (BioRad). Membranes were then stained with ponceau red for 15mins, before washing off using tap water and fixation by a brief wash of 10% acetic acid (Merck) and imaged on a Biorad Chemidoc. Membranes were then stripped of poncea by washing in 10x TBS until no dye was remaining and then incubated with primary antibodies in TBS buffer with 4% skimmed milk, 0.1% Tween for all antibodies used followed by detection with secondary either IR-670 or IR-800 labelled antibodies (LI-COR). The membranes were scanned on Odyssey scanner (LI-COR) and the images collected with Image Studio software.

2.2.7 High Performance Liquid Chromatography

HPLC was performed by Dr Bernard Ramsahoye on isolated RNase treated gDNA. Relative values for 5mC and 5hmC were then normalised to wild-type samples and experimental conditions expressed as a percentage of these.

2.2.8 Tissue Preparation

For all electron microscopy (EM) mice of appropriate age, post-natal day 24 (P24) considered juvenile and P90 or more adult, were live perfused with 4% paraformaldehyde (PFA) (Sigma) 2.5% gluteraldehyde (Agar Scientific) dissolved in 0.1M PB. Perfusion consisted of injection of 0.1ml ketamine (Vetalar), medetomidine (Domitar) solution to cause terminal anaesthesia followed by opening of the chest and administration of fixative through injection into the left atrium after cutting of the pulmonary vein to relieve pressure. Perfusion

was considered complete when the liver appeared cleared of blood and movement in extremities had ceased. Spinal cord optic nerve and sciatic nerve tissue was then dissected and transferred to post fixative solution consisting of 1% gluteraldehyde in 0.1M PB and stored until staining at 4°C.

For OLIG2 QKI7 staining *Lsh*$^{off/off}$ and control P14 and P90+ adult mice were perfused as described for EM with the exception that the fixation and post-fixative used was 4% PFA (Sigma) in phosphate buffered saline (PBS). Optic nerves and spinal cords were dissected and immersed in post-fix for 2 hours at 4°C these were then washed in PBS before dehydration by overnight incubation at 4°C in first 15% followed by 30% sucrose (Fisher Scientific) in PBS.

For all other antibody staining tissue was immersed overnight in 4% PFA (PBS) overnight these were then washed in PBS before dehydration by overnight incubation at 4°C in first 15% followed by 30% sucrose (Fisher Scientific) in PBS.

Tissue was then embedded in OCT (VWR Chemicals) and 10µm sections cut and stored at -20ºC until staining.

2.2.9 Electron Microscopy

Post-fixed tissue was stained using 1% osmium tetroxide in 0.1M PB, dehydrated using graded ethanol series washes, infiltrated with propylene oxide and embedded in TAAB 812 resin. Ultrathin sections; 60nm thick were cut from selected areas, stained in Uranyl Acetate and Lead Citrate then viewed in a Philips CM120 Transmission electron microscope. Images were taken on a Gatan Orius CCD camera. All chemicals were sourced from TAAB Laboratories Equipment Ltd. Percentage myelinated axon counts were performed on all images to prevent selective bias and graphs and statistical tests were generated using weighted averages for the relative contribution of total number of axons for at least 3

biological replicates of each genotype imaged. g-ratio of random samples of axons were obtained using the g-ratio ImageJ plugin (Goebbels et al. 2010).

2.2.10 Immunofluorescence of tissue and cells

For all antibody conditions10µm frozen sections were warmed to room temperature, or 10 minute 4% PFA fixed coverslips containing cells were washed in PBS and then blocked in 4% bovine serum albumin (Sigma) for 1 hour and then stained overnight at 4°C with appropriate antibodies (see table) in blocking solution with 0.2-0.3% Triton X 100 (Sigma). Samples were then washed in PBS before secondary staining for 1hr at room temperature and stained with 1µg/ml DAPI (Sigma). All solutions dissolved in PBS. Comparative cell counts were performed with each channel threshold at the same value in controls and experimental conditions to ensure consistent positive scoring. Graphs and statistical test were generated using weighted averages for the relative contribution of total cells for at least 3 biological replicates of each genotype imaged.

2.2.11 Tissue RNA isolation and cDNA synthesis

Optic nerves from P14 and P90+ animals were added to TRIzol (Ambion) and snap frozen before storage at -70°C. Tissue was homogenised in pools of 4-6 optic nerve pairs per genotype using a dounce homogeniser. RNA was then isolated using Directzol Microprep kit (Zymo Research) or RNase easy miniprep kit (QIAGEN) according to manufacturer's instructions.

2.2.12 Gene expression analysis by qPCR

Reverse transcription to cDNA was carried out using SuperScript II and IV enzymes (Life Technologies) using oligo d(T) primers according to reagent manufacturer's instructions. All analyses of experimental conditions were matched with littermate controls with RNA isolated and cDNA synthesised by the same procedure.

Isolated cDNA was analysed by qPCR using the Roche 480 Light cycler system with manufacturer supplied master mix and either 384 or 96 well plates. All expression levels were normalised to *Gapdh* expression in each sample and shown as $\log_2$ fold change in experimental genotypes, relative to gene expression in control cDNA. Data represents the average of 3 technical replicates (6 total) of 2 biological replicate cDNA pools, generated from the same number of animals for each genotype.

2.2.13 Oligodendrocyte Isolation

1-day prior isolation positive selection plates were coated with Goat Anti-Rat IgG (H+L) solution in PBS and negative selection plates in BSC1 and incubated overnight at 4ºC. On day of dissection, solution was removed from positive selection plates and washed in PBS before addition of αCD140a antibody in 0.2% BSA PBS solution. Mouse brains were dissected, along with meninges, and a single cell suspension was obtained using MACs neural dissociation Kit P (Miltenybiotec) according to manufacturer's instructions. Suspension was passed through a 70µm strainer and 10ml HBSS was added, this was then spun down 300xG for 5 mins and resuspended in 7ml panning buffer before incubation on a washed negative selection plate for 15 mins. Not selected cells in suspension were then transferred to a positive selection plate for 45 minutes at room temperature. Not selected cells were discarded (or retained for DNA isolation). The plate was then washed 10 times in PBS and cells were either scraped in OPC medium before plating and culture or harvested directly from the positive section plate.

2.2.14 RNA-Seq Library preparation

RNA was isolated as previously described from 3 pools of 6 optic nerves and brain samples alongside from a mixture of all 6 mice in each pool. Quality of RNA was then assessed by running on brain RNA on 1.5% agarose gel at 200V for 15 mins in TAE buffer to assess quality via integrity of the ribosomal RNA bands. Libraries were then generated from the 100-200ng yeild from each pool using the TruSeq® Stranded Total RNA Library Prep kit with

Human/Mouse/Rat rRNA illumination beads (Illumina). 15 amplification cycles were used as recommended for low sample input. Libraries were then assessed for quality using the bioanalyser 2100 expert High Sensitivity DNA Assay (Agilent) kit according to manufacturer's instructions pooled and sent for sequencing on 2 lanes of an illumina HiSeq 4000 150PE by Edinburgh Genomics. 1 control library contained reads mapping to no annotated sequence and as a result this and its littermate control were discarded from analysis.

2.2.15 Whole genome bisulphite sequencing library preparation

DNA was isolated from OPCs derived from 3 separate mice per genotype (*Lsh*$^{+/off}$*;Pdgfrα-Cre, Lsh*$^{off/off}$*;Pdgfrα-Cre* and *Lsh*$^{off/off}$) as described earlier. Concentration was then measured using Qbit BR DNA assay and kit according to manufacturer's instructions and 1µg DNA input into bisulphite conversion using EZ DNA Methylation-Gold kit (Zymogen) according to manufacturer's instructions. Libraries were then generated from this DNA using TruSeq® DNA Methylation Kit using 10x amplification cycles according to manufacturer's instructions. Libraries were then assessed for quality using the bioanalyser 2100 expert High Sensitivity DNA Assay (Agilent) kit according to manufacturer's instructions pooled and sent for sequencing on 2 lanes of an illumina HiSeq 4000 150PE by Edinburgh Genomics. 1 control library contained reads mapping to no annotated sequence and as a result this and its littermate control were discarded from analysis.

2.2.16 Differential expression analysis stage specific comparisons

Quality control for libraries was performed on raw data using FastQC v0.112 and Trimmomatic v0.32 to trim low quality and adapter sequences. Remaining reads were then mapped to the mm10 mouse reference transcriptome using STAR v2.5.3a and transcript abundance was quantified with Salmon v0.11.4. Differentially expressed genes between *Lsh*$^{+/off}$ and *Lsh*$^{off/off}$ were called using DESEQ2 v1.22.1 from the estimated read counts output by Salmon. Gene annotations were obtained from the Ensembl database v79.

CNS cell type specific genes were called from RPKM values derived from the Barres brain database (Zhang et al. 2014). Each cell type present in the database were assigned a ratio between RPKM value in the cell type to the mean RPKM in all other cell types. For each cell type genes were then ranked by this ratio and the top 100 deemed specific for a given cell type. In the assignment of genes to different regulatory stages in OL differentiation, stages of regulation and rat genes within those stages were defined in the route publication (Swiss et al. 2011). Mouse homologues for the rat genes were then identified by cross referencing gene names in the Ensembl database. All genes which did not have a mouse homologue were excluded from the analysis. Cell type characteristic genes defined by single cell RNA-seq were extracted directly from the route publication (Marques et al. 2016). Gene ontology analysis was performed using g-profiler v0.6.7 on genes identified to be significantly changed (p-value <0.05) in each direction. All graphs were produced using R in R-studio and analysis was performed by Shaun Webb (Wellcome centre for cell biology bioinformatics core facility) under my direction.

2.2.17 Whole genome bisulphite sequencing analysis

Quality control for libraries was performed on raw data using FastQC v0.112 and Trimmomatic v0.32 to trim low quality and adapter sequences. Surviving reads were then aligned to the mouse mm10 reference genome using Bismark v0.19.0 and CpG methylation and coverage values were provided in the output. Percentage CpG methylation was then calculated for 1kb regions across the genome and these regions were classified based on proximity to annotated genomic features, using ChIPpeakAnno v3.16.0 and the org.Mm.eg.db annotation package in R using the default priorities for feature assignment. Significantly differentially methylated regions (DMRs) between each possible pair of condition sequences were called using DMRseq v1.2.1. These DMRs were then manually filtered to remove regions mapping to the Y chromosome and random contigs. (DMRs were then assigned to genomic features as above. All graphs were produced using R in R-studio

and analysis was performed by Shaun Webb (Wellcome centre for cell biology bioinformatics core facility) under my direction.

Results- Chapter Three- Conditionally Reversible LSH Knock-Out in Mice

3.1 Introduction

Chao Li produced two independent mouse lines from separate ESC clones. Both of these lines produced viable *Lsh*$^{+/off}$ germline converted chimeras, which were crossed into C57Bl/6 background (F1) to generate the strains TV1 and TV2. Animals were not backcrossed C57Bl/6 background for multiple generations so remained largely on a mixed 129/Ola/C57Bl/6 background. A surprising initial observation given previously reported perinatal lethality for *Lsh*$^{-/-}$ (Geiman et al. 2001) *Lsh*$^{+/off}$ x *Lsh*$^{+/off}$ crosses using both strains produced *Lsh*$^{off/off}$ progeny that survive until weaning. Given this result, the importance of the first step in achieving my initial aim of characterising any *Lsh*$^{off/off}$ phenotype of quantifying the extent of ablation *Lsh* mRNA and LSH protein in *Lsh*$^{off/off}$ was highlighted as the most simple explanation for lack of perinatal lethality is incomplete knock-out. Recombination mediated conditional alleles generated with the aim of altering protein expression rely on the ability of the splice acceptor (SA) within the inserted cassette to force incorporation of the polyadenylation signal and cause truncated mRNA transcription from the locus. Complete abolition of protein expression requires no skipping of the SA, as this would result in full-length mRNA transcription and subsequent translation. In addition, incorporation of the inserted cassette in mRNA followed by subsequent splicing into the next exon upstream of the polyadenylation signal would cause production of a potentially functional fusion protein. Because LSH is an enzyme, small amounts of protein produced from a hypomorphic allele has the potential to alter a large proportion of its *in vivo* substrate. Previous hypomorphic mutations in *Lsh* that completely abolish ATPase function and greatly reduce protein expression also survive postnatally, proving conceptually that even small levels of non- LSH function remaining could prevent perinatal lethality (Sun et al. 2004). These two factors

combined with the high levels of redundancy present within systems regulating chromatin structure would make dissection of LSH's *in vivo* function difficult using a hypomorphic allele.

3.2 LSH expression is abolished in *Lsh*$^{off/off}$ and is restored in *Lsh*$^{on/on}$

3.2.1 Full length *Lsh* protein coding transcript is reduced in *Lsh*$^{off/off}$

To quantify the extent of knock-out in *Lsh*$^{off/off}$ at the mRNA level and test if splice variants including the GFPneo-cassette were present in mRNA produced from the *Lsh*^{off} allele I first decided to look in mouse embryonic stem cells (ESCs). When the initial *Lsh*$^{+/off}$ lines were generated in the Stancheva lab, as previous mouse knockouts of *Lsh* displayed an exclusively recessive phenotype (Geiman et al. 2001), these cells were targeted again using the initial homologous recombination vector to produce a homozygous *Lsh*$^{off/off}$ line for characterisation of any potential ESC phenotype. As *Lsh* expression is under the control of an E2F promoter and ESCs spend a large proportion of time in the dividing cell cycle, these cells express LSH at a high level (Raabe et al. 2001, Fan et al. 2003). I reasoned that if unexpectedly spliced variants of *Lsh* mRNA were produced, it will be at a lower level than the GFP-neo-stop fusion mRNA due to the relative strength of the *Engrailed* splice acceptor and its widespread use in other systems (Voss et al. 1998, McClive et al. 1998). Due to the limited sensitivity of any method to look at gene expression, I would also have the maximum chance of detecting improperly spliced transcript where the promoter was most active.

To this end, I isolated total RNA from the double targeted *Lsh*$^{off/off}$ ESCs and the parental *Lsh*$^{+/+}$ E14 ESC line. Polyadenylated mRNA was then reverse transcribed into cDNA using Oligo d(T) primers and PCR performed using primers specific for exon 3, immediately upstream of the GFP-neo-stop cassette and a combination of the short exons 4 and 5. Any products present in the *Lsh*$^{off/off}$ PCR would indicate transcripts that would have improperly

spliced through the GFP-neo-stop to downstream exons, and those larger than 82bp would indicate the presence of the cassette in a fusion mRNA that may be functional (Fig. 3.1A).

I performed qPCR on *Lsh*$^{off/off}$ and *Lsh*$^{+/+}$cDNA. This revealed approximately 3% of improperly spliced transcript being produced in *Lsh*$^{off/off}$, significantly more than in controls lacking reverse transcriptase in the cDNA synthesis reaction (Fig. 3.1B). However, analysis of the melt curves from the products these samples indicate a lower Tm of product present in *Lsh*$^{off/off}$, which is not consistent with splicing through the cassette to produce a larger product. A more sensitive technique to look further into what was being produced from the *Lsh*$^{off/off}$ locus would be northern blotting using a probe either for exons 4 and 5 or GFPneo, however as large amounts of protein producing transcript has been ruled-out, I prioritised confirming LSH knock-out at the protein level.

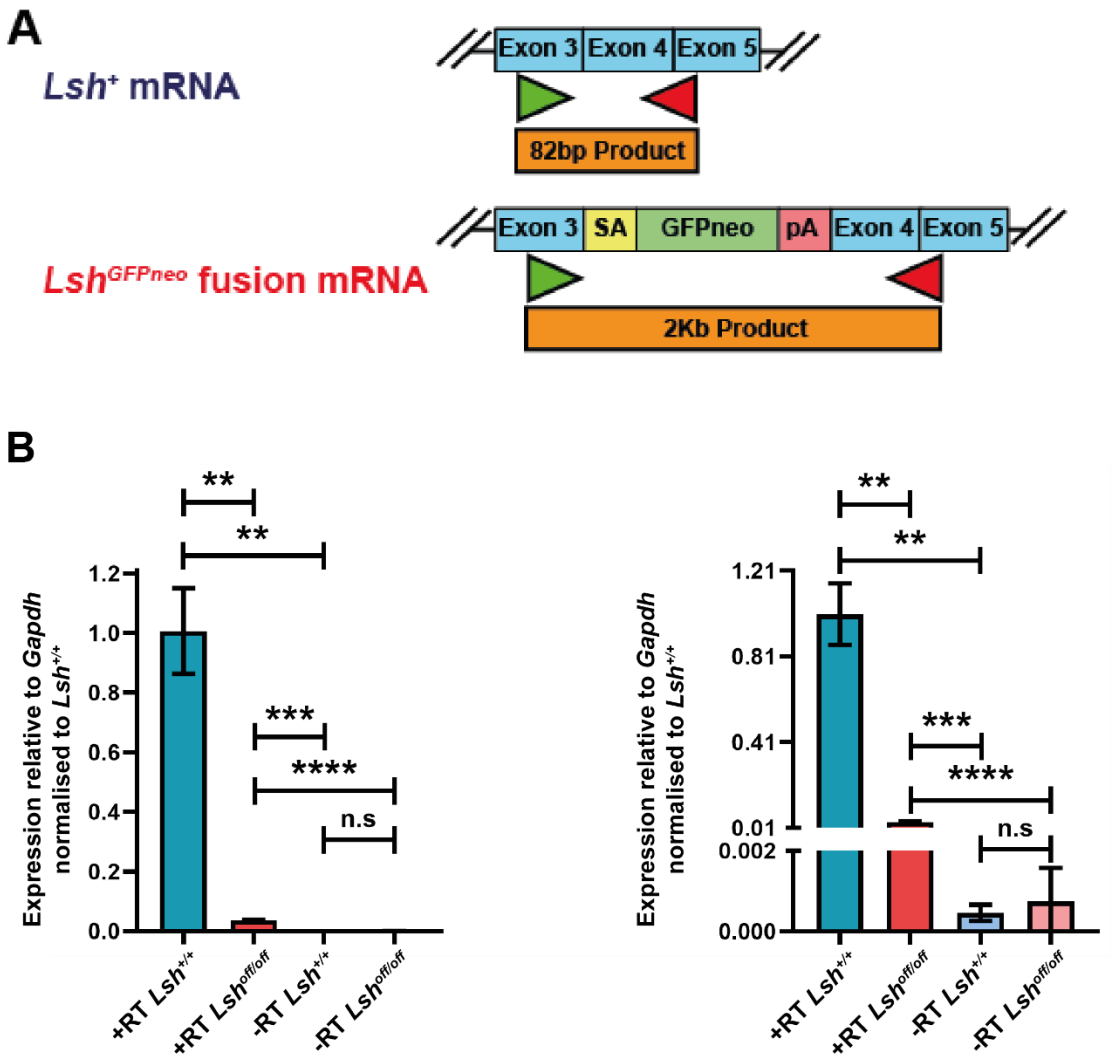

Figure 3-1 qPCR for products spanning insertion cassette of the *Lsh^{off}* allele shows *Lsh^{+}* transcript expression abolished

A) Schematic representation of PCR products made from cDNA in the scenarios of (top) wildtype *Lsh* mRNA being produced and (bottom) the *engrailed* splice acceptor being read through, or cryptic splice acceptors used within the *Gfpneo* cassette insertion. Such a large product is unlikely to be detectable under the same qPCR conditions as the 82bp product.

B) qPCR signal from reverse transcribed ESC mRNA across *Lsh* genotypes and RT conditions. Left graph with contiguous axes and right with split to show levels of expression in conditions producing less product that *Lsh$^{+/+}$*. T-tests with Welch's correction were used to calculate significance, n.s signifies not significant, ****= p<0.00001, ***= p<0.0005, **=p<0.005. Bars represent mean and error bars standard deviation (n=3).

3.2.2 As low as 3% of LSH expression in *Lsh*$^{+/+}$ ESCs is detectable by western blot.

To investigate the extent to which the *Lsh*$^{off/off}$ allele abolishes protein expression, the sensitivity of currently available antibodies for LSH protein in western blots first needed to be determined. In order to determine this sensitivity, I needed to assess the minimum proportion of protein from wild-type cells detectable in the assay. To increase sensitivity of detection, a protein extract from a source for which a comparison between *Lsh*$^{+/+}$and *Lsh*$^{off/off}$ could be made and that would have high levels of LSH is also required.

To achieve this, Irina Stancheva prepared nuclear protein extracts from E13.5 embryos (see previous section for reasoning). To control for differing efficiency of transfer to nitrocellulose membranes depending on protein concentration present, nuclear protein from *Lsh*$^{+/+}$ embryos and *Lsh*$^{-/-}$ MEFs, a previously established knock-out of LSH generated by an independent laboratory (Geiman et al. 2001), was mixed in differing ratios of *Lsh*$^{+/+}$ nuclear extract with *Lsh*$^{-/-}$ MEF nuclear extract. 60µg of these dilutions and were loaded to an acrylamide gel along with *Lsh*$^{off/off}$ embryo nuclear extract. Equality of loading was confirmed by probing with a αHDAC1 antibody (Fig. 3.2A). The same membrane was then probed using 3 different antibodies raised to different regions of the LSH protein. LSH was detectable to the minimum proportion of *Lsh*$^{+/+}$nuclear extract tested (3%) using the N-terminal rabbit polyclonal antibody and was undetectable in *Lsh*$^{off/off}$ extract under optimal exposure for quantification (Fig.3.2B). Probing for other antibodies resulted in less sensitive detection, but in no condition was LSH detected in *Lsh*$^{off/off}$ extract (Fig3.2C, D). No antibody condition was able to detect any LSH protein in the previous knock-out. Following on from this I used the same approach for *Lsh*$^{+/+}$ and *Lsh*$^{off/off}$ ESCs to see if any protein was detectable in a more highly expressing cell type. Again, LSH was detectable up to the 3% dilution, but this time even with the less sensitive mouse monoclonal antibody (Fig.3.2E). From these experiments I concluded that *Lsh*$^{off/off}$ knocks-out at least 97% of LSH protein in mouse embryos, and possibly more limited by the sensitivity of the assay.

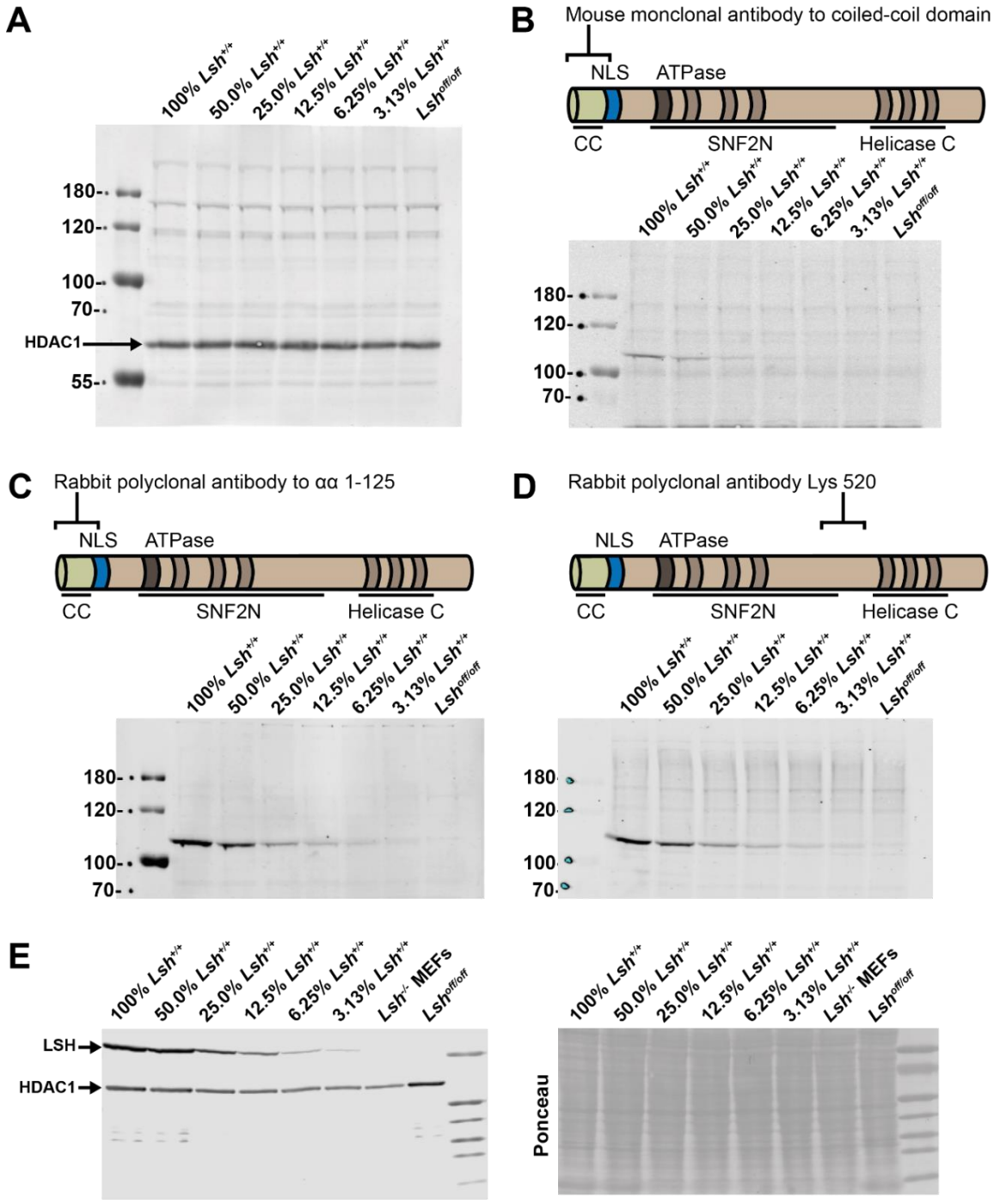

Figure 3-2 Western blot titrations determining LSH antibody sensitivity shows at least 97% depletion of LSH in *Lsh*$^{off/off}$

A) Staining for HDAC1 on a nitrocellulose transferred SDS-PAGE gel loaded with decreasing concentrations of *Lsh*$^{+/+}$ embryonic extract, mixed with increasing concentrations of *Lsh*$^{-/-}$ extract.
B) Schematic representation of epitope location of a mouse monoclonal antibody used to stain the membrane shown in (A). Signal is detectable up to 12.5% of *Lsh*$^{+/+}$ extract, with no increase in background at higher molecular weight.
C) As (B) but showing the epitope of a rabbit polyclonal antibody. Signal detectable to 3% with low background in all lanes.
D) As (B) and (C) with schematic showing epitope for rabbit polyclonal antibody raised to a more c-terminal region of LSH, again protein datable to 3% of *Lsh*$^{+/+}$ levels with no increase in background or higher molecular weight bands in *Lsh*$^{off/off}$. MW indicated in kDa on A-D.
E) A blot of mouse ESC protein extracts loaded in the same titration scheme as described above probed with mouse monoclonal αLSH antibody. Panel on right shows equal loading by ponceau staining.

3.2.3 LSH expression is abolished in MEFs derived from *Lsh*$^{off/off}$ mice and restored in MEFs derived from mice converted to

The western blot titration experiment only looks at expression in 1 individual *Lsh*$^{off/off}$ animal and the double target ESC line. It is conceivable clonal variation between the lines that were used to generate *Lsh*$^{off/off}$ animals and genetic background may have an impact on LSH expression. It is also necessary to test if conversion to *Lsh*$^{on/on}$ (Fig. 1.1) is capable of restoring LSH expression to *Lsh*$^{+/+}$ levels as intended. One possibility that would lead to reduced expression of full length LSH, or production of a fusion protein with impaired function, is the presence of the GFPneo-stop cassette leading to unexpected splicing events, even following change in orientation.

To address these possibilities, I used primary MEF cell lines isolated from *Lsh*$^{off/off}$, *Lsh*$^{+/off}$, *Lsh*$^{+/+}$ and *Lsh*$^{on/on}$ mice by Natalia Torrea, another PhD student in the former Stancheva lab. *Lsh*$^{+/on}$ mice were generated from crossing of the TV2 *Lsh*$^{+/off}$ line into a line possessing constitutively expressed FLPo recombinase (C57BL/6-Tg(CAG-Flpo)1Afst/Ieg). Progeny from this cross possessing *Flpo* and therefor considered converted to *Lsh*$^{+/on}$, were then crossed into *Lsh*$^{+/+}$ mice to remove the *Flpo* allele. Non-littermate *Lsh*$^{+/on}$ progeny from this cross were then crossed to produce *Lsh*$^{on/on}$ animals. MEFs were used for testing the expression of LSH because large amounts of material could be collected from them and the relatively high level of expression compared to tissue from mice. Primary MEF cell lines were readily available from Natalia's project and due to their retained ability to undergo cellular senescence and limited number of divisions following isolation from the animal, may be less prone to potential artefacts associated with immortalisation and prolonged growth in culture (such as aneuploidy).

qPCR on all the lines tested surprisingly revealed *Lsh* expression around 12% of *Lsh*$^{+/+}$ in *Lsh*$^{off/off}$ and importantly *Lsh*$^{on/on}$ cells have restored *Lsh* expression and *Lsh*$^{+/off}$ expression is approximately 50% of *Lsh*$^{+/+}$. I speculate that due to much lower levels of expression in

MEFs, variability between samples is much higher than in ESCs. Interestingly detection of transcript in *Lsh*$^{-/-}$ MEFs suggests a non-protein coding transcript may be produced including this splice junction in these cells (Fig. 3.3A). Any conclusion beyond reduction in transcript in *Lsh*$^{off/off}$ and restoration in *Lsh*$^{on/on}$ would require further experiments (such as the northern blot suggested in the previous section) due to the limitation of this PCR, especially at the lower levels of transcript present in MEFs.

To determine sensitivity of LSH protein detection I performed a similar titration to that described in the previous section. I mixed nuclear extract from *Lsh*$^{+/+}$ primary MEFs with the *Lsh*$^{-/-}$ previously published immortalised line, with a decreasing ratio of *Lsh*$^{+/+}$ material in each tested sample. This revealed LSH expression was detectable up to approximately 6% of *Lsh*$^{+/+}$ levels, less than that possible in ESCs, likely due to increased promoter activity due to MEF's slower division rate (Fig.3.3B). To address the issue of possible clonal variation or genetic background effecting LSH expression in *Lsh*$^{off/off}$ and whether protein expression is restored in *Lsh*$^{on/on}$ I did a western blot of nuclear extract on 2 MEF lines from *Lsh*$^{off/off}$ and *Lsh*$^{on/on}$ mice. These support the evidence from the titration experiments that LSH is not detectable in *Lsh*$^{off/off}$ and that LSH expression is restored in *Lsh*$^{on/on}$ from the qPCR and endpoint PCR experiments (Fig. 3.3C).

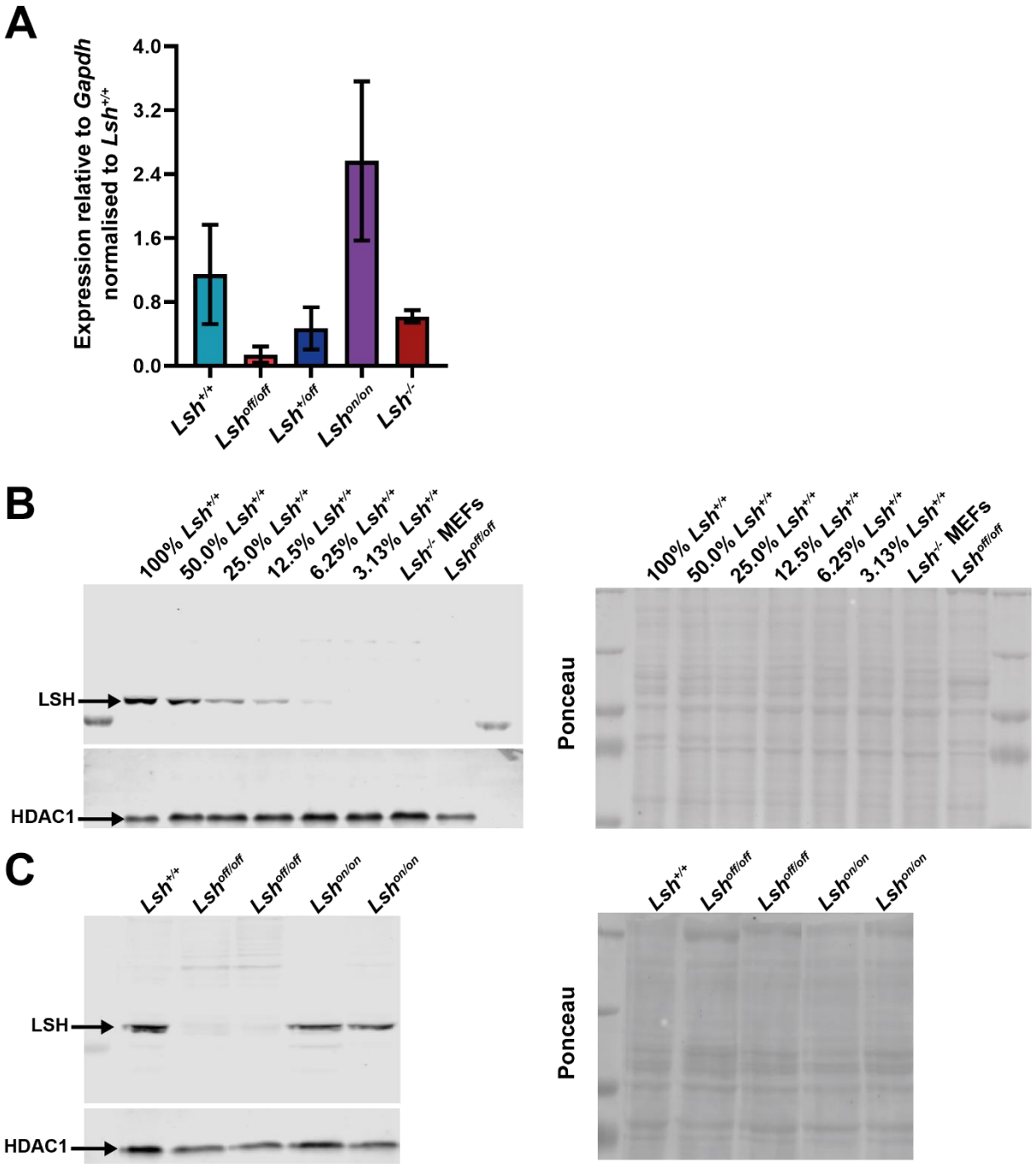

Figure 3-3 qPCR and western blot analysis for primary MEF cell lines replicates protein abolition in *Lsh^{off}* observed in embryos and restoration of LSH expression in *Lsh^{on}*

A) qPCR using splice junction specific primers for cDNA derived from *Lsh* mRNA in primary MEF cell lines. Bars represent mean and error bars standard (n=3).
B) Staining for LSH using n-terminal rabbit polyclonal antibody and HDAC1 on a nitrocellulose transferred SDS-PAGE gel loaded with decreasing concentrations of *Lsh$^{+/+}$* primary MEF extract, mixed with increasing concentrations of *Lsh$^{-/-}$* extract and *Lsh$^{off/off}$* MEF extract. Panel on right shows equal loading by ponceau staining.
C) Staining for LSH using n-terminal rabbit polyclonal antibody and HDAC1 on a nitrocellulose transferred SDS-PAGE gel loaded with *Lsh$^{+/+}$*, 2 *Lsh$^{off/off}$* and 2 *Lsh$^{on/on}$* primary MEF cell lines. Panel on right shows equal loading by ponceau staining.

3.3 *Lsh*$^{off/off}$ mice survive to adulthood but are not healthy. This phenotype is rescued in *Lsh*$^{on/on}$

Initial expectations in the Stancheva lab on production of *Lsh*$^{off/off}$ mice were that, like the previous global knockout of the gene, this genotype would result in perinatal lethality. The strategy for dissecting LSH's function in development would therefor revolve around analysis of embryos and restoring and abolishing expression protein in specific tissues at different developmental stages and study potential phenotypes that arose. This surprisingly proved not to be the case.

3.3.1 *Lsh*$^{+/off}$ animals are fertile whereas *Lsh*$^{off/off}$ mice are sterile and survive to adulthood to varying extents depending on genetic background.

In order to investigate the viability of mouse strains with the *Lsh*^{off} allele, I have analysed all data on the litter sizes produced from crosses of various genotypes. Crossing of heterozygous *Lsh*$^{+/off}$ (*Lsh*$^{+/off}$ × *Lsh*$^{+/off}$) animals within the 129/Ola/C57Bl/6 mixed background produces litters of sizes comparable to *Lsh*$^{+/off}$ × *Lsh*$^{+/+}$ crosses (Fig. 3.4A). Altering genetic background from that of the initial chimeras by crossing *Lsh*$^{+/off}$ strains into the C57BL/6/CBA Tg(CAG-cre/Esr1*)5Amc strain (hereby termed LSH ER-CRE, Allele termed *TgEr-Cre*) and the (129X1/SvJ x 129S1/Sv)F1-Kitl+ Gt(ROSA)26Sor strain (termed LSH ROSA26 ER-CRE, allele termed *Rosa26Er-Cre*) also doesn't significantly affect litter sizes (Fig. 3.4A). To see if the perinatal lethality phenotype seen in previous *Lsh* knockouts was observable in the *Lsh*^{off} lines, I analyzed the proportion of mice born surviving until weaning across our strains. Interestingly, this revealed a small but statistically significant decrease in proportion of mice making it to weaning in *Lsh*$^{+/off}$*; TgEr-Cre* x *Lsh*$^{+/off}$ compared to *Lsh*$^{+/off}$ x *Lsh*$^{+/+}$ and *Lsh*$^{+/off}$ x *Lsh*$^{+/off}$ compared to *Lsh*$^{+/off}$ × *Lsh*$^{+/+}$ but not *Lsh*$^{+/off}$*; Rosa26Er-Cre* (Fig.3.4B). Chi-squared analysis of genotypes produced from the 4 crosses shows that there is a significant reduction in *Lsh*$^{off/off}$ animals from the expected Mendelian ratio in *Lsh*$^{+/off}$ × *Lsh*$^{+/off}$ and *Lsh*$^{+/off}$*; TgEr-Cre* x *Lsh*$^{+/off}$, but not *Lsh*$^{+/off}$ × *Lsh*$^{+/+}$ or *Lsh*$^{+/off}$*; Rosa26Er-*

Cre x *Lsh*$^{+/off}$ (Fig.3.4C, D, E, F). Suggesting that significantly more lethality exists in the *Lsh*$^{off/off}$ before weaning than *Lsh*$^{+/off}$ when large numbers of mice are analysed (n=767). The fact that this is detectable in *Lsh*$^{+/off}$*; TgEr-Cre* x *Lsh*$^{+/off}$ and not *Lsh*$^{+/off}$*; Rosa26Er-Cre* despite similar numbers of mice being analysed (n=166 and n=131 respectively), also suggests some effect of this line's background in exacerbating this lethality.

Figure 3-4 *Lsh*$^{+/off}$ crosses produce homozygous *Lsh*$^{off/off}$ progeny to a normal Mendelian ratio dependent on genetic background

A) Boxplots showing litter sizes from *Lsh*^{off} crosses in different genetic backgrounds. P-values are the result of unpaired t-tests on comparisons of conditions. Whiskers representative of upper and lower quartiles, n=39, 120, 28 and 28 litters respectively.
B) Boxplots showing percentages of mice born across *Lsh*^{off} line crosses. P-values sre the result of Mann-Whitney non-parametric tests due to non-normal distribution present in samples. Bounds of boxes represent minimum and maximum values, n numbers as with (A)
C) Observed and expected rations of mice born from *Lsh*$^{+/+}$ × *Lsh*$^{+/off}$ crosses.
D) Observed and expected rations of mice born from *Lsh*$^{+/off}$ × *Lsh*$^{+/off}$ crosses.
E) Observed and expected rations of mice born from *Lsh*$^{+/off}$ × *Lsh*$^{+/off}$*;TgEr-Cre* crosses.
F) Observed and expected rations of mice born from *Lsh*$^{+/+}$ × *Lsh*$^{+/off}$*; Rosa26ErCre* crosses.
P-values on graphs C-F the result of Chi-squared test comparing expected vs observed numbers.

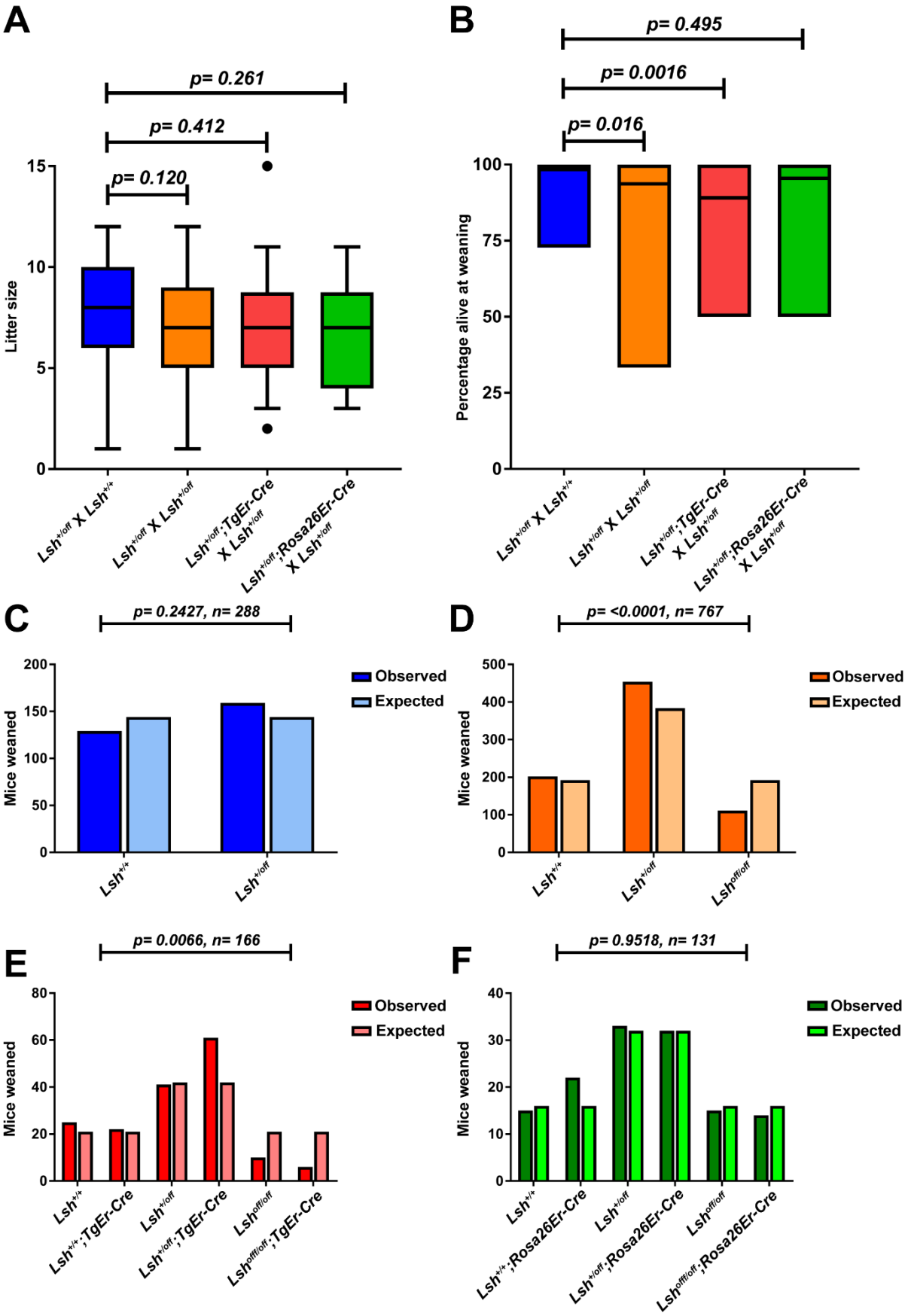
A
p= 0.261
p= 0.412
p= 0.120
Litter size
15
10
5
0
Lsh+/off X Lsh+/+
Lsh+/off X Lsh+/off
Lsh+/off;TgEr-Cre X Lsh+/off
Lsh+/off;Rosa26Er-Cre X Lsh+/off
B
p= 0.495
p= 0.0016
p= 0.016
Percentage alive at weaning
100
75
50
25
0
Lsh+/off X Lsh+/+
Lsh+/off X Lsh+/off
Lsh+/off;TgEr-Cre X Lsh+/off
Lsh+/off;Rosa26Er-Cre X Lsh+/off
C
p= 0.2427, n= 288
Mice weaned
200
150
100
50
0
Observed
Expected
Lsh+/+
Lsh+/off
D
p= <0.0001, n= 767
Mice weaned
500
400
300
200
100
0
Observed
Expected
Lsh+/+
Lsh+/off
Lshoff/off
E
p= 0.0066, n= 166
Mice weaned
80
60
40
20
0
Observed
Expected
Lsh+/+
Lsh+/+;TgEr-Cre
Lsh+/off
Lsh+/off;TgEr-Cre
Lshoff/off
Lshoff/off;TgEr-Cre
F
p= 0.9518, n= 131
Mice weaned
40
30
20
10
0
Observed
Expected
Lsh+/+
Lsh+/+;Rosa26Er-Cre
Lsh+/off
Lsh+/off;Rosa26Er-Cre
Lshoff/off
Lshoff/off;Rosa26Er-Cre

3.3.2 *Lsh*$^{off/off}$ mice have growth retardation, ataxia and tremor phenotypes that are rescued in *Lsh*$^{on/on}$.

In order to address the first aim of my thesis, I now set out to see if there was any obviously phenotypes in *Lsh*$^{off/off}$ animals which would prove amenable to more in-depth study.

Early observation of *Lsh*$^{off/off}$ mice revealed an obvious tremor and ataxia phenotype (see appendix video 3), which often led to animals being culled due to welfare concerns. Mice were lean and slightly decreased length compared to *Lsh*$^{+/off}$ littermates (Fig.3.5A). Another immediate observation was that *Lsh*$^{on/on}$ animals are fertile, but *Lsh*$^{on/on}$ x *Lsh*$^{on/on}$ crosses produce reduced litter sizes compared to other lines, though a similar proportion make it to weaning as *Lsh*$^{+/off}$ × *Lsh*$^{+/+}$ and significantly higher proportion than *Lsh*$^{+/off}$ × *Lsh*$^{+/off}$ (Fig.3.5B). To analyse the extent of the reduced body weight and growth phenotype, I have plotted combined weekly weights across monitored litters in *Lsh*^{off} *and Lsh*^{on} mouse lines. *Lsh*$^{+/off}$ and *Lsh*$^{on/on}$ mice show a growth in body weight comparable to *Lsh*$^{+/+}$ animals, but *Lsh*$^{off/off}$ males and females have a reduction in growth from approximately 5 weeks post-weaning, followed by a gradual decline immediately in males starting at week 9 for females (Fig. 3.5C). As a large proportion of *Lsh*$^{off/off}$ animals were being found dead post-weaning, the severity of the body weight and neurological phenotype were monitored according to a scoring system (see materials and methods) for all homozygous animals across *Lsh*^{off} and *Lsh*^{on} lines, and a humane endpoint defined. Data from all maintained mice shows survival of *Lsh*$^{off/off}$ animals starts to drop around 7 weeks post-weaning onwards, with no death seen in the other genotypes within this timeframe (Fig.3.5D). We did not continue maintaining mice beyond 10 weeks to determine maximum *Lsh*$^{off/off}$ survival as priority was given to other experiments that required mice before endpoint was reached. Plotting neurological scoring of *Lsh*$^{off/off}$, *Lsh*$^{on/on}$ and *Lsh*$^{+/off}$ animals reveals a large variation in severity of *Lsh*$^{off/off}$ phenotype, though it was apparent in all but 1 of 24 animals immediately post-weaning. Importantly there is also no phenotype observable in non-*Lsh*$^{off/off}$ genotypes, indicating this is not a genetic background effect of the strain (Fig.3.5E).

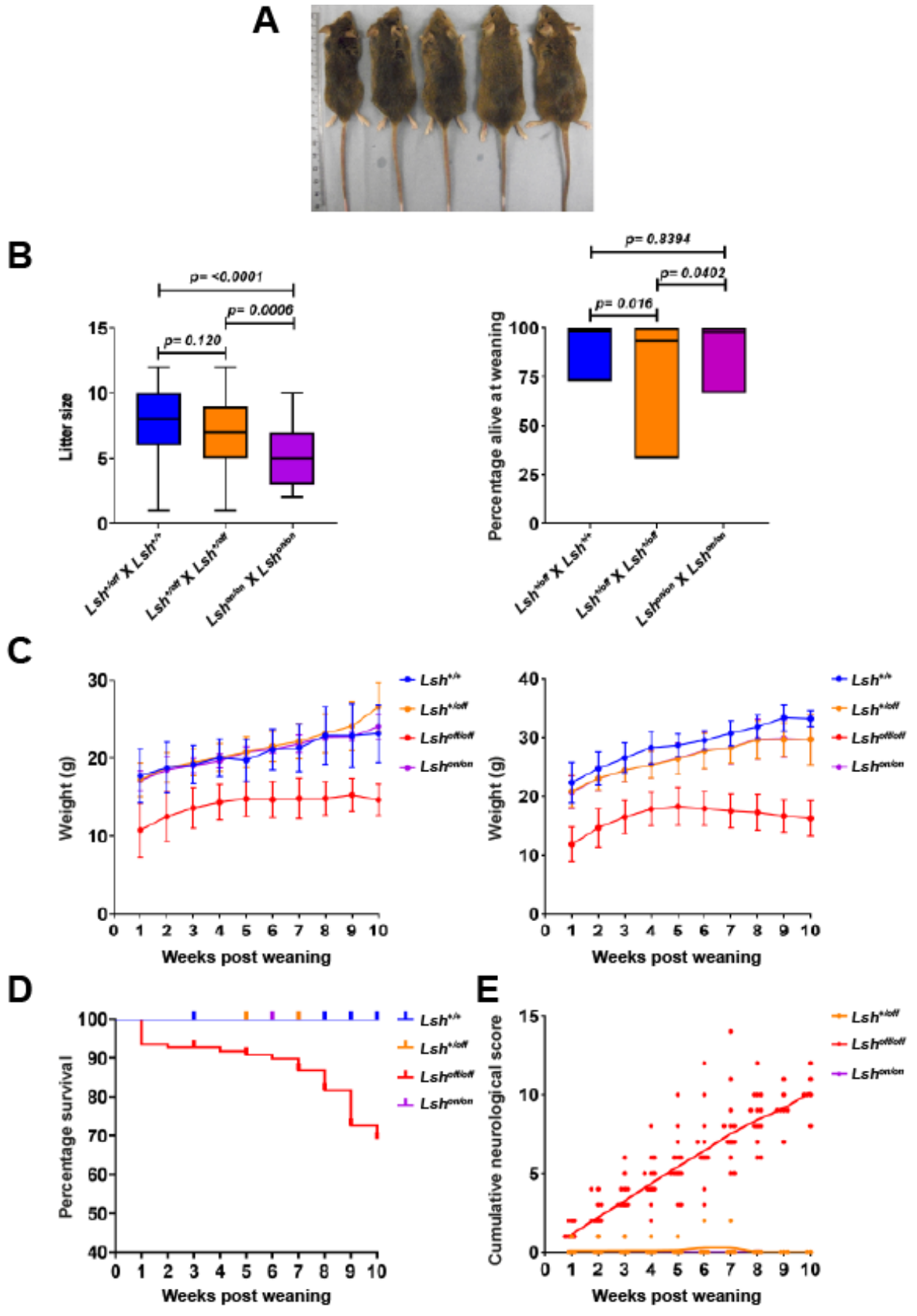
A
B
p= <0.0001
p= 0.0006
p= 0.120
Litter size
Lsh+/lof X Lsh+/+
Lsh+/lof X Lsh+/lof
Lsh lof/lof X Lsh lof/lof
p= 0.8394
p= 0.0402
p= 0.016
Percentage alive at weaning
Lsh+/lof X Lsh+/+
Lsh+/lof X Lsh+/lof
Lsh on/on X Lsh on/on
C
Weight (g)
Weeks post weaning
Lsh+/+
Lsh+/lof
Lsh lof/lof
Lsh on/on
Weight (g)
Weeks post weaning
Lsh+/+
Lsh+/lof
Lsh lof/lof
Lsh on/on
D
Percentage survival
Weeks post weaning
Lsh+/+
Lsh+/lof
Lsh lof/lof
Lsh on/on
E
Cumulative neurological score
Weeks post weaning
Lsh+/lof
Lsh lof/lof
Lsh on/on

Figure 3-5 *Lsh*$^{off/off}$ has a growth retardation, neurological and survival phenotype that is rescued in *Lsh*$^{on/on}$

A) Boxplots showing litter sizes from *Lsh*^{on} and *Lsh*^{off} crosses. P-values result on unpaired t-test comparisons of conditions. Whiskers representative of upper and lower quartiles, n=39, 120 and 34 respectively.
B) Boxplots showing percentages of mice born in *Lsh*^{on} and *Lsh*^{off} crosses. P-values the result of Mann-Whitney non-parametric tests due to non-normal distribution present in samples. Bounds of boxes represent minimum and maximum values, n numbers as with (A)
C) Line graph of mean weights post-weaning for females of *Lsh*$^{+/+}$, *Lsh*^{on} and *Lsh*^{off} genotypes. Error bars show standard deviation, maximum n numbers=10, 48, 39 and 4 respectively, though this varies between timepoints for the first 3 genotypes due to culling and deaths.
D) Line graph of mean weights post-weaning for males of *Lsh*$^{+/+}$, *Lsh*^{on} and *Lsh*^{off} genotypes. Error bars show standard deviation, maximum n numbers=12, 41, 46 and 6 respectively though this varies between timepoints for the first 3 genotypes due to culling and deaths.
E) Scatter plot of neurological score for *Lsh*$^{+/+}$, *Lsh*^{on} and *Lsh*^{off} genotypes, maximum n numbers=13, 89, 109 and 8 respectively though this varies between timepoints for the first 3 genotypes due to culling for use in other experiments and death.

3.3.3 Adult *Lsh*$^{off/off}$ mice DNA is hypomethylated in multiple tissues and *Lsh*$^{off/off}$ mice have atrophied optic nerves and other organs show

To investigate if *Lsh*$^{off/off}$ mice have a functional knock-out of LSH *in vivo* and narrow down the location of a cellular cause for the observed phenotype, tissue was dissected from *Lsh*$^{off/off}$ and *Lsh*$^{+/off}$ control animals and analysed. An immediate observation was, strikingly, optic nerves from *Lsh*$^{off/off}$ mice are smaller than their heterozygote counterparts and appear almost transparent in phenotypically severe animals (Fig. 3.6A). Notably, although there is a reduction in girth, this transparency is not observable in the peripheral nervous system sciatic nerve in the same animal (Fig.3.6B). It's important to note though, other organs differ morphologically depending on genotype, with spleen much smaller and paler colour in *Lsh*$^{off/off}$ animals (Fig.3.6C).

To address if LSH is functionally knocked-out, I isolated gDNA from brain, spleen and kidney and sent for HPLC to determine 5-methyl-cytosine (5mC) content relative to cytosine. This shows hypomethylation of DNA compared to *Lsh*$^{off/off}$ from around 70% of *Lsh*$^{+/off}$ in brain to around 60% in spleen (Fig. 3.6C). In addition, we looked at the presence of 5-hydroxymethyl cytosine, a read out for the dynamic removal of 5mC (Pastor et al. 2013), which interestingly showed the greatest disparity in spleen (Fig. 3.6D), the tissue with the greatest proportion of rapidly dividing cells (Bachman et al. 2014).

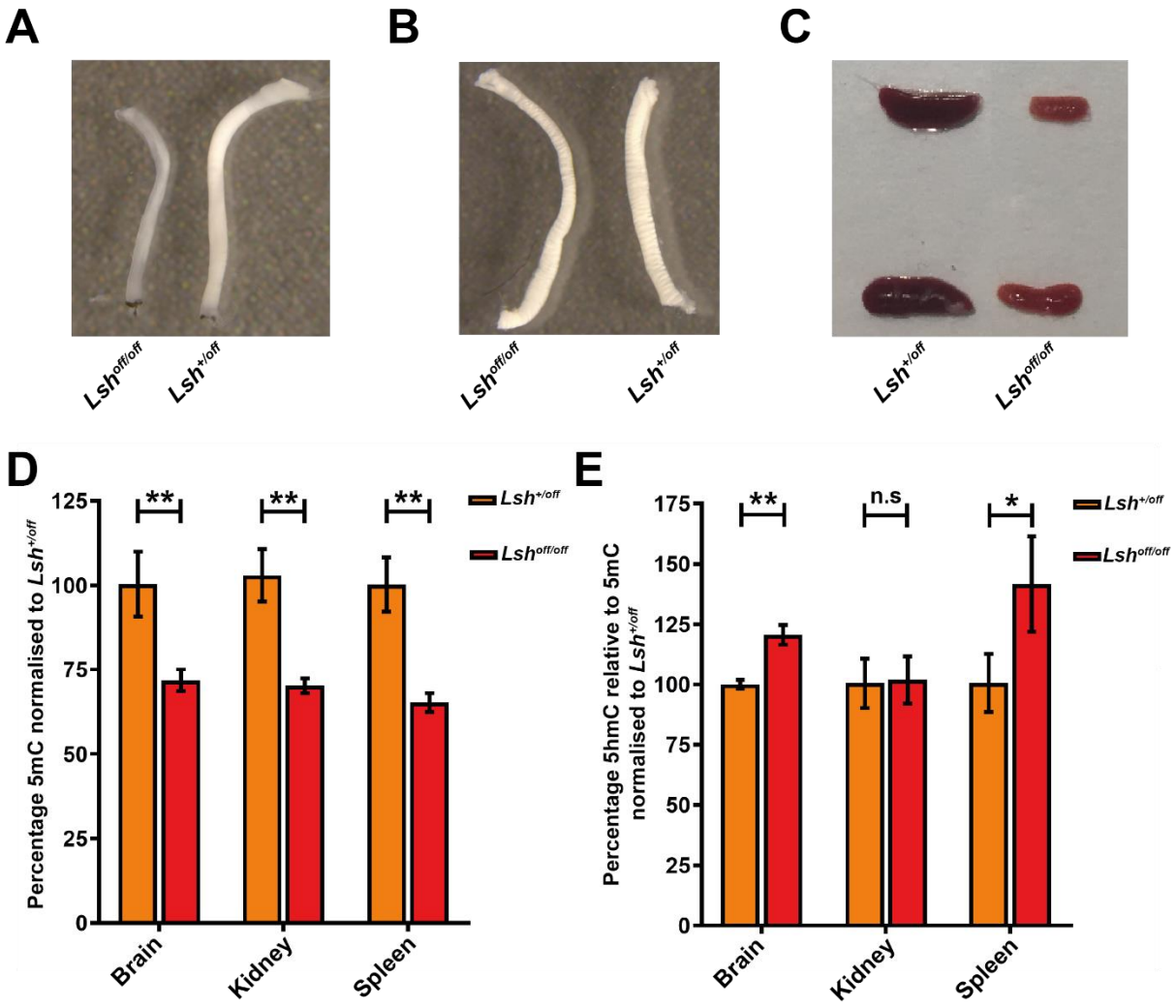

Figure 3-6 There are morphological and DNA methylation phenotypes across *Lsh*$^{off/off}$ tissues

A) Light microscopy image of P90 *Lsh*$^{+/off}$ and *Lsh*$^{off/off}$ optic nerve.
B) Light microscopy image of P90 *Lsh*$^{+/off}$ and *Lsh*$^{off/off}$ sciatic nerve (same animal as above).
C) Light microscopy image of 2 P90 *Lsh*$^{+/off}$ and *Lsh*$^{off/off}$ spleens.
D) HPLC analysis of 5 methyl-cytosine in DNA isolated from *Lsh*$^{+/off}$ and *Lsh*$^{off/off}$ tissue.
E) HPLC analysis of 5' hydroxymethyl-cytosine in DNA isolated from *Lsh*$^{+/off}$ and *Lsh*$^{off/off}$ tissue. Bars on D and E represent a mean of 5mC or 5hmC percentages normalised to *Lsh*$^{+/off}$ levels respectively (mean considered 100%) error bars show standard deviation (n=3) and P-values calculated using unpaired T-tests. *=P<0.05, **=P< 0.005 and n.s signifies not significant.

3.4 Summary

There is detectable signal in PCR using primers either side of the wild-type mRNA exon 3,4,5 splice junction in *Lsh*$^{off/off}$ ESCs, though melt curve analysis shows this is not the result of wild-type *Lsh* transcript production. Likely due to lower expression levels, this *Lsh*$^{off/off}$ product is not above the level of noise in MEF cDNA. LSH protein is reduced at least 94% in *Lsh*$^{off/off}$ MEFs and 97% in *Lsh*$^{off/off}$ ESCs. In these conditions, full length LSH, or a fusion protein of LSH and the protein product of the inserted GFPneo cassette is not detectable. This reduction or abolition in LSH is sustained in *Lsh*$^{off/off}$ across variation in genetic background. Breeding of *Lsh*^{off} possessing mice into an *FLPo* strain leads to restoration of LSH expression at the RNA and protein level in progeny homozygous for SA-GFPneo-STOP insertion. This suggests inversion of the cassette successfully abolishes SA recognition, allowing full-length protein to be produced. *Lsh*$^{off/off}$ embryos can make it to term and genetic background does have some effect of *Lsh*$^{off/off}$ viability. Due to the differences between the LSH ER-CRE and LSH ROSA26 ER-CRE insertions, the difference in post-natal viability observed could be due to differing doses of CRE/ESR1 fusion protein caused by multiple insertions of the *CAG-cre/Esr1* transgene. In addition, differences in expression between the *Cag* and *Sor* promoters rather than the differing strain backgrounds introduced to *Lsh*$^{+/off}$ could be responsible for altered lethality. Nonetheless, the ability to breed a more perinatal lethality-like phenotype into *Lsh*^{off} strains hints that through more extensive backcrossing of lines the *Lsh*$^{-/-}$ phenotype could be recapitulated in our knockout lines

As it's not possible to confirm 100% LSH knock-out in *Lsh*$^{off/off}$ mice, the argument can always be made that any phenotype present in these mice that differs from previous reports of a widely accepted *Lsh* knock-out are due to tiny amounts of residual functional protein being present. However, as discussed earlier, recently mutations in the human *Lsh* gene (*Hells*), that truncate LSH protein early into the protein and abolish all characterised enzymatic activity and functional domains, have recently been associated with ICF

syndrome (Thijssen et al. 2016). This shows that functional *Lsh* knock-out is compatable with post-natal mammalian life, making the prospect less unreasonable to be true also in mouse. Also encouraging levels of methylation in $Lsh^{off/off}$ seem to be similarly reduced to previous lines. Mice also develop and unexpected neurological phenotype, which intriguingly fits with previously characterized lines lacking nervous system myelination (Orian et al. 1994). In order to fulfil the aims of my project I chose to focus on characterizing the cellular defects present in this phenotype in $Lsh^{off/off}$ animals, and to see if there truly is a lack in myelin in $Lsh^{off/off}$ and where this lack in localized to, with an aim to narrow down a cellular cause.

Results- Chapter Four- LSH Knock-out Leads to Hypomyelination and an Oligodendrocyte Differentiation Defect

4.1 Introduction

To test the hypothesis that the ataxia and tremor phenotype was in fact due to myelination and try and narrow down when and where LSH expression was essential for this process, I needed to perform a rigorous characterisation of myelin throughout the central nervous system. Characterisation of the precise defect, which could be due to a mechanical inability for differentiated cells to produce or wrap myelin, an inability for cells to properly differentiate or survive due to intrinsic or extrinsic factors, or because neurons themselves are not amenable to myelination, would also shed light on the cellular cause of the *Lsh*$^{off/off}$ phenotype. The most sensitive way to achieve this characterisation is through transmission electron microscopy on nervous system tissue.

4.2 *Lsh*$^{off/off}$ mice have reduced myelination throughout development, but to differing extents depending on axonal/tissue specific environments

4.2.1 *Lsh*$^{off/off}$ mice have substantial hypomyelination throughout adulthood, specifically in the central nervous system

I performed transmission electron microscopy (TEM) on osmium tetroxide stained sections of post-natal day 90 optic nerve, corpus callosum and spinal cord from *Lsh*$^{off/off}$ and *Lsh*$^{+/off}$ animals, to control for any dominant negative effect of the LSH-GFPneo fusion protein may have on myelination. Example images show there is indeed an obvious lack of myelin (dark staining regions) wrapped around axons (circular cross sections) in all the CNS tissues tested (Fig. 4.1A, B, C). To test if this was due to an in ability of all cells to synthesis the components of myelin, or a problem specific to OLs, the myelinating cells of the CNS, I also performed TEM on sciatic nerves, a peripheral nervous system tissue myelinated by Schwann cells. There was no obvious difference between genotypes (Fig. 4.1D).

However, some myelination was still visible in *Lsh*$^{off/off}$ indicating the presence of some mOLs. To be confident that this phenotype was apparent across animals in the population, and to get a better indication of the amount of residual myelin, I counted the proportion of myelinated axons in a sample of 200 axons per animal in the optic nerve and spinal cord of 3 individuals per genotype. This revealed the extent of myelination differs quite widely between more and less severely affected *Lsh*$^{off/off}$ animals, (Fig.4.1E). In addition, it appears as though spinal cord in *Lsh*$^{off/off}$ is substantially more myelinated (in terms of percentage with any myelin) than optic nerve. An important aspect of the phenotype that can hint at the role of LSH in myelination is whether the ability to establish myelin in development is impaired, or whether there is a loss following aging. The former would suggest a differentiation defect, or large-scale death in the OL population and the latter that LSH is important for long-term OL survival. To distinguish between these two possibilities, I performed TEM on optic nerves

from P24 animals, which normally represents the peak of developmental myelination (Foran and Peterson 1992). A lack of myelination analogous to those in older animals was observable in example images in optic nerve, although again spinal cord appears to be less severely affected (Fig.4.1F).

It is unclear from the percentage myelinated axon analysis if the *Lsh*$^{off/off}$ hypomyelination is the result of individual variation, or a variegated pattern of myelination across the CNS of *Lsh*$^{off/off}$ animals, and the small region sectioned in a given individual happening to be relatively well myelinated. When looking at a few images of corpus callosum from the same *Lsh*$^{off/off}$ animal, small patches where more myelin is present are observable that might be consistent with a variegated phenotype (Fig.4.1G). However, I chose not to perform a more rigorous analysis into whether this is consistent with variegation, due to the overwhelmingly phenotype present even in less severely affected *Lsh*$^{off/off}$ animals, and instead chose to focus more on the cellular cause of the phenotype.

Figure 4-1 *Lsh*$^{off//off}$ animals are hypomyelinated throughout the CNS throughout development but retain myelin in the PNS

A) Representative TEM images of myelin in P90 *Lsh*$^{+/off}$ *and Lsh*$^{off/off}$ optic nerve
B) Representative TEM images of myelin in P90 *Lsh*$^{+/off}$ *and Lsh*$^{off/off}$ corpus callosum
C) Representative TEM images of myelin in P90 *Lsh*$^{+/off}$ *and Lsh*$^{off/off}$ spinal cord
D) Representative TEM images of myelin in P90 *Lsh*$^{+/off}$ *and Lsh*$^{off/off}$ sciatic nerve
E) Mean percentage myelinated axons in *Lsh*$^{+/off}$ and *Lsh*$^{off/off}$ tissue from a sample of 200 axons from 3 individuals, error bars represent S.E.M and p-values calculated using unpaired t-tests between genotypes within a tissue. *=P<0.05.
F) Representative TEM images of myelin in P24 *Lsh*$^{+/off}$ *and Lsh*$^{off/off}$ optic nerve and spinal cord
G) Images of P90 *Lsh*$^{off/off}$ corpus callosum illustrating the variation in myelination across different regions in the same animal. Images taken from the same tract of callosal axons.

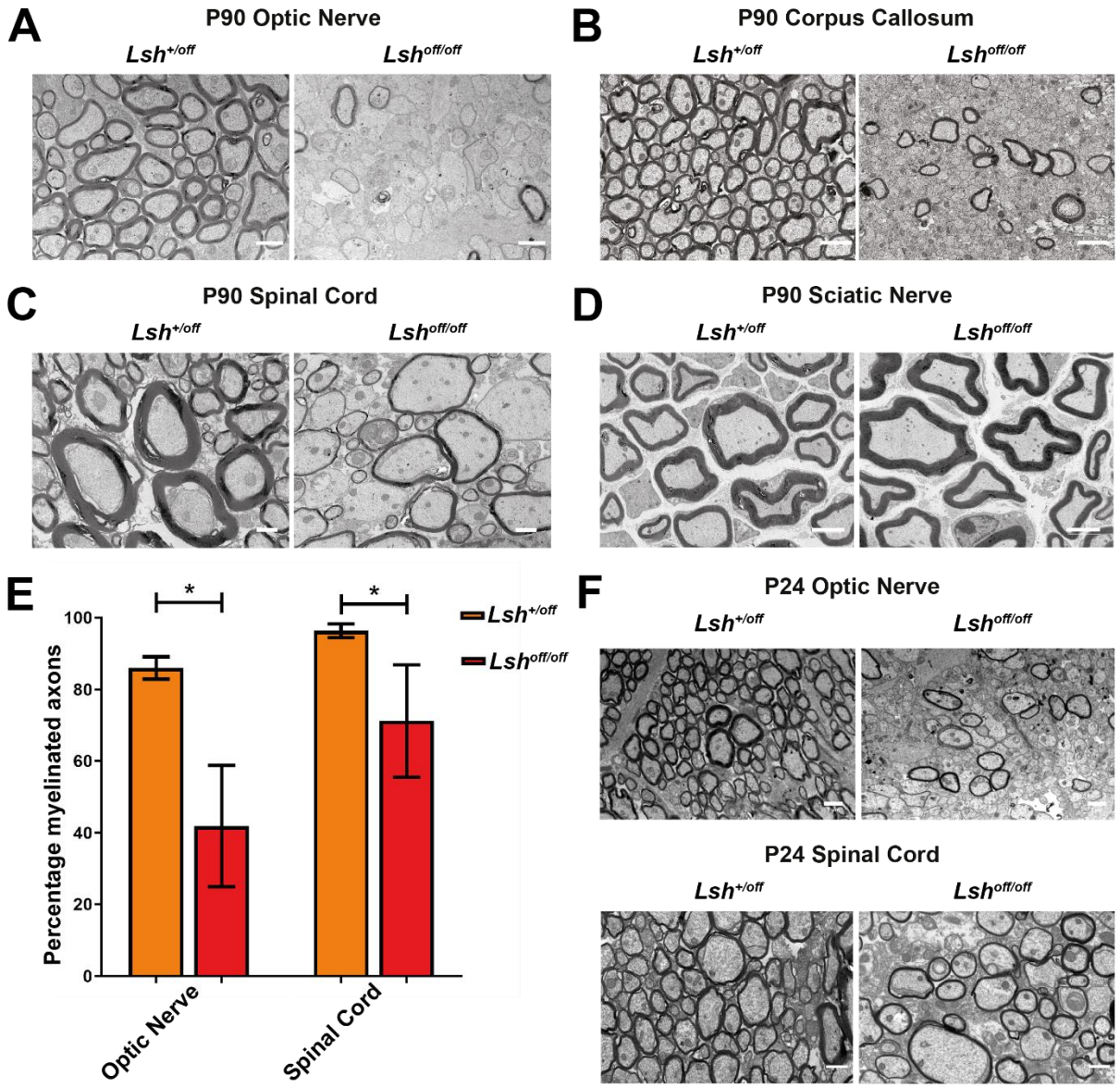
A
P90 Optic Nerve
Lsh+/off
Lshoff/off
B
P90 Corpus Callosum
Lsh+/off
Lshoff/off
C
P90 Spinal Cord
Lsh+/off
Lshoff/off
D
P90 Sciatic Nerve
Lsh+/off
Lshoff/off
E
Percentage myelinated axons
100
80
60
40
20
0
*
*
Lsh+/off
Lshoff/off
Optic Nerve
Spinal Cord
F
P24 Optic Nerve
Lsh+/off
Lshoff/off
P24 Spinal Cord
Lsh+/off
Lshoff/off

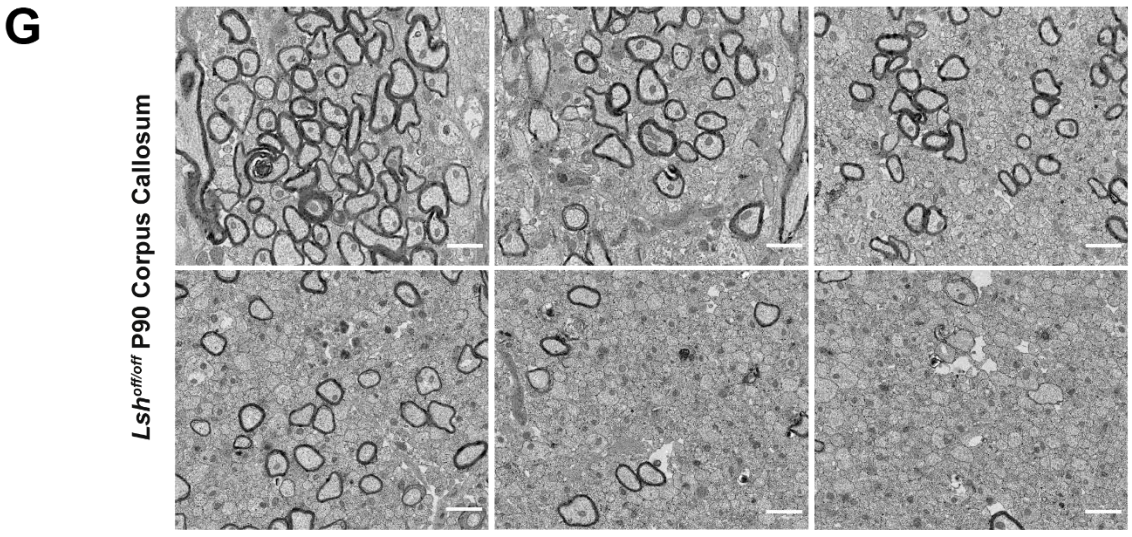
G
Lshoff/off P90 Corpus Callosum

4.2.2 *Lsh*$^{off/off}$ mice have a similar axon density and calibre range to *Lsh*$^{+/off}$ but the relationship between axon calibre and myelination is maintained only for larger axons.

One feature of myelin is the tendency for larger diameter axons to be more likely myelinated and to a greater thickness than smaller axons (Hildebrand et al. 1993). When this relationship breaks down, it can indicate an impairment of response to differentiation signals secreted by axons or for axons to secrete these signals (Makinodan et al. 2012, Mensch et al. 2015, Almeida et al. 2011). To investigate if these are factors influencing the *Lsh*$^{off/off}$ phenotype I measured percentage of myelinated axons in the *Lsh*$^{off/off}$ optic nerve in various ranges of axon calibre. Larger calibre axons are not significantly more likely to be myelinated than small calibre ones in optic nerve (Fig.4.2A). This may be due to the earlier discussed lack of ability to react to axon signalling from the relatively low diameter of axons present in the optic nerve or could be due to another factor in the tissue environment. Therefor to test if axon diameter could be sensed at larger sizes and in other tissues, I performed similar analysis on the larger axons in the spinal cord. Here we can see that at the largest axon strata, calibre does influence myelination, with >0.7μm^2 axons being myelinated to a much greater extent than smaller axons, and more even than comparable sizes in optic nerve (Fig. 4.2B).

The conclusion from myelination analysis is the result of an OL defect could be confounded by differences in axon density and size between *Lsh*$^{off/off}$ and *Lsh*$^{+/off}$. It is conceivable the *Lsh*$^{off/off}$ neurological phenotype is the result of an inability of neurons to develop and form effective networks in the CNS, independently of myelin. This could, in turn, have a knock-on effect on myelination. An observation consistent with this would a reduction in axon density or size in *Lsh*$^{off/off}$. To test this hypothesis, I measured the frequency of neurons across different axon calibres in our 200 axon/animal samples, along with total density of axons in *Lsh*$^{off/off}$ optic nerve and spinal cord compared to *Lsh*$^{+/off}$. There is no significant difference in size distribution of axon calibre in the sampled axons measured (Fig.4.2C, D). Density of

neurons in *Lsh*$^{off/off}$ tends to be higher than *Lsh*$^{+/off}$ though this difference is not statistically significant in either tissue and is possibly due to the reduced size of *Lsh*$^{off/off}$ tissue (Fig.3.6A) forcing the same number of neurons to be in a smaller space (Fig. 4.2E).The g-ratio of a myelinated axon is the ratio of axon area excluding myelin to that including it. It is used as an index of to what extent myelination of a neuron performs its function of insulating the electrical signals sent through the fibre (Chomiak and Hu 2009). If LSH functions in OL survival alone, or there is a truly variegated phenotype where some OLs myelinate normally, and others don't, you may expect for this g-ratio to be maintained in those axons that do receive myelination in *Lsh*$^{off/off}$. To see if this is the case, I measured g-ratios from 275 myelinated axons in *Lsh*$^{off/off}$ and *Lsh*$^{+/off}$ optic nerve and spinal cord, to consider a range of axon diameters. In both conditions, *Lsh*$^{off/off}$ neurons had a consistently lower g-ratio (Fig, 4.2F). To see if this was consistent across all fibre diameters, I plotted g-ratio against axon area for the 275 neurons. The trend of high g-ratio in *Lsh*$^{off/off}$ holds across tissue and diameter (Fig.4.2G, H).

Figure 4-2 Axon calibre increases percentage myelinated axons and myelin thickness for axons *Lsh*$^{off/off}$, though is still reduced in both criterions compared to *Lsh*$^{+/off}$ at P90

A) Size stratified mean percentage myelinated axons in a sample of 200 axons across 3 animals per genotype in optic nerve.
B) Size stratified mean percentage myelinated axons in a sample of 200 axons across 3 animals per genotype in spinal cord. Error bars represent SEM in A and B, P-values calculated by 2-way ANOVA and shown for the axon area factor for A and B.
C) Bar chart showing numbers of axons across different calibre stratifications in the same optic nerve sample as A and B.
D) Bar chart showing numbers of axons across different calibre stratifications in the same spinal cord sample as A and B.
E) Average axon density across *Lsh*^{off} genotypes and tissues, >1000 axons sampled per the 3 animals analysed.,
F) g-ratios across *Lsh*^{off} genotypes and tissues, 275 axons samples across 3 animals per genotype
G) g-ratios across *Lsh*^{off} genotypes stratified by axon diameter, using the same sample as (F) for spinal cord.
H) g-ratios across *Lsh*^{off} genotypes stratified by axon diameter, using the same sample as (F) for optic nerve.

Unpaired t-tests were used to calculate p-values for E and F. For all data n.s signified not significant ***=P<0.0005 *****=P<0.00001.

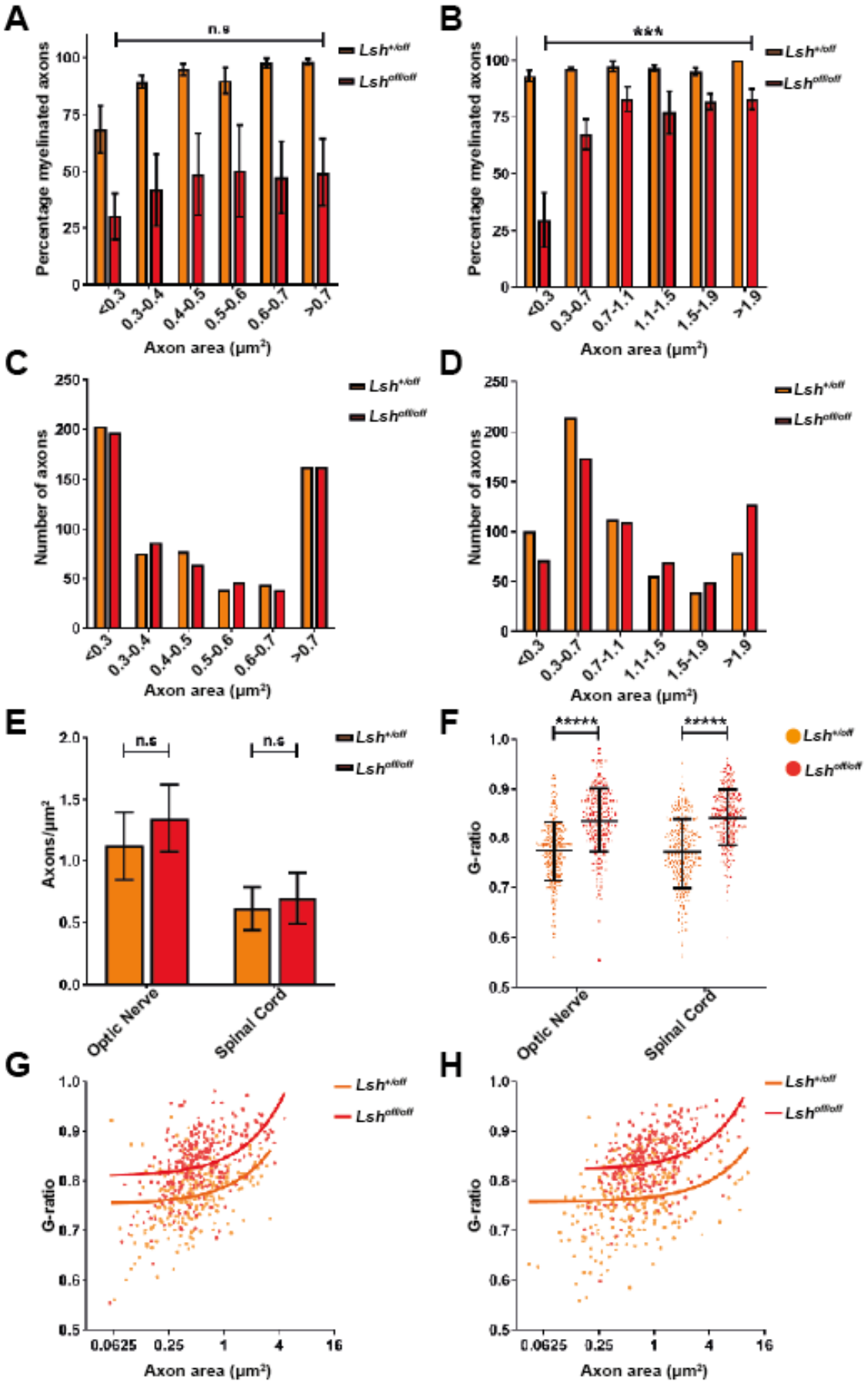
A
n.s
Percentage myelinated axons
100
75
50
25
0
<0.3
0.3-0.4
0.4-0.5
0.5-0.6
0.6-0.7
>0.7
Axon area (µm²)
Lsh+/off
Lshoff/off
B
***
Percentage myelinated axons
100
75
50
25
0
<0.3
0.3-0.7
0.7-1.1
1.1-1.5
1.5-1.9
>1.9
Axon area (µm²)
Lsh+/off
Lshoff/off
C
Number of axons
250
200
150
100
50
0
<0.3
0.3-0.4
0.4-0.5
0.5-0.6
0.6-0.7
>0.7
Axon area (µm²)
Lsh+/off
Lshoff/off
D
Number of axons
250
200
150
100
50
0
<0.3
0.3-0.7
0.7-1.1
1.1-1.5
1.5-1.9
>1.9
Axon area (µm²)
Lsh+/off
Lshoff/off
E
n.s
n.s
Axons/µm²
2.0
1.5
1.0
0.5
0.0
Optic Nerve
Spinal Cord
Lsh+/off
Lshoff/off
F
*****
*****
G-ratio
1.0
0.9
0.8
0.7
0.6
0.5
Optic Nerve
Spinal Cord
Lsh+/off
Lshoff/off
G
G-ratio
1.0
0.9
0.8
0.7
0.6
0.5
0.0625
0.25
1
4
16
Axon area (µm²)
Lsh+/off
Lshoff/off
H
G-ratio
1.0
0.9
0.8
0.7
0.6
0.5
0.0625
0.25
1
4
16
Axon area (µm²)
Lsh+/off
Lshoff/off

4.3 *Lsh*$^{off/off}$ mice have an oligodendrocyte differentiation defect

The experiments outlined above point to a cellular defect specific to the CNS rather than the production of myelin in general, that is not fully penetrate across all cells in a lineage, varies according to anatomical location, as well as varying greatly between animals. Large axons are still capable of stimulating OLs to myelinate, but even when they do, this is to a lesser extent than *Lsh*$^{+/off}$. The extent to which OLs myelinate axons often increases with maturity (Flores et al. 2008), indicating that those that can myelinate in *Lsh*$^{off/off}$ are still earlier in the differentiation process than *Lsh*$^{+/off}$. Because of this and LSH's previously characterised role in developmental gene regulation (Myant et al. 2011), I hypothesised that LSH is required to enhance OL differentiation, possibly from neural precursor cell (NPC) stage in the embryo and/or OPC stage postnatally. As LSH is canonically associated with the deposition of DNA methylation and a repressive chromatin environment (Muegge 2005), one possibility would be a failure to repress genes that inhibit progression through the OL lineage. Connections have also been made between LSH and the survival of NPCs in *in vitro* differentiation assays in another knock-out of the protein ((Han et al. 2017) and there is a decreased ability for cells to proliferate with a *Lsh* hypomorph mutation (Sun et al. 2004). Despite the fact we see near normal, or increased axon density in *Lsh*$^{off/off}$, it remains possible that OLs, or other glial cells are affected by such a phenotype and either die or fail to proliferate and properly distribute throughout the CNS, causing the myelination defect. To distinguish between these possibilities, I set out to characterise the distribution and lineage progression of OLs throughout development. As the OL lineage has been extensively characterised in mouse, with distinct marker genes existing for different lineage stages (Fig.1.1) I decided to interrogate this lineage stage specific gene expression in *Lsh*$^{off/of}$ at the RNA and protein level.

4.3.1 At post-natal day 14 there is a reduction of mature oligodendrocytes in the *Lsh*$^{off/off}$ optic nerve and an increase in oligodendrocyte precursor cell marker expressing cells

Post-natal day 14 (P14) is a peak of developmental OL differentiation in mouse (Foran and Peterson 1992). As the lack of myelination in *Lsh*$^{off/off}$ is present throughout adulthood, I reasoned that if LSH indeed was required for the majority of OL differentiation during development, I would expect to see a decrease in lineage specific markers associate with differentiation at this timepoint. I also decided to look initially in optic nerve as it's a pure white matter tract in the brain and so avoids complications that may arise from differences between white and grey matter OLs and previous experiments show it is hypomyelinated in *Lsh*$^{off/off}$. Due to large size differences between *Lsh*$^{off/off}$ and *Lsh*$^{+/off}$ optic nerves, I reasoned that the best way to assess the relative abundance of different lineage stages would be to count relative to the number of DAPI positive nuclei, as appose to area. Despite their decrease in optic nerve size, *Lsh*$^{off/off}$ animals retain a similar number of cells in optic nerve sections (Fig.4.3A, B). Staining of P14 optic nerve for the TF OLIG2, which is ubiquitously expressed throughout the OL lineage, reveals that *Lsh*$^{off/off}$ mice have a similar number of OL cells in the CNS (Fig.4.3A, C). Co-staining with QKI7 an RNA-binding protein specific for mOLs when present with OLIG2, reveals however that there is a decrease in the number of mOLs in *Lsh*$^{off/off}$ (Fig.4.3A, D).

It's possible that a similar number of OL lineage cells, but decrease in those expressing mature markers, is the result of OL lineage cells being unable to upregulate a specific mature marker, while normally expressing others. Therefor to investigate if this truly was a reduction in differentiated OLs, I performed similar staining, but using NG2, a marker or OPCs when co-staining with OLIG2. If OL lineage cells were unable to progress beyond the OPC stage of differentiation, I would expect to see an equivalent increase in NG2 positive cells to the decrease in QKI7 OLIG2 positive cells seen previously. Although there was a

statistically significant increase in NG2 OLIG2 cells of 30% in *Lsh*$^{off/off}$ this is lower in magnitude than the >40% decrease in OLIG2 QKI7 positive cells, in addition, the percentage of OLIG2 NG2 is lower than that of OLIG2 QKI7 in both genotypes (Fig. 4.3E, F). This result suggests that some OPCs are capable of downregulating OPC markers during development, but the proportion capable of progressing to the next stage in the lineage is reduced the closer they get to terminal differentiation to myelinating OLs. To investigate if this was in fact the case, I performed qPCR on reverse transcribed optic nerve mRNA from P14 optic nerves. The pattern of mRNA expression for OL differentiation genes differs somewhat from protein expression (Fig.4.3G). *Lsh*$^{off/off}$ optic nerves show a robust under expression of mature stage differentiation markers, consistent with immunofluorescence experiments, however OPC markers are not all consistently over expressed (Fig. 4.3H). This supports the idea that most OL lineage cells can repress OPC genes during differentiation in *Lsh*$^{off/off}$ and the problem lies largely with failure to upregulate genes involved in myelination and differentiation.

Figure 4-3 There is a reduction in mature oligodendrocytes and increase in OPC numbers in *Lsh*$^{off/off}$ P14 optic nerve

A) Representative images of DAPI, OLIG2 and QKI7 staining of *Lsh*$^{+/off}$ and *Lsh*$^{off/off}$ P14 optic nerve.
B) Average number of cells in section imaged between genotypes.
C) Percentage of DAPI positive cells also staining for OLIG2 between genotypes
D) Percentage of DAPI positive cells also staining for OLIG2 and QKI7 between genotypes
E) Representative images of DAPI, OLIG2 and NG2 staining of *Lsh*$^{+/off}$ and *Lsh*$^{off/off}$ P14 optic nerve.
F) Percentage of DAPI positive cells also staining for OLIG2 and QKI7 between genotypes
G) Schematic of gene expression in oligodendrocyte lineage progression
H) qPCR of P14 optic nerve cDNA for myelin associated genes.

Error bars on all samples represent standard deviation, unpaired t-tests using Welch's correction were used for p-value calculation. *=P<0.05, **=P<0.005. n=3 animals/genotypes for A-F with 4 sections counted per animal (>500 cells). See materials and methods for qPCR replicate strategy.

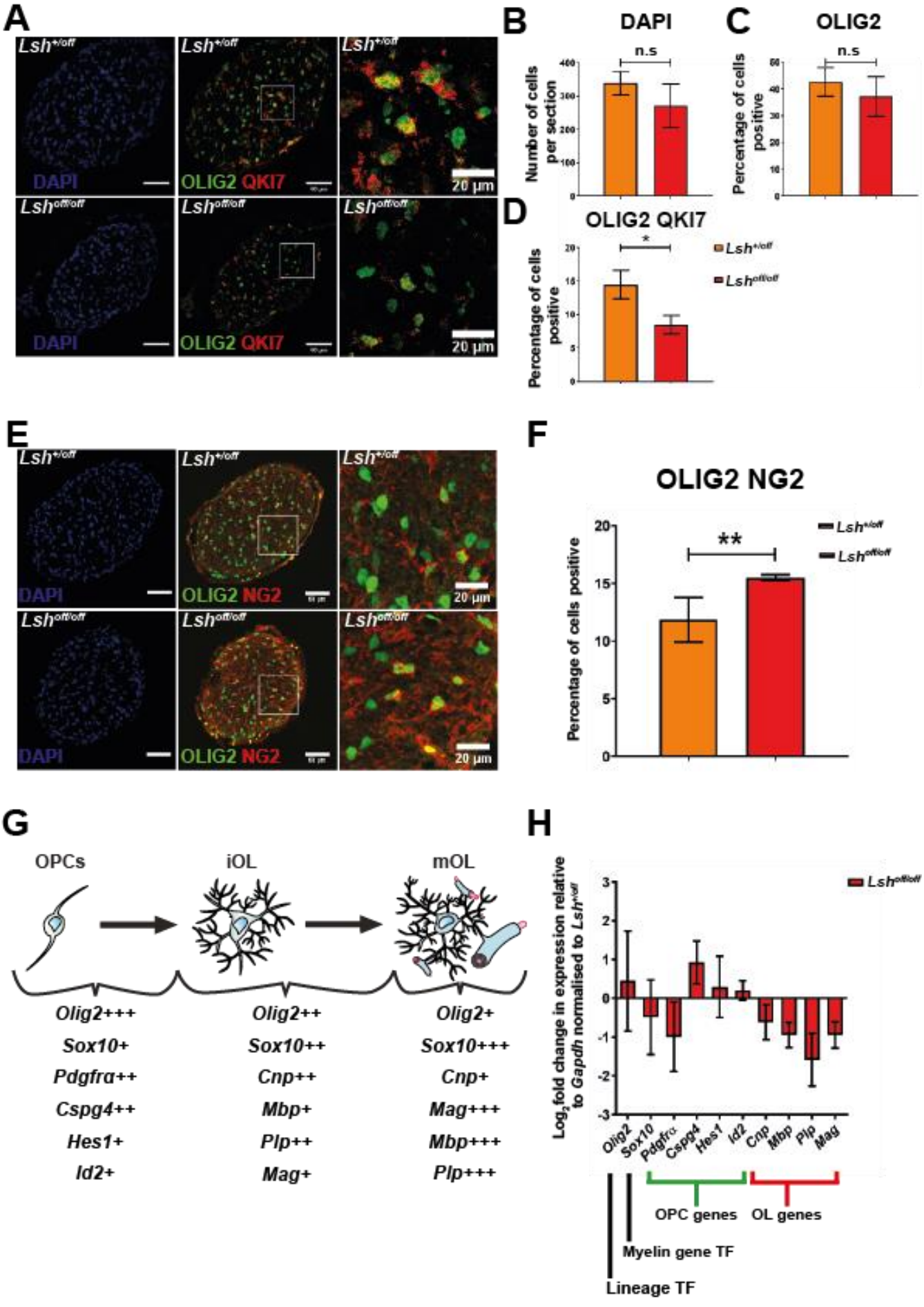
A
Lsh+/off
Lsh+/off
Lsh+/off
DAPI
OLIG2 QKI7
20 µm
Lsh off/off
Lsh off/off
Lsh off/off
DAPI
OLIG2 QKI7
20 µm
B
DAPI
n.s
Number of cells per section
C
OLIG2
n.s
Percentage of cells positive
D
OLIG2 QKI7
*
Percentage of cells positive
Lsh+/off
Lsh off/off
E
Lsh+/off
Lsh+/off
Lsh+/off
DAPI
OLIG2 NG2
20 µm
Lsh off/off
Lsh off/off
Lsh off/off
DAPI
OLIG2 NG2
20 µm
F
OLIG2 NG2
**
Percentage of cells positive
Lsh+/off
Lsh off/off
G
OPCs
iOL
mOL
Olig2+++
Sox10+
Pdgfrα++
Cspg4++
Hes1+
Id2+
Olig2++
Sox10++
Cnp++
Mbp+
Plp++
Mag+
Olig2+
Sox10+++
Cnp+
Mag+++
Mbp+++
Plp+++
H
Log2 fold change in expression relative to Gapdh normalised to Lsh+/off
Lsh off/off
Olig2
Sox10
Pdgfrα
Cspg4
Hes1
Id2
Cnp
Mbp
Plp
Mag
OPC genes
OL genes
Myelin gene TF
Lineage TF

4.3.2 The differentiation defect seen at P14 in *Lsh*$^{off/off}$ persists and is exacerbated at P90.

At the P90 stage we see extensive hypomyelination of the CNS, however it is still possible that the differentiation defect seen at P14 is the result in a delay of OL differentiation, that could correct itself later in development. In this case, the cause of the myelin phenotype would be separate from the ability to regulate gene expression during differentiation e.g. once differentiated OLs are still unable to wrap axons. To test if this was the case, I performed similar cell marker comparisons between genotypes at P90 as to at P14. Total cell numbers and OLIG2 positive cell percentage at P90 are again similar between genotypes (Fig.4.4A, B,C). The reduction in OLIG2 QKI7 double positive cells is exacerbated on aging to P90 (Fig.4.4A, D). NG2 OLIG2 at P90 staining however reveals a larger increase in NG2 OLIG2 positive cells in *Lsh*$^{off/off}$ than at P14, but still proportionally smaller than the decrease in OLIG2 QKI7 positive cells (Fig.4.4E, F). qPCR of reverse transcribed P90 mRNA is also consistent with immunofluorescence and P14 experiments (Fig4.4G). Taken together, this data shows that the failure to upregulate myelination and differentiation genes is persistent throughout development.

Figure 4-4 There is a reduction in mature oligodendrocytes and increase in OPC numbers in the P90 *Lsh*$^{off/off}$ optic nerve

A) Representative images of DAPI, OLIG2 and QKI7 staining of *Lsh*$^{+/off}$ and *Lsh*$^{off/off}$ P90 optic nerve.
B) Average number of cells in section imaged between genotypes.
C) Percentage of DAPI positive cells also staining for OLIG2 between genotypes
D) Percentage of DAPI positive cells also staining for OLIG2 and QKI7 between genotypes
E) Representative images of DAPI, OLIG2 and NG2 staining of *Lsh*$^{+/off}$ and *Lsh*$^{off/off}$ P90 optic nerve.
F) Percentage of DAPI positive cells also staining for OLIG2 and QKI7 between genotypes
G) qPCR of P90 optic nerve cDNA for myelin associated genes.
Error bars on all samples represent standard deviation, unpaired t-tests using Welch's correction were used for p-value calculation. *=P<0.05, **=P<0.005, ***=P<0.0005. n=3 animals/genotype for A-F with 4 sections counted per animal (>500 cells). See materials and methods for qPCR replicate strategy.

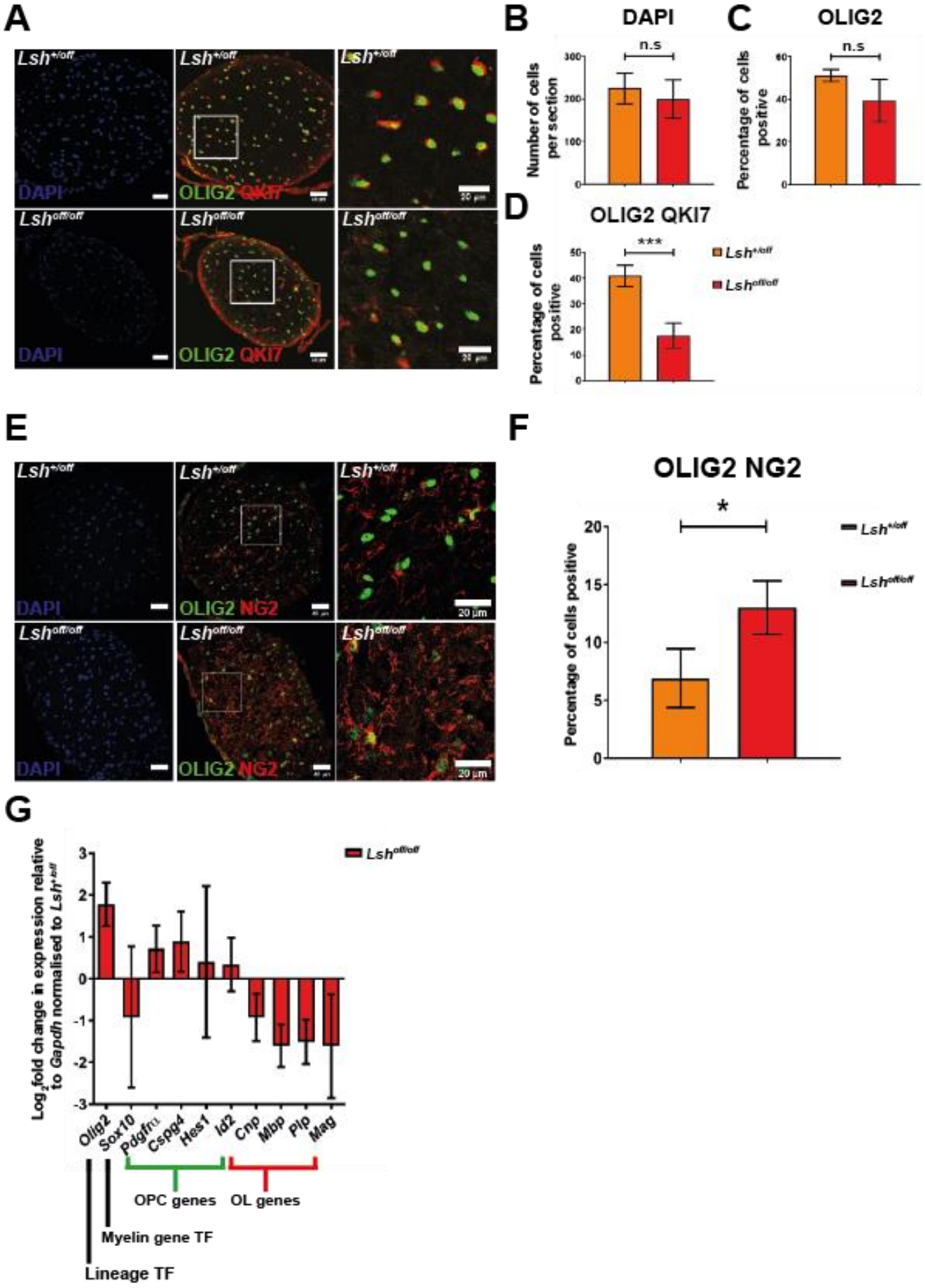
A
Lsh+/off
Lshoff/off
DAPI
OLIG2 QKI7
20 µm
B
DAPI
n.s
Number of cells per section
C
OLIG2
n.s
Percentage of cells positive
D
OLIG2 QKI7
***
Lsh+/off
Lshoff/off
Percentage of cells positive
E
DAPI
OLIG2 NG2
20 µm
F
OLIG2 NG2
*
Lsh+/off
Lshoff/off
Percentage of cells positive
G
Lshoff/off
Log2 fold change in expression relative to Gapdh normalised to Lsh+/off
Olig2
Sox10
Pdgfrα
Cspg4
Hes1
Id2
Cnp
Mbp
Plp
Mag
OPC genes
OL genes
Myelin gene TF
Lineage TF

4.3.3 Spinal cord oligodendrocytes progress further in differentiation than optic nerve, but still fail to terminally differentiate to myelinating oligodendrocytes

As a less severe defect was seen in percentage myelinated axons in P90 spinal cord compared to optic nerve, I hypothesised that *Lsh*$^{off/off}$ spinal cord OLs would be able to progress, on average, to a later stage of differentiation than those in optic nerve. To test this, I performed OLIG2 and QKI7 staining in spinal cord of P90 *Lsh*$^{+/off}$ and *Lsh*$^{off/off}$ animals. Cell numbers and OLIG2 positive cell percentage again remain similar between genotypes (Fig4.5A, B, C) but strikingly, the percentage of OLIG2 QKI7 positive cells, largely due to 1 animal, showed a tendency to increase in *Lsh*$^{off/off}$ (Fig.4.5A, D). As newly formed OLs express QKI7 higher than long matured OLs (Y. Chen et al. 2007), it's possible this is the result of *Lsh*$^{off/off}$ spinal cord being in a still earlier stage of OL differentiation than *Lsh*$^{+/off}$ however still able to progress beyond the stage optic nerve OL lineage cells can. As the counts for the immunofluorescence was highly variable in the animals stained, I performed qPCR on reverse transcribed mRNA from spinal cord white matter from *Lsh*$^{+/off}$ and *Lsh*$^{off/off}$ to see if expression marker genes in mRNA were consistent with the protein data. Under expression of only *Mag* was detectable with other late stage marker genes unchanged (Fig4.5E). *Olig2* is also the only gene expressed higher in OPCs that as overexpressed, as it is in P90 optic nerve. This is consistent with the idea that a less severe OL defect exists in the spinal cord than optic nerve of *Lsh*$^{off/off}$, in concordance with the TEM data looking at myelin.

Figure 4-5 There is no reduction in mature oligodendrocytes in the P90 *Lsh*$^{off/off}$ spinal cord, though some gene expression changes are present at the mRNA level

A) Representative images of DAPI, OLIG2 and QKI7 staining of *Lsh*$^{+/off}$ and *Lsh*$^{off/off}$ P90 spinal cord.
B) Average number of cells in section imaged between genotypes.
C) Percentage of DAPI positive cells also staining for OLIG2 between genotypes
D) Percentage of DAPI positive cells also staining for OLIG2 and QKI7 between genotypes
E) qPCR of P90 spinal cord cDNA for myelin associated genes.
Error bars on all samples represent standard deviation, unpaired t-tests using Welch's correction were used for p-value calculation. *=P<0.05, **=P<0.005, ***=P<0.0005. n=3 animals/genotypes for A-D with 1 section counted per animal (>1000 cells). See materials and methods for qPCR replicate strategy.

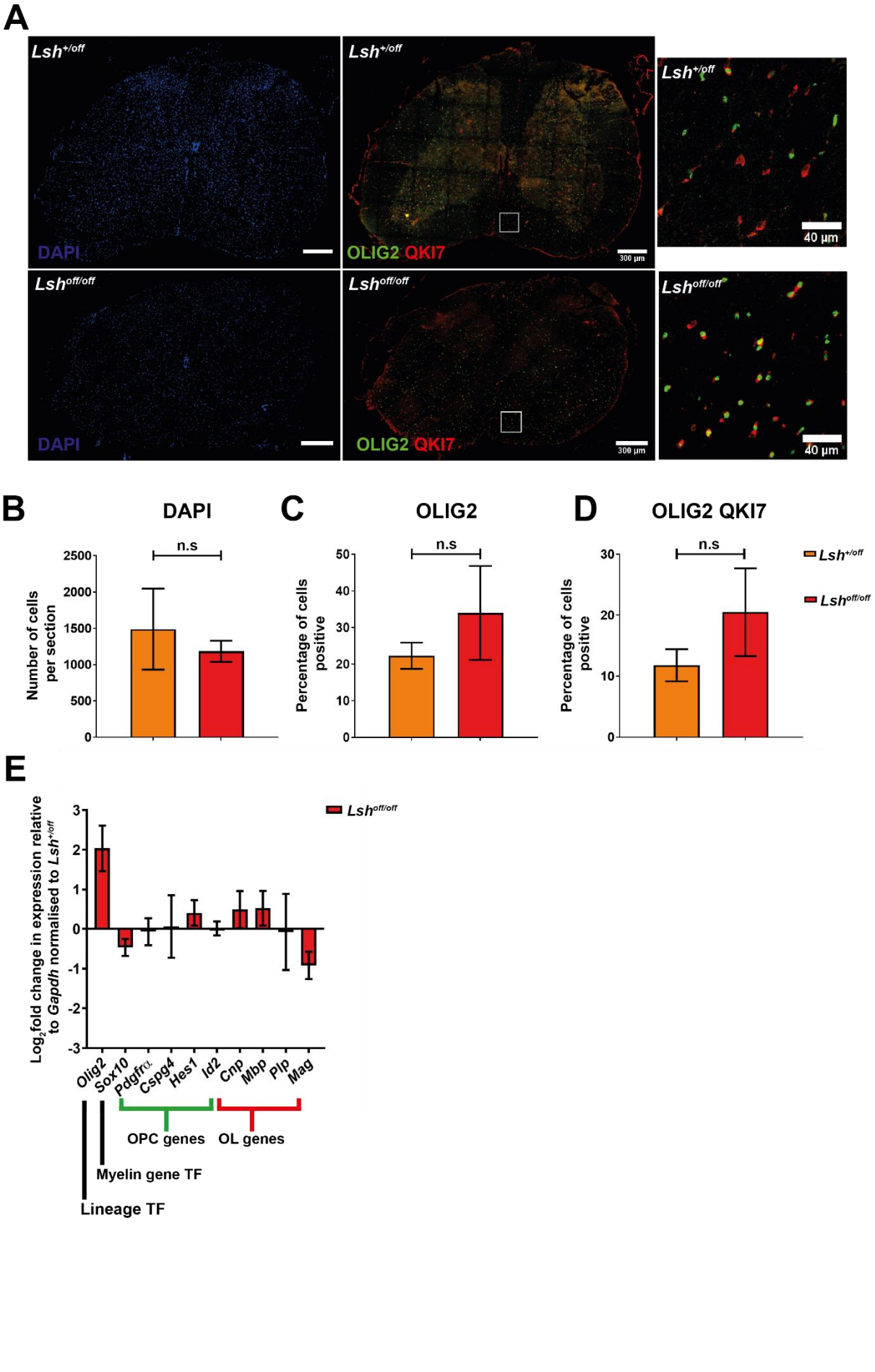
A
Lsh+/off
DAPI
OLIG2 QKI7
300 µm
40 µm
Lshoff/off
B
DAPI
n.s
Number of cells per section
C
OLIG2
Percentage of cells positive
D
OLIG2 QKI7
Lsh+/off
Lshoff/off
E
Log2fold change in expression relative to Gapdh normalised to Lsh+/off
Olig2
Sox10
Pdgfrα
Cspg4
Hes1
Id2
Cnp
Mbp
Plp
Mag
OPC genes
OL genes
Myelin gene TF
Lineage TF

4.4 Summary

TEM confirms the hypothesis based on mouse phenotype and tissue observations that *Lsh*$^{off/off}$ CNS is exclusively hypomyelinated. This hypomyelination is present throughout all axon calibres in the CNS, though increased frequency and thickness of myelination suggests ability to respond to axonal signalling is intact in *Lsh*$^{off/off}$. Marker gene expression analysis shows a robust reduction of mOLs in optic nerve throughout development, accompanied by a more modest increase in OPCs. This points to LSH deficiency causing an OL differentiation defect, but it remains unclear whether this is the result of extrinsic factors or is intrinsic to OPC gene regulation. To address this question and aim 2) of the project, I will exploit the conditionally reversible LSH system to see if LSH is required in OPCs and when in development its expression is essential.

Results- Chapter Five- The *Lsh*$^{off/off}$ myelination defect is cell autonomous to OPCs in the CNS, and LSH expression is only required early in life

5.1 Introduction

TEM analysis of myelin structure and marker gene expression profiling support that the myelin phenotype is indeed caused by a defect in OL differentiation. Myelin is reduced in all CNS tissues and developmental timepoints analysed A similar number of OLIG2 positive cells being present in *Lsh*$^{off/off}$ tissue to *Lsh*$^{+/off}$ suggests that this defect occurs in the OPC to mOL transition. OPC markers are upregulated and mOL (markers are reduced in all tissues and developmental timepoints analysed, albeit inconsistently in certain marker genes. The lesser extent and consistency of OPC marker gene over-expression compared to mature markers suggests the stage at which the majority *Lsh*$^{off/off}$ OL lineage cells arrest is intermediate between OPC and myelinating cells. Inhibitors of differentiation such as *Id2* and *Hes1* show no change in *Lsh*$^{off/off}$, suggesting the initial hypothesis of failure to silence these factors in *Lsh*$^{off/off}$ being the cause of the phenotype is not the case. It is possible that this differentiation defect is the result of abolition LSH expression within OL lineage cells preventing proper regulation of crucial genes to lineage progression. However, greater severity of the phenotype in optic compared to spinal cord could also be evidence that tissue specific environment can overcome the differentiation block to an extent. An alternative explanation is intrinsic differences in spinal cord and optic nerve OLs, which has been studied extensively (Richardson et al. 2006), lead to differing requirements for differentiation, and that LSH is more essential for the implementation of the optic nerve OPC requirements than spinal cord. To test if the *Lsh*$^{off/off}$ phenotype is indeed cell autonomous to the OL lineage, I decided to exploit the conditionally reversable nature of the *Lsh*^{off} allele and

characterise a mouse strain where *Lsh*$^{off/off}$ was converted to *Lsh*$^{on/on}$ specifically in OLs by breeding into a line where CRE recombinase is expressed under the control of a *Pdgrα* promoter, which is expressed exclusively in OPCs in the CNS (Sim et al. 2011).

5.2 Conversion to *Lsh*$^{on/on}$ in OPCs rescues the *Lsh*$^{off/off}$ myelination phenotype

5.2.1 *Lsh*$^{off/off}$*; Pdgfrα-Cre* animals do not develop ataxia or tremors in adulthood

The loxP and lox411 sites of the *Lsh*^{off} allele are orientated such that CRE expression and nuclear localisation causes an inversion of the SAGFPneoPA cassette. The splice acceptor can then no longer be recognised and full-length protein LSH is produced (Fig.5.1A). FLPo mediated conversion and expression rescue is shown in Fig.1.2 and ER-CRE mediated rescue of expression on tamoxifen treatment (experiment performed by Natalia Torrea). To see if this Cre mediated conversion of the *Lsh*^{off} allele in PDGFRα expressing cells caused any detectable change in embryonic lethality compared to *Lsh*$^{off/off}$ I analysed the litter sizes from crosses of *Lsh*$^{+/off}$*; Pdgfrα-Cre* × *Lsh*$^{+/off}$*.* Litters of comparable size to *Lsh*$^{+/off}$ × *Lsh*$^{+/off}$ and *Lsh*$^{+/off}$ × *Lsh*$^{+/+}$ are produced (Fig.5.1B). If the cellular defect responsible for the low levels of perinatal lethality seen in our *Lsh*^{off} line is within PDGFRα expressing cells, I would expect to see an over representation of *Lsh*$^{off/off}$; *Pdgfrα-Cre* animals resulting from *Lsh*$^{+/off}$*;Pdgfrα-Cre* × *Lsh*$^{+/off}$ crosses, and a reduced proportion of animals making it to weaning. There is no the significant decrease in proportion of mice weaned seen in *Lsh*$^{+/off}$ × *Lsh*$^{+/+}$ in *Lsh*$^{+/off}$*;Pdgfrα-Cre* × *Lsh*$^{+/off}$ showing there is not a detectable increase in embryonic lethality (Fig. 5.1C). The proportion weaned is also not significantly different from *Lsh*$^{+/off}$ × *Lsh*$^{+/off}$, which does show reduced size compared to *Lsh*$^{+/off}$ × *Lsh*$^{+/+}$, suggesting there may be a small intermediate perinatal lethality phenotype in the *Lsh*$^{off/off}$*;Pdgfrα-Cre* line. However, as shown in chapter 3 genetic background can impact this phenotype in *Lsh*^{off} lines and it should be noted that the lack of detectable lethality may be due to the fewer number of litters analysed (n=120 vs n=43 respectively). The mendelian ratio of genotypes

produced also does not differ significantly from those expected by chance in *Lsh*$^{+/off}$*;Pdgfrα-Cre* × *Lsh*$^{+/off}$ crosses as it does in *Lsh*$^{+/off}$ × *Lsh*$^{+/off}$*,* again reduced n-number may render a difference undetectable. An important observation however is that *Lsh*$^{off/off}$*; Pdgfrα-Cre* is not enriched in litters above that of *Lsh*$^{off/off}$ and if anything is decreased (Fig. 5.1D). This indicates that conversion to *Lsh*$^{on/on}$ in OPCs in the CNS and other cells outside of the CNS does not rescue the perinatal lethality associated with *Lsh*$^{off/off}$. I next decided to test if the post-weaning growth defect seen in *Lsh*$^{off/off}$ is rescuable in *Lsh*$^{off/off}$*; Pdgfrα-Cre*. Though the phenotype is which is less apparent in this genetic background, indicated by a less drastic difference between *Lsh*$^{off/off}$ animals and *Lsh*$^{+/off}$ litter mates seen in both males and females that in the *Lsh*^{off} line not possessing *Pdgfrα-Cre*, there is a tendency for reduced weight compared to *Lsh*$^{+/off}$*;Pdgfrα-Cre* that is not completely rescued in *Lsh*$^{off/off}$ (Fig. 5.1E, F). If a lack of LSH specifically in OL lineage cells is responsible for the developmental lack of myelin in the *Lsh*$^{off/off}$ CNS, and this in turn is responsible for neurological phenotype in *Lsh*$^{off/off}$ mice, I would expect rescue of the phenotype in *Lsh*$^{off/off}$*; Pdgfrα-Cre*. To test this I analysed blind scoring of littermate matched *Lsh*$^{off/off}$*;Pdgfrα-Cre, Lsh*$^{off/off}$ and *Lsh*$^{+/off}$*;Pdgfrα-Cre* (control) animals. *Lsh*$^{off/off}$*; Pdgfrα-Cre* do not possess a comparable neurological phenotype to *Lsh*$^{off/off}$ post weaning, though some animals scored for mild ataxia immediately following weaning (Fig.5.1G) (Appendix video 5).

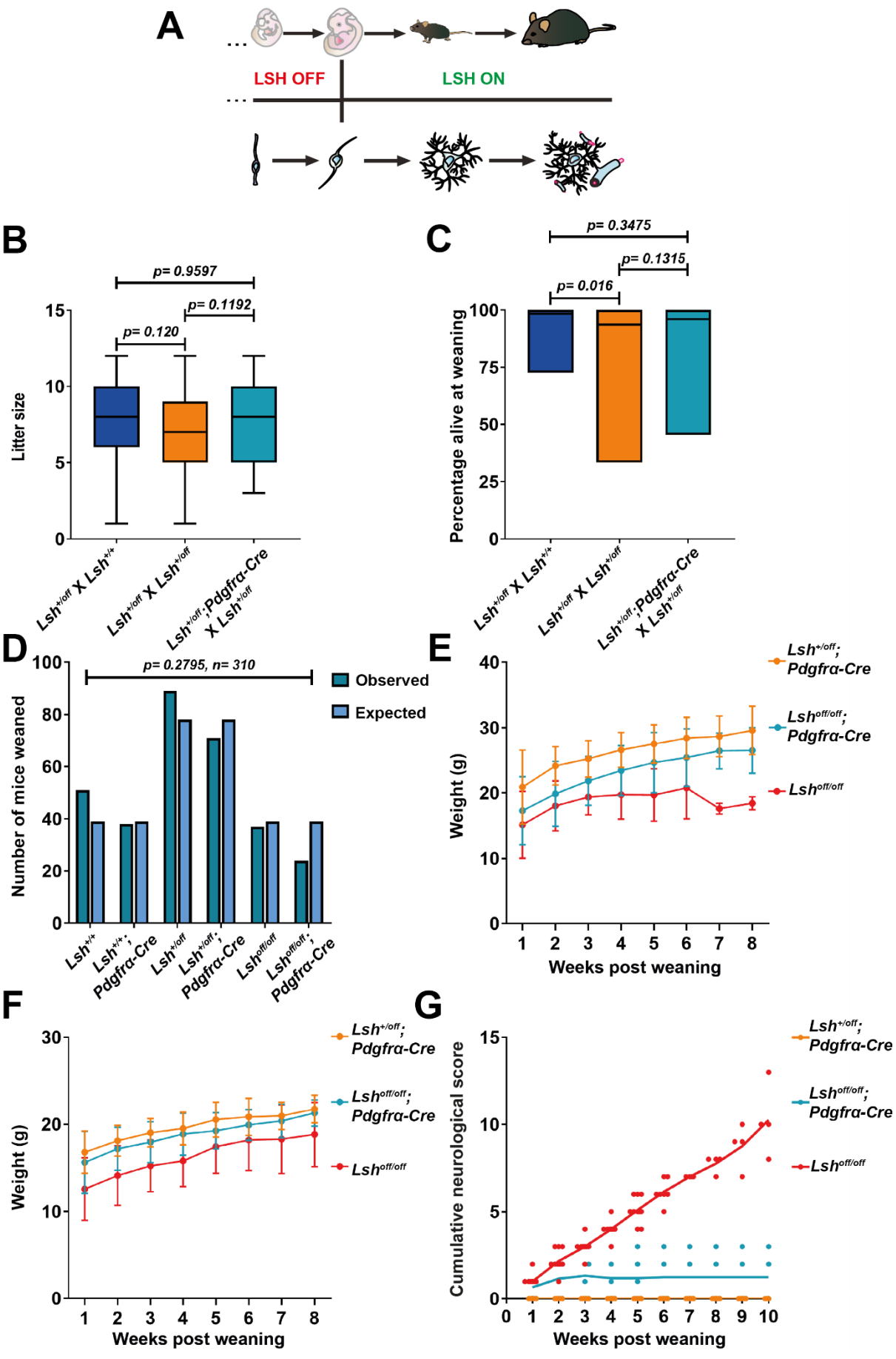
A
LSH OFF
LSH ON
B
p= 0.9597
p= 0.1192
p= 0.120
Litter size
Lsh+/off X Lsh+/+
Lsh+/off X Lsh+/off
Lsh+/off;Pdgfrα-Cre X Lsh+/off
C
p= 0.3475
p= 0.1315
p= 0.016
Percentage alive at weaning
D
p= 0.2795, n= 310
Observed
Expected
Number of mice weaned
Lsh+/+
Lsh+/+; Pdgfrα-Cre
Lsh+/off
Lsh+/off; Pdgfrα-Cre
Lsh off/off
Lsh off/off; Pdgfrα-Cre
E
Lsh+/off; Pdgfrα-Cre
Lsh off/off; Pdgfrα-Cre
Lsh off/off
Weight (g)
Weeks post weaning
F
Lsh+/off; Pdgfrα-Cre
Lsh off/off; Pdgfrα-Cre
Lsh off/off
Weight (g)
Weeks post weaning
G
Lsh+/off; Pdgfrα-Cre
Lsh off/off; Pdgfrα-Cre
Lsh off/off
Cumulative neurological score
Weeks post weaning

Figure 5-1 Cre mediated conversion to *Lsh^{on}* in the oligodendrocyte lineage rescues neurological phenotypes of *Lsh$^{off/off}$*

A) Schematic representation of the timing of *Lsh* allele conversion in the *Pdgfrα-Cre* line (off to on)
B) Boxplots showing litter sizes from *Lsh^{off}* and *Lsh^{off}; Pdgfrα-Cre* crosses. P-values result on unpaired t-test comparisons of conditions. Whiskers representative of upper and lower quartiles, n=39, 120 and 43 respectively.
C) Boxplots showing percentages of mice born in *Lsh^{on}* and *Lsh^{off}; Pdgfrα-Cre* crosses. P-values the result of Mann-Whitney non-parametric tests due to non-normal distribution present in samples. Bounds of boxes represent minimum and maximum values, n numbers as with (B).
D) Observed and expected rations of mice born from *Lsh$^{+/off}$; Pdgfrα-Cre* × *Lsh$^{+/off}$* crosses.P-values on graph the result of Chi-squared test comparing expected vs observed numbers.
E) Line graph of mean weights post-weaning for males of *Lsh$^{+/off}$; Pdgfrα-Cre, Lsh$^{off/off}$; Pdgfrα-Cre* and *Lsh$^{of/offf}$* genotypes. Error bars show standard deviation, maximum n numbers=10, 12, and 7 respectively, though this varies between timepoints due to culling and deaths.
F) Line graph of mean weights post-weaning for females of *Lsh$^{+/off}$; Pdgfrα-Cre, Lsh$^{off/off}$; Pdgfrα-Cre* genotypes. Error bars show standard deviation, maximum n numbers=22, 15, and 17 respectively though this varies between timepoints for the first 2 genotypes due to culling and deaths.
G) Scatter plot of neurological score for *Lsh$^{+/off}$; Pdgfrα-Cre, Lsh$^{off/off}$; Pdgfrα-Cre* genotypes, maximum n=32, 27 and 24 respectively though this varies between timepoints for the first 3 genotypes due to culling for use in other experiments and death.

5.2.2 *Lsh$^{off/off}$;Pdgfrα-Cre* leads to conversion from *Lsh^{off}* to *Lsh^{on}* specifically in oligodendrocyte lineage cells. OPCs derived from *Lsh$^{off/off}$* animals however cannot be cultured using standard conditions

To support the conclusion of the neurological phenotype analysis that OL lineage specific rescue of LSH expression from the OPC stage in development rescues the myelin phenotype, I sought to verify that conversion from the *Lsh^{off}* to *Lsh^{on}* was occurring in OPCs specifically in *Lsh$^{off/off}$;Pdgfrα-Cre*. To do this, I isolated OPCs from P7 mouse brain using a well-established adaptation of an immunopanning protocol. To verify that this protocol does indeed lead to a separation of specifically OPCs, and to investigate the purity of this population, I performed immunostaining on the OPC fraction of this isolation plated onto coverslips for *Lsh$^{+/+}$* animals. This revealed that 88% ± 2% of cells isolated were positive for the OPC specific marker NG2 (Fig.5.2A), with the remaining cells looking from DAPI staining as if they were dead. Isolation of gDNA from the OPC, whole brain homogenate and the OPC depleted fraction in this protocol (what remains following positive selection) in *Lsh$^{off/off}$;Pdgfrα-Cre* followed by allele specific PCR amplification (Fig.5.2B) reveals conversion to *Lsh^{on}* specifically in OPCs (Fig.5.2C).

The gold standard for evidence that the differentiation defect is autonomous to OL lineage cells would be to remove OPCs from their *in vivo* environment and test the ability for *Lsh*$^{off/off}$ cells to differentiate. To attempt this, I isolated cells from *Lsh*$^{+/off}$ and *Lsh*$^{off/off}$ and attempted to expand them under well-established culture conditions(Emery and Dugas 2013). It was quickly apparent, on multiple attempts, *Lsh*$^{off/off}$ OPCs could not survive in culture long enough for analysis of differentiation (Fig.5.2D). This provides evidence that the *in vivo* environment of *Lsh*$^{off/off}$ OPCs confers a greater compacity to support OPCs than that *in vitro*. It is also possible that the growth factors supplemented to OPCs in culture force *Lsh*$^{off/off}$ to divide more than they have an ability to do so, and thus leads to cell death. However, as this doesn't seem to be the case *in vivo*, due to the similar number of OLIG2 positive cells observed between genotypes, rather than speculate further I focused efforts n characterisation of the *in vivo* phenotype of *Lsh*$^{off/off}$*;Pdgfrα-Cre.*

Figure 5-2 *Lsh*$^{off/off}$*;Pdgfrα-Cre* leads to specific conversion to *Lsh*$^{on/on}$ in OPCs

A) Representative image of DAPI and NG2 staining in isolated OPCs, n=3 isolations using different animals.
B) Schematic explaining expected PCR products from different SAGFPneoPA cassette orientation in *Lsh*^{GFPneo} animals.
C) Image of agarose gel running allele specific PCR products across OPC isolation fractions in rescue and control genotypes.
D) Representative light microscopy images of *Lsh*$^{off/off}$ OPC failure to proliferate under standard culture conditions.

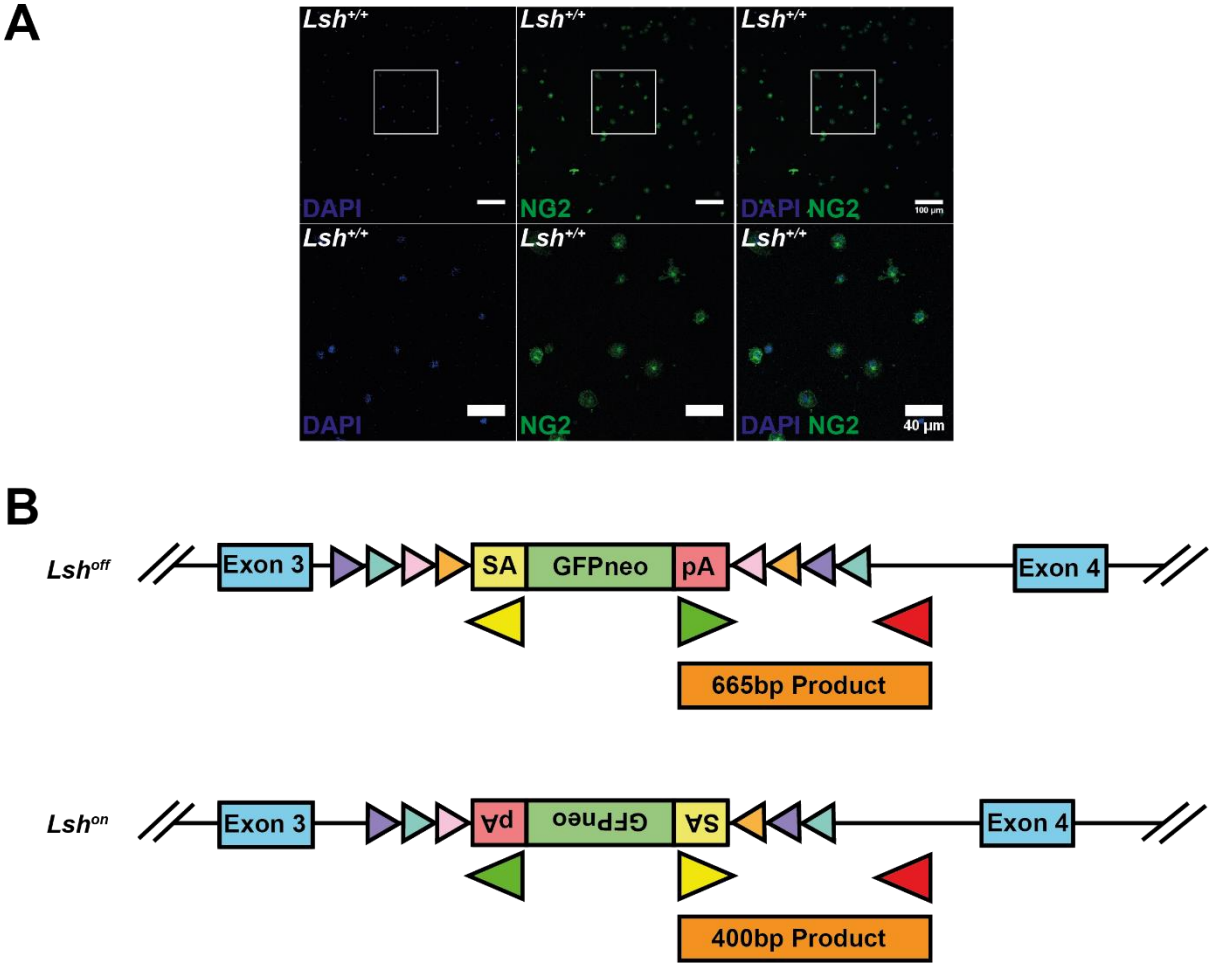
A
Lsh+/+
DAPI
NG2
DAPI NG2
100 µm
40 µm
B
Lshoff
Exon 3
SA
GFPneo
pA
Exon 4
665bp Product
Lshon
400bp Product
C
Lshoff/off
Lshoff/off; Pdgfra-Cre
Whole brain
Not selected
OPC fraction
Lshoff PCR
Lshon PCR
D
Lsh+/off D2
Lsh+/off D7
Lshoff/off D2
Lshoff/off D7
20 µm

5.2.3 Adult *Lsh$^{off/off}$; Pdgfrα-Cre* animals are myelinated grossly normally and do not have an oligodendrocyte differentiation defect

To see if and to what extent OL lineage specific rescue of LSH expression rescues the myelination in *Lsh$^{off/off}$* I performed TEM on axons from the most severely affected tissue in *Lsh$^{off/off}$,* optic nerve. It was immediately apparent that *Lsh$^{off/off}$;Pdgfrα-Cre* possessed no apparent myelin phenotype whereas *Lsh$^{off/off}$* littermates were severely hypomyelinated (Fig.5.3A). This supports the conclusion of the neurological scoring analysis, that conversion to *Lsh^{on}* in the OL lineage rescues the myelin phenotype and the presumption that neurological phenotype was the result of lack of myelin. To see if rescue in myelination was accompanied by rescue of OL differentiation, I performed a similar analysis of stage specific OL lineage marker genes as I had done for *Lsh$^{off/off}$* animals in chapter 4. DAPI positive cells numbers in adult optic nerves taken at P90 to P120 were consistent between all genotypes (Fig. 5.3B, C). *Lsh$^{off/off}$;Pdgfrα-Cre* does show an increase in OLIG2 positive cells compared to other genotypes (Fig. 5.3B, D). OLIG2 and QKI7 staining shows a complete rescue in mOL numbers in *Lsh$^{off/off}$;Pdgfrα-Cre* to the level of *Lsh$^{+/off}$;Pdgfrα-Cre* controls and a reduction in *Lsh$^{off/off}$* littermate controls comparable to that seen in non-*Pdgfrα-Cre* possessing line (Fig5.3B, E). qPCR of OL stage specific marker genes also shows comparable levels of expression in *Lsh$^{off/off}$;Pdgfrα-Cre* to *Lsh$^{+/off}$;Pdgfrα-Cre*, with maybe a decrease in mOL genes, though to a smaller extent than in *Lsh$^{off/off}$* (Fig. 4.4) (Fig.5.3F). Taken together, these data rule out rescue being a consequence of breeding *Lsh^{off}* into a different genetic background. The rescue is also to an extent that wild-type-like numbers of mature of OLs were detectable, ruling out other CNS cell-types as exacerbating factors in the *Lsh$^{off/off}$* phenotype.

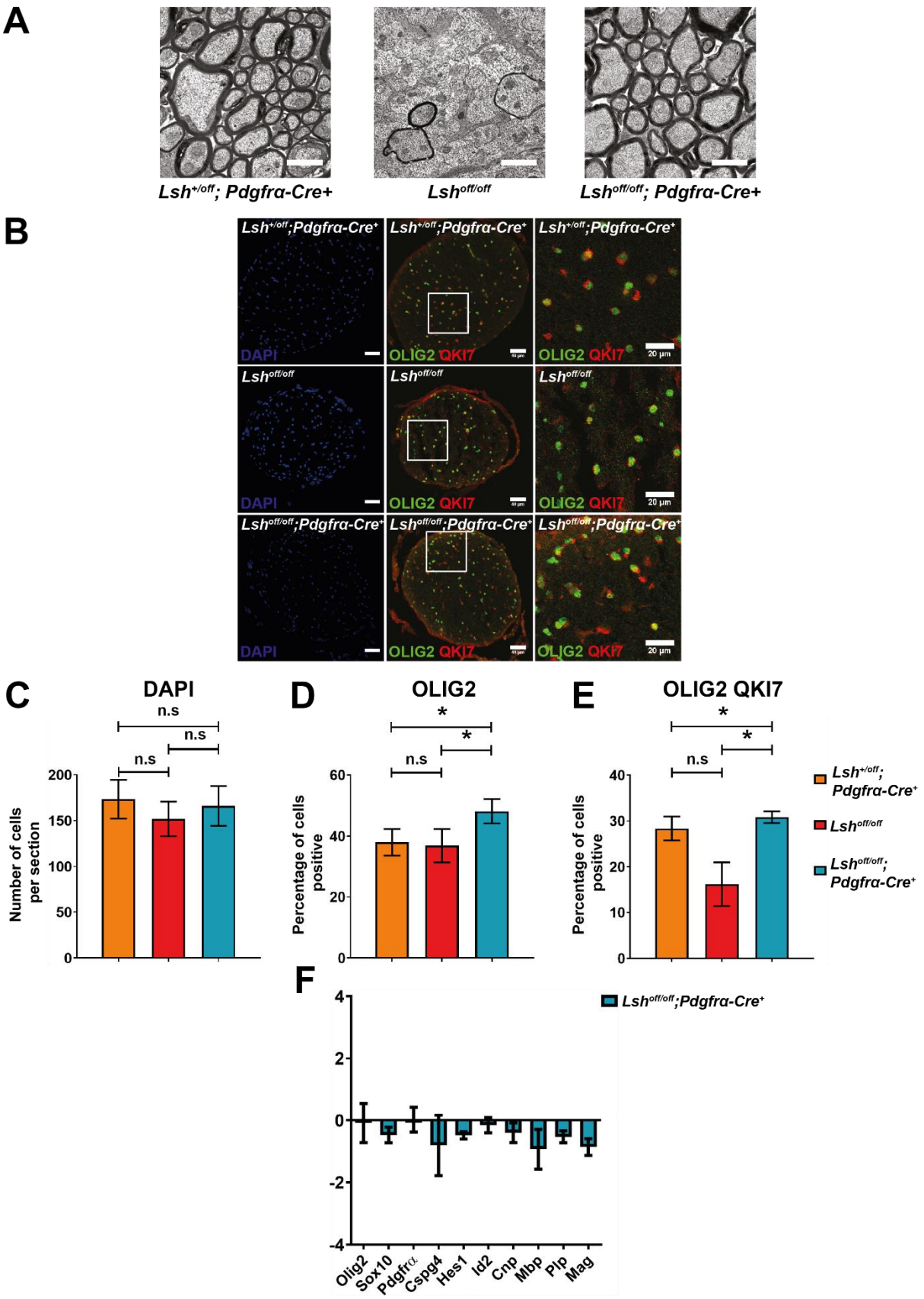
A
Lsh+/off; Pdgfrα-Cre+
Lshoff/off
Lshoff/off; Pdgfrα-Cre+
B
Lsh+/off;Pdgfrα-Cre+
Lshoff/off
Lshoff/off;Pdgfrα-Cre+
DAPI
OLIG2 QKI7
20 µm
C
DAPI
n.s
n.s
n.s
Number of cells per section
200
150
100
50
0
D
OLIG2
*
*
n.s
Percentage of cells positive
60
40
20
0
E
OLIG2 QKI7
*
*
n.s
Percentage of cells positive
40
30
20
10
0
Lsh+/off; Pdgfrα-Cre+
Lshoff/off
Lshoff/off; Pdgfrα-Cre+
F
Lshoff/off;Pdgfrα-Cre+
4
2
0
-2
-4
Olig2
Sox10
Pdgfrα
Cspg4
Hes1
Id2
Cnp
Mbp
Plp
Mag

Figure 5-3 Cre mediated conversion to *Lsh^{on}* in the oligodendrocyte lineage rescues the cellular phenotype of *Lsh$^{off/off}$*

A) Representative TEM images of myelin in P90 *Lsh$^{+/off}$;Pdgfrα-Cre*, *Lsh$^{off/off}$; Pdgfrα-Cre* and *Lsh$^{off/off}$* littermate optic nerves.
B) Representative images of DAPI, OLIG2 and QKI7 staining of *Lsh$^{+/off}$;Pdgfrα-Cre*, *Lsh$^{off/off}$; Pdgfrα-Cre* and *Lsh$^{off/off}$* P90 optic nerves.
C) Average number of cells in section imaged between genotypes.
D) Percentage of DAPI positive cells also staining for OLIG2 between genotypes.
E) Percentage of DAPI positive cells also staining for OLIG2 and QKI7 between genotypes.
F) qPCR of P90 optic nerve cDNA for myelin associated genes.
Error bars on all samples represent standard deviation, unpaired t-tests using Welch's correction were used for p-value calculation. *=P<0.05. n=3 animals/genotypes for A-F with 4 sections counted per animal (>500 cells). See materials and methods for qPCR replicate strategy.

5.3 Conversion to *Lsh$^{off/off}$* specifically in OPCs causes no neurological phenotype

The *Pdgfrα* driven CRE converts *Lsh^{off}* to *Lsh^{on}* in OPCs, which arise at E12.5 (Pringle and Richardson 1993) and the allele remains converted from then on in development. The possibilities that LSH is required prior to differentiation to mOL or during the differentiation, remain indistinguishable by the experiments performed so far. In order to distinguish between these possibilities, and further narrow down a cellular cause for the *Lsh$^{off/off}$* myelination phenotype, I again descended to exploit the conditionally reversible knock-out system. Crossing of *Lsh$^{on/on}$* animals where the *Lsh^{off}* allele was converted using the FLPo recombinase in previous generations, into the *Pdgfrα-Cre* possessing line, results in mice that specifically convert to *Lsh^{off2}* in OLs in the CNS. As the half-life of LSH protein in OPCs is unknown, some remaining LSH in the OL lineage cells of these animals can't be ruled out, but this would be further diluted in an individual cell through division following conversion

If LSH is required during differentiation from OPCs to mOLs therefor, I reasoned that these OPC conditional knock-out animals may still possess a myelination phenotype, albeit it milder than in *Lsh$^{off/off}$* due to the remaining LSH protein. In contrast if LSH was required exclusively early in development then I would expect *Lsh$^{on/on}$;Pdgfrα-Cre* animals would show no myelin phenotype. The *Lsh$^{off/off}$;Pdgfrα-Cre* experiment has suggested there are

also phenotypes that are not linked to OPC LSH expression, such as body weight, I would expect animals that are *Lsh*$^{on/on}$ in all tissue but OPCs not be subject to these. To address these possibilities and support the conclusions of the rescue experiment, I therefore set out to characterise phenotype of *Lsh*$^{on/on}$*;Pdgfrα-Cre* animals.

5.3.1 *Lsh*$^{on/on}$*; Pdgfrα-Cre* animals are born at a normal mendelian ratio and have no detectable phenotype

In *Lsh*$^{on/on}$*;Pdgfrα-Cre Lsh*^{on} is in theory converted to *Lsh*^{off} specifically in the OL lineage from E12.5 (Fig.5.5A). To test if this is the case at the genetic level, I performed an allele specific PCR on gDNA isolated from *Lsh*$^{on/on}$*;Pdgfrα-Cre* and *Lsh*$^{on/on}$ optic nerve, which are enriched for OL lineage cells and ear tissue, which also expresses PDGFRα in the majority of cells at some point during development (Andrae et al. 2014). *Lsh*^{off} is present to a much higher level in both tissues in *Lsh*$^{on/on}$*;Pdgfrα-Cre*, and completely absent in *Lsh*$^{on/on}$ (Fig. 5.5B). Characterisation of the *Lsh*$^{on/on}$*;Pdgfrα-Cre* phenotype requires a comparison to animals in the same genetic background which would not be expected to possess any phenotype. As *Lsh*$^{+/off}$ animals have no detectable phenotype, and these animals have a single *Lsh*^{off} allele in PDGFRα expressing cells. I reasoned that the use of *Lsh*$^{on/+}$*;Pdgfrα-Cre* animals would fit this requirement as they would also be heterozygous *Lsh*^{off} in OPCs, but express LSH to wild-type levels in other cell types, as would *Lsh*$^{on/on}$*;Pdgfrα-Cre*.

Lsh$^{on/on}$ animals are fertile but show a reduction in litter sizes in comparison to *Lsh*$^{+/off}$ X *Lsh*$^{+/+}$ crosses and outcrossing of the *Lsh* lines has previously been shown to influence perinatal lethality (Fig. 3.3). If these phenotypes are solely the result of outcrossing *Lsh* lines and not the specific alleles there possess, they may be apparent in *Lsh*$^{on/on}$*;Pdgfrα-Cre* and be a potential confounding factor is connecting phenotype to OPC specific knock-out. To test if any embryonic lethality is associated with PDGFRα expressing cell specific deletion of LSH or if the fertility phenotype seen in *Lsh*$^{on/on}$ is still present on outcrossing the *Lsh*^{on} line to *Pdgfrα-Cre* I analysed litter sizes in *Lsh*$^{on/+}$*;Pdgfrα-Cre* × *Lsh*$^{on/on}$ crosses. There is no

detectable reduction in litter sizes compared to *Lsh*$^{+/off}$ × *Lsh*$^{+/+}$ and increase compared to *Lsh*$^{on/on}$ × *Lsh*$^{on/on}$ and *Lsh*$^{+/off}$ × *Lsh*$^{+/off}$ (Fig. 5.5C). In addition I analysed the proportion of *Lsh*$^{on/+}$*;Pdgfrα-Cre* × *Lsh*$^{on/on}$ litters making it to weaning, and this is unchanged compared to other genotypes (Fig.5.5D). *Lsh*$^{on/on}$*; Pdgfrα-Cre* mice were also born to the expected Mendelian ratio (Fig. 5.5E) and do not possess a growth phenotype in male or females (Fig.5.5F, G). In addition, *Lsh*$^{on/on}$*; Pdgfrα-Cre* animals do not possess a neurological phenotype (Appendix video 6).

Figure 5-4 OPC specific knock-out has no detectable breeding or growth phenotype

A) Schematic representation of the timing of *Lsh* allele conversion in the *Pdgfrα-Cre* line (on to off)
B) Image of agarose gel running allele specific PCR products across OPC isolation fractions in knock-out and control genotypes.
C) Boxplots showing litter sizes from *Lsh*^{off}, *Lsh*^{on} and *Lsh*^{on}*; Pdgfrα-Cre* crosses. P-values result on unpaired t-test comparisons of conditions. Whiskers representative of upper and lower quartiles, n=39, 12, 34 and 15 respectively.
D) Boxplots showing percentages of mice born in *Lsh*^{off}, *Lsh*^{on} and *Lsh*^{on}*; Pdgfrα-Cre* crosses. P-values the result of Mann-Whitney non-parametric tests due to non-normal distribution present in samples. Bounds of boxes represent minimum and maximum values, n numbers as with (B).
E) Observed and expected rations of mice born from *Lsh*$^{+/on}$*; Pdgfrα-Cre* × *Lsh*$^{on/on}$ crosses. P-values on graph the result of Chi-squared test comparing expected vs observed numbers.
F) Line graph of mean weights post-weaning for males of *Lsh*$^{+/on}$*; Pdgfrα-Cre* × *Lsh*$^{on/on}$*; Pdgfrα-Cre* genotypes. Error bars show standard deviation, n=4 and 6 respectively.
G) Line graph of mean weights post-weaning for females of *Lsh*$^{+/off}$*; Pdgfrα-Cre, Lsh*$^{off/off}$*; Pdgfrα-Cre* genotypes. Error bars show standard deviation, n=4 and 6 respectively.

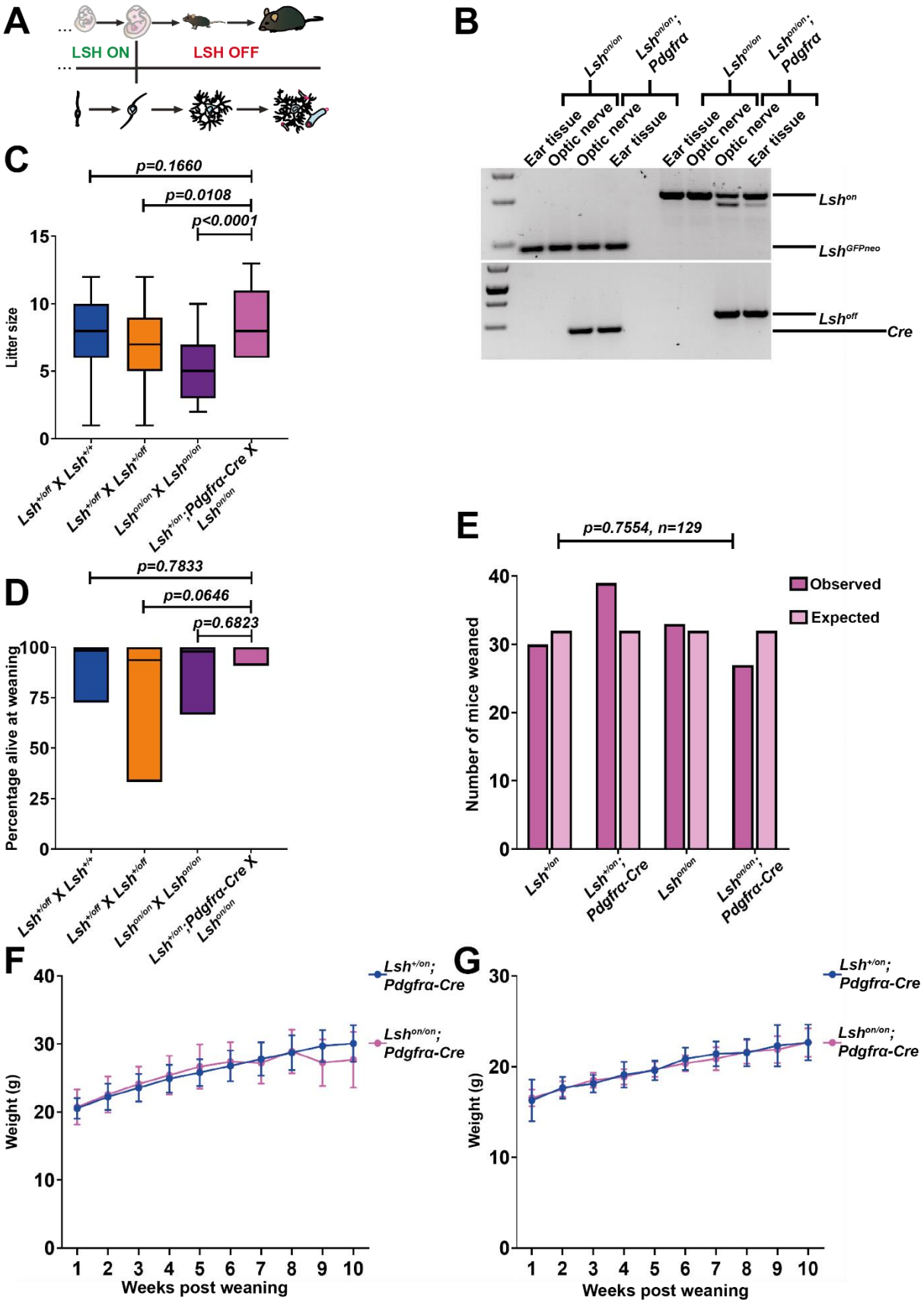
A
LSH ON
LSH OFF
B
Lsh^on/on
Lsh^on/on; Pdgfra
Ear tissue
Optic nerve
Lsh^on
Lsh^GFPneo
Lsh^off
Cre
C
p=0.1660
p=0.0108
p<0.0001
Litter size
Lsh+/off X Lsh+/+
Lsh+/off X Lsh+/off
Lsh on/on X Lsh on/on
Lsh+/on;Pdgfra-Cre X Lsh on/on
D
p=0.7833
p=0.0646
p=0.6823
Percentage alive at weaning
E
p=0.7554, n=129
Observed
Expected
Number of mice weaned
Lsh+/on
Lsh+/on; Pdgfra-Cre
Lsh on/on
Lsh on/on; Pdgfra-Cre
F
Lsh+/on; Pdgfra-Cre
Lsh on/on; Pdgfra-Cre
Weight (g)
Weeks post weaning
G
Lsh+/on; Pdgfra-Cre
Lsh on/on; Pdgfra-Cre
Weight (g)
Weeks post weaning

5.3.2 *Lsh$^{on/on}$; Pdgfrα-Cre* animals are myelinated grosely normally and do not have an oligodendrocyte differentiation defect

As mentioned earlier, the lack of a growth phenotype was expected in *Lsh$^{on/on}$;Pdgfrα-Cre* due to *Lsh$^{on/on}$* being present in non-PDGFRα expressing cells and the persistence of a mild growth phenotype in *Lsh$^{off/off}$;Pdgfrα-Cre* suggesting that these cells were at least not entirely responsible for reduced weight. The perinatal phenotype not being present may be due to the susceptibility of the small effect seen in *Lsh$^{off/off}$* to be altered due to outbreeding of the strain. However, the non-statistically significant tendency for *Lsh$^{+/off}$;Pdgfrα-Cre* × *Lsh$^{+/off}$* to have a reduced proportion of animals reaching weaning is not present in *Lsh$^{+/on}$;Pdgfrα-Cre* × *Lsh$^{on/on}$*, which more closely resembles *Lsh$^{+/off}$* × *Lsh$^{+/+}$* crosses. This suggests again that this phenotype is caused by the lack of LSH expression in non PDGFRα expressing cells.

The lack of observable neurological phenotype in *Lsh$^{on/on}$;Pdgfrα-Cre* when mice were aged up until 1 year, suggests that also no myelin phenotype is present. It is conceivable that OPC specific knock-out of LSH could still confer an OL differentiation defect, albeit to a much lesser extent than seen in *Lsh$^{off/off}$*. One might even expect this scenario to be the case if small amounts of LSH remain in OL lineage cells due to lack of degradation following expression being abolished at E12.5. Therefor to see if any evidence of myelination or OL differentiation defect could be found at the molecular level and test the hypothesis that LSH is not required in the OPC to mOL differentiation to any extent, I performed characterisation of OL stage specific marker gene expression in P120-P200 *Lsh$^{on/on}$; Pdgfrα-Cre* animals.

TEM analysis of myelin in the optic nerve of 3 individuals of *Lsh$^{on/on}$;Pdgfrα-Cre* and *Lsh$^{on/+}$;Pdgfrα-Cre* revealed no obvious signs of reduced myelin thickness or coverage (Fig. 5.6A). DAPI and immunostaining for OLIG2 reveal similar total cell numbers and OL lineage cell numbers in *Lsh$^{on/on}$;Pdgfrα-Cre* and *Lsh$^{on/+}$;Pdgfrα-Cre* (Fig.5.6B, C, D). The percentage of mOLs staining for OLIG2 and QKI7 also remains the same between genotypes (Fig. 19B, E). Finally qPCR of reverse transcribed optic nerve mRNA for OL stage specific marker

genes revealed, if anything, a slight over expression of mOL associated genes in *Lsh$^{on/on}$;Pdgfrα-Cre* (Fig.5.6F).

Figure 5-5 Cre mediated conversion to *Lsh^{off}* in the oligodendrocyte lineage does not lead to the cellular phenotype observed in *Lsh$^{off/off}$*

A) Representative TEM images of myelin in P90 *Lsh$^{+/on}$;Pdgfrα-Cre*, *Lsh$^{on/on}$; Pdgfrα-Cre* littermate optic nerves.
B) Representative images of DAPI, OLIG2 and QKI7 staining of *Lsh$^{+/on}$;Pdgfrα-Cre*, *Lsh$^{on/on}$; Pdgfrα-Cre* P90 optic nerves.
C) Average number of cells in section imaged between genotypes.
D) Percentage of DAPI positive cells also staining for OLIG2 between genotypes.
E) Percentage of DAPI positive cells also staining for OLIG2 and QKI7 between genotypes.
F) qPCR of P90 optic nerve cDNA for myelin associated genes.
Error bars on all samples represent standard deviation, unpaired t-tests using Welch's correction were used for p-value calculation. *=P<0.05. n=3 animals/genotypes for A-F with 4 sections counted per animal (>500 cells). See materials and methods for qPCR replicate strategy.

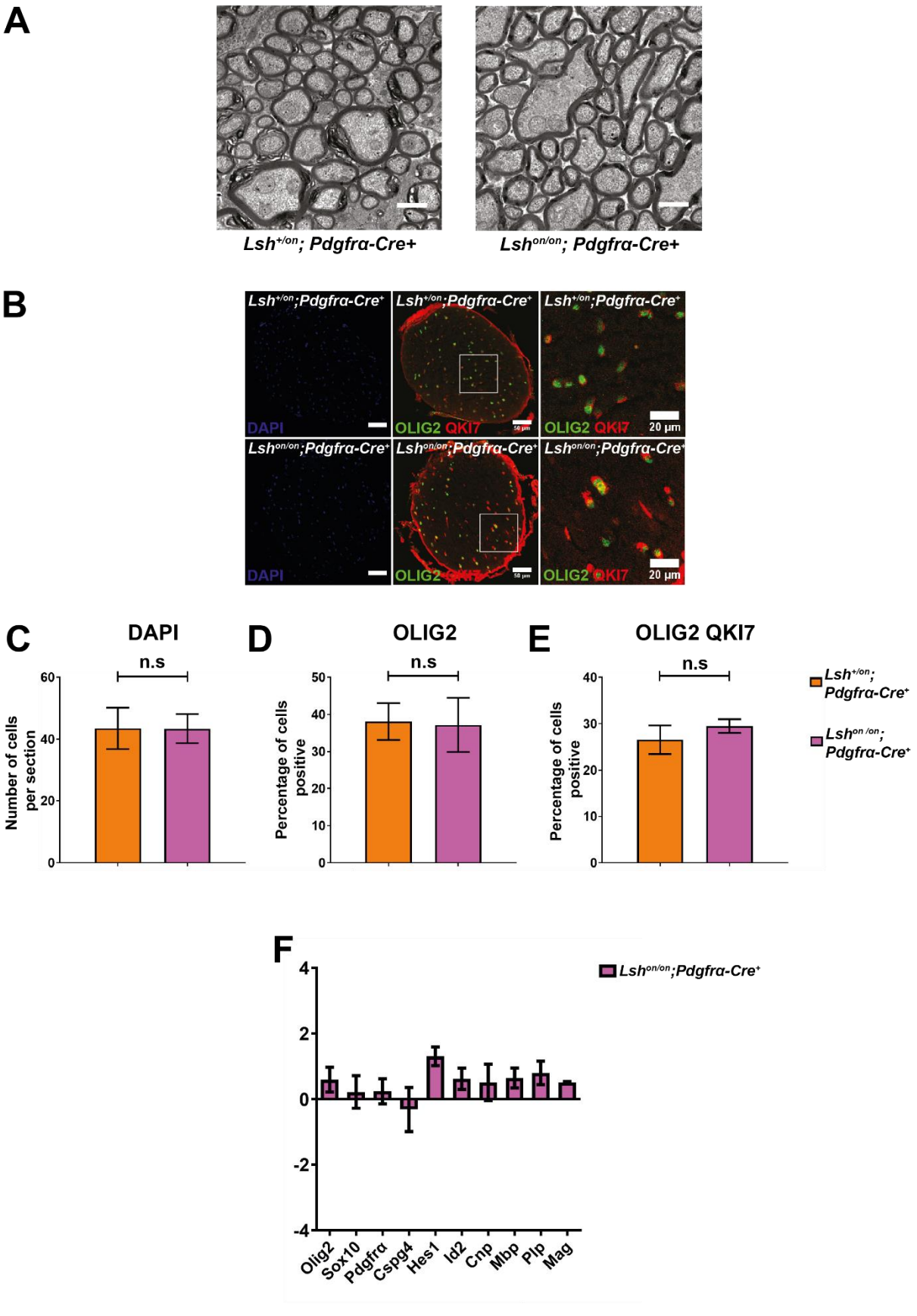
A
Lsh+/on; Pdgfrα-Cre+
Lshon/on; Pdgfrα-Cre+
B
Lsh+/on;Pdgfrα-Cre+
Lshon/on;Pdgfrα-Cre+
DAPI
OLIG2 QKI7
20 µm
C
DAPI
n.s
Number of cells per section
D
OLIG2
n.s
Percentage of cells positive
E
OLIG2 QKI7
n.s
Percentage of cells positive
Lsh+/on; Pdgfrα-Cre+
Lshon /on; Pdgfrα-Cre+
F
Lshon/on;Pdgfrα-Cre+
Olig2
Sox10
Pdgfra
Cspg4
Hes1
Id2
Cnp
Mbp
Plp
Mag

5.4 Summary

The *Lsh*$^{off/off}$ defect in OL differentiation is rescued on early life expression of LSH in OPCs, with a partial growth phenotype possibly still remaining. This strongly suggests that the OL differentiation defect is cell autonomous to OPCs. However somewhat counter to my initial expectations when initially proposing the OPC specific knock-out experiment, these data support that LSH is not required in the OL lineage for differentiation, at least when this knock-out occurs later than an undefined but relatively early period after E12.5 in development. This would rule out expression being required during OPC to mOL differentiation. But it does not rule out that conversion achieved in *Lsh*$^{off/off}$*;Pdgfrα-Cre* enables the crucial function in OL differentiation to occur in development, but later than it usually would in a wildtype situation. While further experiments into the precise timing of LSH requirement in OL development would potentially shed light on LSH's molecular function, the evidence in this chapter supports some LSH requirement in OPCs prior to differentiation.

A major problem in studying the molecular mechanism of LSH deficiency in OL differentiation is distinguishing between the primary effects of LSH on transcription, that may be causal in the phenotype, and secondary transcriptional changes that are the result of failed OL differentiation. I now know the defect occurs within OPCs, and not following their initiation of differentiation to OLs. Therefore, presumably, primary effects of the LSH deficiency will be present, but secondary effects of failure of *Lsh*$^{off/off}$ OPCs to differentiate will be absent.

To test the hypothesis that LSH's function in regulation of chromatin state is causal in the OL differentiation defect, I will need to compare chromatin state in undifferentiated OPCs, prior to the accumulation of secondary effects, but where primary effects of LSH deficiency are presumably still detectable.

Results- Chapter Six- LSH is required for activation of late stage oligodendrocyte genes, but genome-wide methylation patterns in OPCs are largely unchanged

6.1 *Lsh*$^{off/off}$ mice can silence inhibitors of oligodendrocyte differentiation but do not effectively silence non-CNS genes and fail to upregulate genes involved in crucial to myelination

6.1.1 Introduction

Rescue of LSH expression in OPCs results in rescue of the myelin phenotype, indicating that it is cell autonomous to OPCs. However, the *Pdgfrα* promoter is active in the gut and other organ systems that may have a organism wide effect on phenotype (Andrae et al. 2014). As no culture or differentiation of *Lsh*$^{off/off}$ OPCs can be carried out removing them from their *in vivo* environment, a potential role for these systems in the *Lsh*$^{off/off}$ myelin phenotype cannot be ruled out. Perturbation of these systems would cause effects in other cell types in addition to OLs, therefor I would expect analysis of expression changes in *Lsh*$^{off/off}$ compared to *Lsh*$^{+/off}$ to reveal major changes in genes expressed in non-OL CNS cell types.

In addition, previous analyses of marker gene expression do not consider the entirety of relevant gene expression for the OL lineage, and despite not being consistent with the data so far, it remains possible that genes known to be inhibitors differentiation are the causal factors in preventing *Lsh*$^{off/off}$ differentiation. It also remains possible, as marker gene expression profiling so far suggests, that expression of key genes required for differentiation to progress and are unable to be upregulated in the absence of LSH.

To see if any evidence can be gathered supporting either de-repression of inhibitors of differentiation, or repression of genes required for progress in differentiation, and to see if other CNS cell types show a perturbation in *Lsh*$^{off/off}$, I decided to perform RNA-sequencing to interrogate relative transcript levels in *Lsh*$^{+/off}$ and *Lsh*$^{off/off}$ optic nerve.

6.1.2 *Lsh*$^{off/off}$ optic nerves show no consistent change in expression of genes specific to CNS cell types, apart from those in the oligodendrocyte lineage

To limit the influence of individual variation on differential expression calls in *Lsh*$^{off/off}$ and due to limitations in the amount of material that could be collected from optic nerve, I made sequencing libraries from 2 pools of 6 optic nerve pairs per genotype. Sequencing of these libraries revealed 566 genes significantly over-expressed greater than 2-fold and 312 genes under-expressed greater than 2-fold, with the principle component separating libraries explaining 76% of variation between them, and genotypes clustering on opposite sides of this component (Fig, 6.1A, B). The biased towards over-expression being consistent with LSH's canonical role as a gene repressor.

To shed light on whether these mis-expressed genes were associated with particular CNS cells types, I first needed to define a group of genes whose expression could be said to be specific to a particular cell type. To do this, we used the Barres RNA-seq database (Zhang et al. 2014).The assumption being that the majority of genes that are expressed highly in a specific cell type over all others, would reflect genes expressed highly by the cell type in *in vivo*. A factor confounding this assumption is the cell types of the Barres dataset have been subjected to the manipulations of *in vitro* culture. We reasoned that expression artefacts of this culture, such as high expression of cell cycle genes due to a maintained state of division, or cell death genes due to increased turnover of cells grown *in vitro*, would be largely common to multiple cell types and therefore not deemed specific by the analysis. Another confounding factor I predicted would be the possibility that specific sub-types of cells isolated and cultured would not be representative of the full diversity of expression

patterns *in vivo*. I reasoned that although bias towards the particular sub-type of cells sequenced in this data would be inevitable, the broad trends in cell type specific gene expression would be captured by the analysis and comparison to other datasets would be capable of corroborating its conclusions.

To define the top 100 specific genes for each cell type genes were simply assigned a ratio for expression in RPMK in a given cell type to the mean of RPKM in all other cell types. They were then ranked by this ratio, and the top 100 considered specific. When the RPKM is plotted for these top 100 genes for each Barre's cell type on the same axes as all other cell types, the degree of specificity of these genes to a cell type can be assessed (Fig. 6.2A, B, C, D, E, F, G). The highest expression of top 100 specific genes in other cell types was seen, predictably, among different stages of the OL lineage (Fig.6.2C, D, E). There was also some expression of the top 100 OPC specific genes within microglia (Fig 6.2F). This is consistent with the reported ~10% microglial contamination present in the Barres isolations (Zhang et al. 2014). Another noticeable pattern was that OPC specific genes seemed to have a much lower expression in RPKM than newly formed oligodendrocytes (NFOLs) and myelinating oligodendrocytes (MOLs), median RPKM 10.9, 26.9 and 29.1 respectively. This could partly explain when plotting transcript per million TPM values of each specific gene set in the *Lsh*$^{+/off}$ and *Lsh*$^{off/off}$ dataset reveals a higher level of expression for NFOL and MOL genes than OPC genes even in *Lsh*$^{off/off}$ where myelin is lacking (Fig.6.2H). When looking at a relative quantification of specific transcripts in each cell type between genotypes however it becomes apparent that there is only a directionally consistent change in expression for MOL and to a lesser extent NFOL specific genes, with median values being reduced compared to *Lsh*$^{+/off}$ (Fig.6.2I). There is also more of a mixture of under and over expressed transcripts for OPC specific genes and those for CNS cell types other than MOLs.

Consistent with major changes in cell type specific gene expression only occurring in later stage OL lineage genes, analysis of the adjusted p-value for expression changes in genes

revealed most changes in non-MOL genes were not significant, while over 50% of genes assigned to be specific for MOLs were above $p<0.05$ threshold (Fig. 6.2J).

Taken together this supports the hypothesis that upregulation of mOL genes are responsible for the *Lsh*$^{off/off}$ differentiation defect, and that cells are in fact able to effectively silence the major proportion of inhibitors of differentiation, or at least those that are specific to OPCs in relation to other CNS cell types. In addition, the lack of major consistent changes in specific gene sets for other CNS cell types, while not ruling out some perturbation of these cell types, suggests there isn't a major scarcity or abundance of these cell types in the *Lsh*$^{off/off}$ CNS, consistent with the idea that the phenotype is indeed autonomous to the OL lineage.

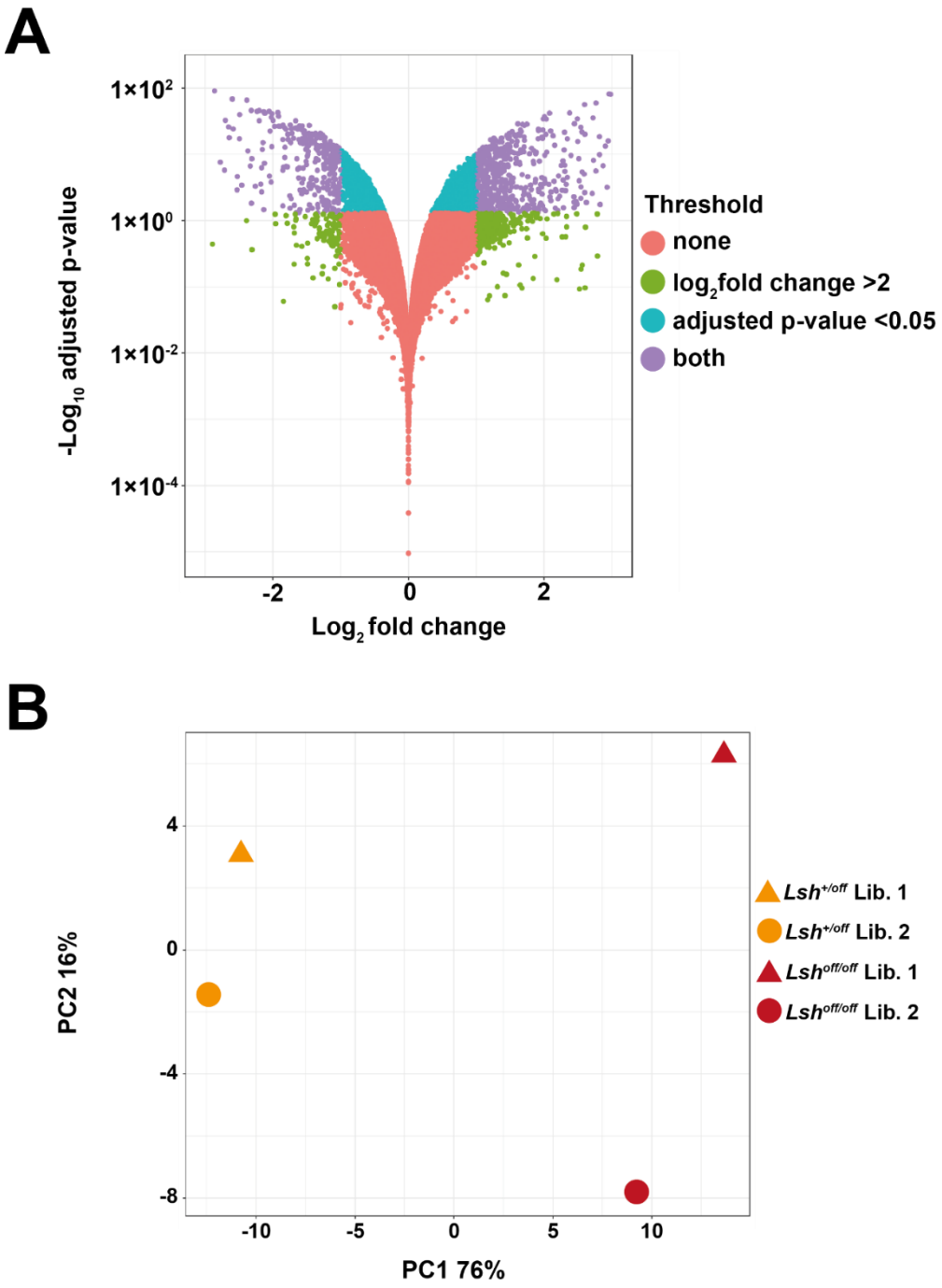

Figure 6-1 There is widespread misexpression of genes in the Lshoff/off CNS, with a skew towards overexpression

A) Volcano plot differential gene expression in *Lsh*$^{off/off}$ optic nerve as determined by RNA-seq. 566 genes are significantly over-expressed greater than 2-fold and 312 genes are under-expressed greater than 2-fold, p-value defined as <0.05 FDR=0.01.

B) Principle component analysis of the 4 analysed RNA-seq libraries. The greatest variation between samples is determined by genotype with opposite genotype libraries further from each other than they are from like genotypes.

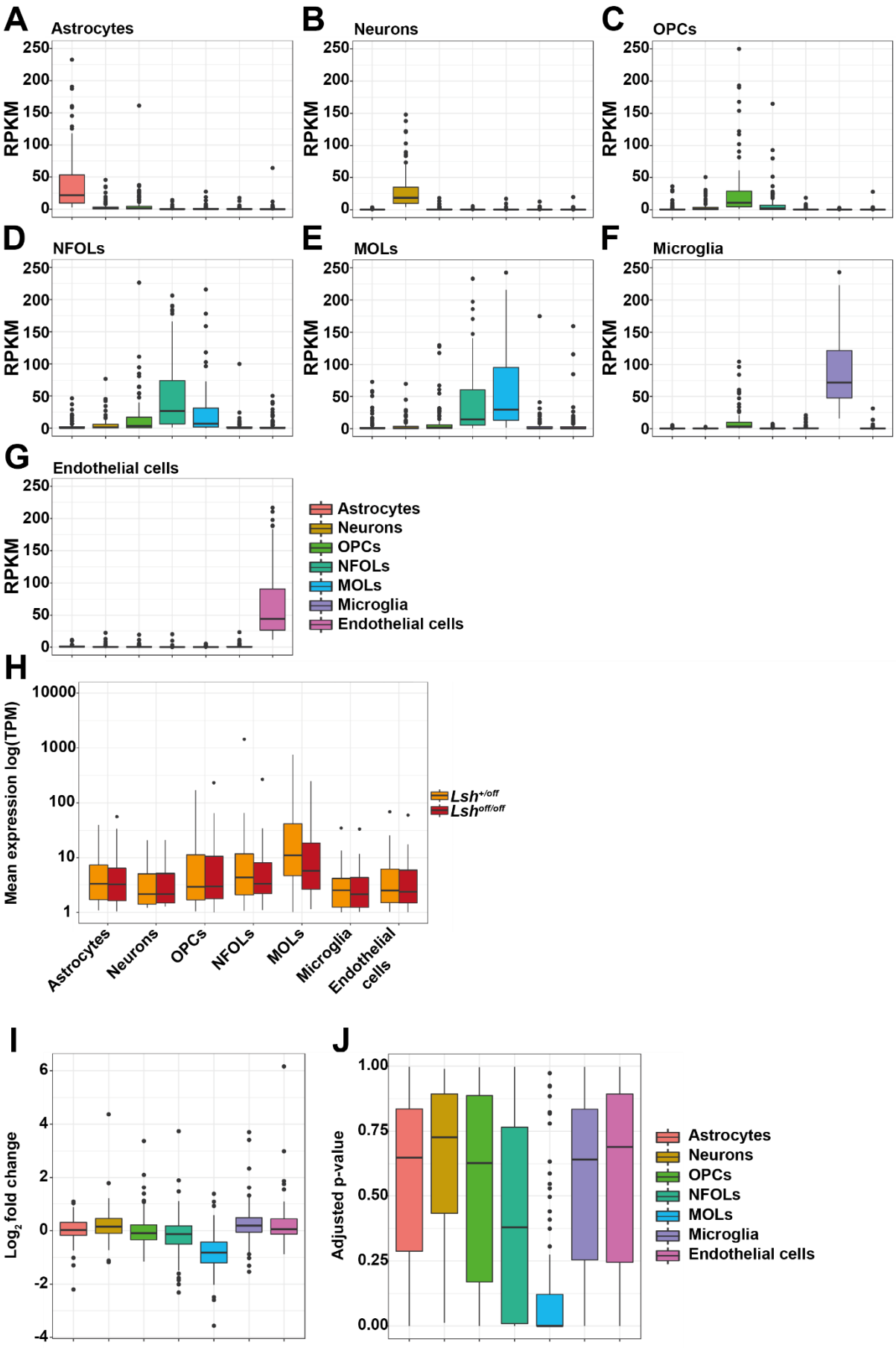
A
Astrocytes
B
Neurons
C
OPCs
D
NFOLs
E
MOLs
F
Microglia
G
Endothelial cells
RPKM
Astrocytes
Neurons
OPCs
NFOLs
MOLs
Microglia
Endothelial cells
H
Mean expression log(TPM)
Lsh+/off
Lshoff/off
I
Log2 fold change
J
Adjusted p-value

Figure 6-2 Mature oligodendrocyte specific genes are robustly under-expressed in *Lsh*$^{off/off}$ but there is not extensive overexpression of OPC genes, or misexpression of genes associated with other CNS cell types

A-G) Boxplots of expression of top 100 CNS cell type specific genes across CNS cell types.
H) The mean expression of top 100 cell type specific genes in both genotypes in TPM.
I) Boxplots of fold change in expression in *Lsh*$^{off/off}$ relative to *Lsh*$^{+/off}$ for top 100 cell type specific genes across CNS cell types.
J) Boxplots showing adjusted p-value for top 100 cell type specific genes across CNS cell types. Lines represent median gene fold change with upper and lower box limits defining upper and lower quartiles, dots are >2 standard deviations from the mean.

6.1.3 Patterns in oligodendrocyte lineage stage specific gene expression are consistent across *in vitro* and *in vivo* datasets

Comparison of genes mis-expressed in *Lsh*$^{off/off}$ optic nerve to those identified to be specific to CNS cell types in the Barres RNA-seq database supports previous experiments suggesting that mOL genes are under-expressed and OPC genes are not over-expressed to a similar extent. The artefacts of the *in vitro* isolation and culture performed in the Barres experiments to some extent reduces the relatability of conclusions reached about *in vivo* OL differentiation in *Lsh*$^{off/off}$. In addition, the approach used to define specific sets of genes relies on comparison to non-OL CNS lineages. Commonalities in highly expressed genes within the whole OL lineage, regardless of differentiation stage, will therefore be excluded from any comparison despite possibly being expressed more highly at a particular stage of OL differentiation. There is also an uneven coverage across cell types for Barres defined specific genes in the optic nerve RNA-seq. MOL specific genes tend to produce in greater transcript numbers in the *in vitro* differentiated MOLs than OPC specific genes are expressed in OPC. This is likely also the case *in vivo* as TPM values for MOL specific genes are higher even in *Lsh*$^{off/off}$ optic nerve, despite the lack of myelin. Changes in expression of genes that are well covered are more likely to be detected by RNA-seq differential expression analysis, so a bias to detecting differences in MOL genes is a conceivable explanation for the patterns seen when comparing *Lsh*$^{off/off}$ fold changes to the Barres data. To further test the hypothesis that in *Lsh*$^{off/off}$ primarily mOL genes are mis-regulated in the

OL lineage, I therefor decided to perform comparisons on other publicly available data sets where stage specific gene expression information could be inferred.

One such dataset is derived from microarray-based gene expression comparisons of rat OL lineage cells stimulated to differentiate *in vitro* at set timepoints following initiation of differentiation (Swiss et al. 2011). As rat OPCs can be cultured more readily *in vitro* than the mouse OPCs used in Barres' experiments, the degree of microglial contamination is reduced. Stage specificity is also defined purely based on comparisons within the OL lineage, enabling calling of genes expressed in other CNS cell types to a specific OL differentiation stage. When we plot the mouse homologues of the genes defined as characteristic of different timepoints in differentiation by this study, late stage genes most clearly show a trend for directional change in expression in $Lsh^{off/off}$ (Fig.6.3A). Over-expression of a subset of early-stage downregulated genes, as well as genes that do not fit the general trend of later the timepoint can be detected. Deviations to from the general trend could be ascribed differences between *in vitro* culture vs *in vivo* differentiation or to differences between rat and mouse OPC differentiation. Another explanation for these could be the reduced transcript number in the optic nerve RNA-seq compared to the consistently under-expressed late stage OL genes that we see in the Barres comparison. When plotting the expression in $Lsh^{+/off}$ onto the stage specific genes, low expression genes over-expressed in the early downregulated category, that would not be subject to coverage bias, are detectable (Fig.6.3B). This suggests coverage cannot fully explain the late stage OL specific effect seen in $Lsh^{off/off}$.

To attempt to address the confounding factors introduced by artefacts associated with *in vitro* differentiation, and those caused by species differences between rat and mouse, we also plotted the $Lsh^{off/off}$ optic nerve expression changes stratified according defined to be characteristic of different lineage stages, across organism development by single cell RNA sequencing of mouse tissue (Marques et al. 2016). Here a tree building approach to cell type

definition was used by the authors whereby cells within a stage of OL differentiation would be separated from others based on differences in gene expression. I reasoned that an advantage of this approach would be, due to limited coverage available in single-cell sequencing, that only the most highly expressed OPC genes, or those most specific to OPCs would characterise a lineage stage. When comparing genes which define the branches between OPCs, NFOLs and MOLs generically, we again see a consistent pattern of MOL and NFOL defining gene under-expression, and little overexpression of OPC defining genes (Fig.6.4A). In addition, when plotting the expression values for each defining gene set, we see that even relatively highly expressed OPC genes are not over-expressed in *Lsh*$^{off/off}$ (Fig.6.4B). The single cell analysis also defines different sub-types OLs within different stages of differentiation. When using the author's definition for more specific OL sub-types, we see that under-expression in *Lsh*$^{off/off}$ optic nerve is most apparent in the MOL2 and MOL6 subtype, with MOL3 largely being unchanged (Fig. 6.4C). Interestingly, NFOL2 but not NFOL1 showed under-expression in *Lsh*$^{off/off}$ and myelin-forming oligodendrocyte-2 (MFOL2), but not MFOL1 genes shows under-expression. The fact that under-expression isn't generic to all sub-types, hints at a specific class of genes in OL differentiation requiring LSH for upregulation. It is also consistent with the observation that some OLs progress further in differentiation than others in *Lsh*$^{off/off}$, such as those in the spinal cord. However, more functional and anatomical characterisation of each OL sub-type is required to support these possibilities. It may be that the unchanged cell types are not present in adult optic nerves. In this scenario the fact that these potentially absent sub-types show no consistent under-expression in *Lsh*$^{off/off}$ acts as a negative control for e conclusions reached regarding other OL sub-types.

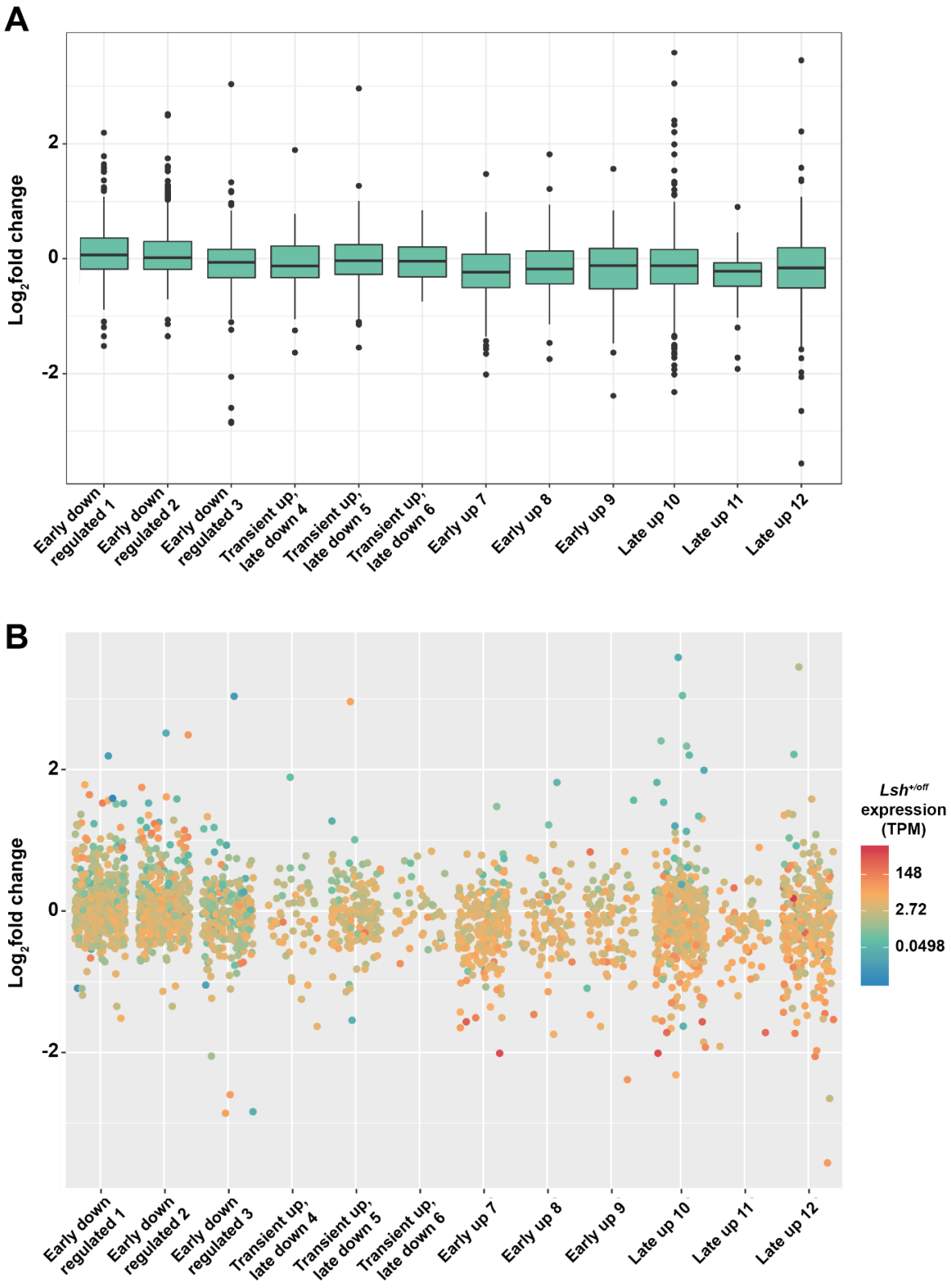

Figure 6-3 Comparison to other oligodendrocyte lineage stage specific gene expression datasets supports conclusion that primarily mature oligodendrocyte genes are mis-expressed

A) Boxplots of fold change in *Lsh*$^{off/off}$ relative to *Lsh*$^{+/off}$ stratified by gene regulatory clusters defined by Swiss et al. Lines represent median gene fold change with upper and lower box limits defining upper and lower quartiles, dots are >2 standard deviations from the mean.

B) Jitter plot of the same data as show in A colour coded by expression in *Lsh*$^{+/off}$ in TPM. Genes with low expression comparable to that of OPCs do have detectable folds changes in gene expression.

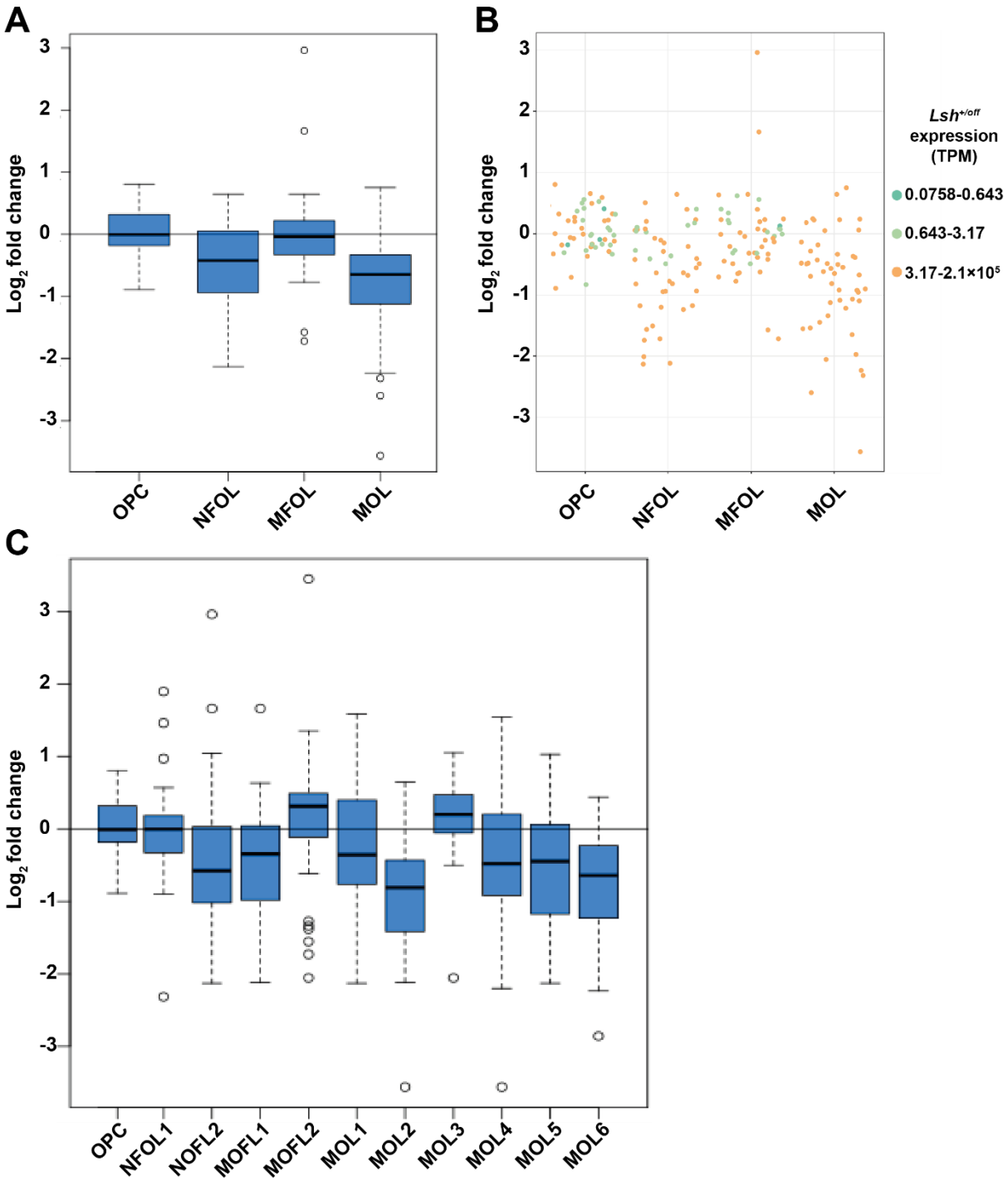

Figure 6-4 Comparison of relative *Lsh*$^{off/off}$ gene expression of oligodendrocyte subtype defining genes from single cell *in vivo* data sets reveals that not all oligodendrocyte subtypes under-express genes *Lsh*$^{off/off}$

A) Boxplots show log_2 fold change in *Lsh*$^{off/off}$ relative to *Lsh*$^{+/off}$ stratified by oligodendrocyte stage defining genes derived from Marques et al.

B) Jitter plot of the same data as show in A, colour coded by expression in *Lsh*$^{+/off}$ in TPM. Genes with low expression show less of a tendency to change than higher expressed mature oligodendrocyte genes.

C) Boxplots show log_2 fold change in *Lsh*$^{off/off}$ relative to *Lsh*$^{+/off}$ stratified by oligodendrocyte subtype defining genes derived from Marques et al. In A and C lines represent median gene fold change with upper and lower box limits defining upper and lower quartiles, dots are >2 standard deviations from the mean.

6.1.4 *Lsh*$^{off/off}$ fails to upregulate genes involved in cholesterol biosynthesis

Analysis so far supports conclusions from previous marker gene expression characterisation in *Lsh*$^{off/off}$ optic nerve that OL lineage cells arrest in differentiation to mOLs at some stage following OPC, but prior to the upregulation of mOL genes. However, not all mOL associated genes are mis-regulated in *Lsh*$^{off/off}$. This leads me to the hypothesis that a specific process or processes required for the differentiation of mOLs is perturbed.

To test these hypotheses, I performed gene ontology analysis on genes significantly under-expressed in *Lsh*$^{off/off}$ optic nerve greater than 2-fold. Strikingly, genes involved in sterol and lipid biosynthesis were most significantly overrepresented amongst the under-expressed genes (Fig. 6.5A.). Cholesterol biosynthesis is a well-known pathway required for OL differentiation (Chrast et al. 2011). Recently, it has been discovered that Imidazole antifungal drugs and many known drugs used to enhance OL differentiation work exclusively through the regulation of production 8,9-unsaturated sterols, an intermediate in cholesterol biosynthesis, with accumulation of these sterols enhancing differentiation (Hubler et al. 2018). Analysis of specific genes required at the key steps of the sterol biosynthesis, defined by Hubler et al., identified a decrease in components upstream of synthesis of the 8-9-unsaturated sterols, with those downstream of lanosterol production also showing a decrease in expression, notably *cyp51* with a 2.7-fold decrease (Fig. 24B). Also, these genes are nearly all significantly differentially expressed between conditions to a high p-value (Fig. 6.5C). This suggests that accumulation of 8,9-unsaturated sterols is prevented in *Lsh*$^{off/off}$ due to lack of upstream intermediates in their biosynthesis and supports that a lack of cholesterol synthesis, and not downstream metabolism of 8,9-unsaturated is responsible for a lack of differentiation. Whether this is a direct effect of LSH being unable to directly regulate these genes in *Lsh*$^{off/off}$ or a secondary effect caused by mis-regulation of other genes that then go on to effect sterol biosynthetic gene expression is not discernible from analysis of this experiment, however.

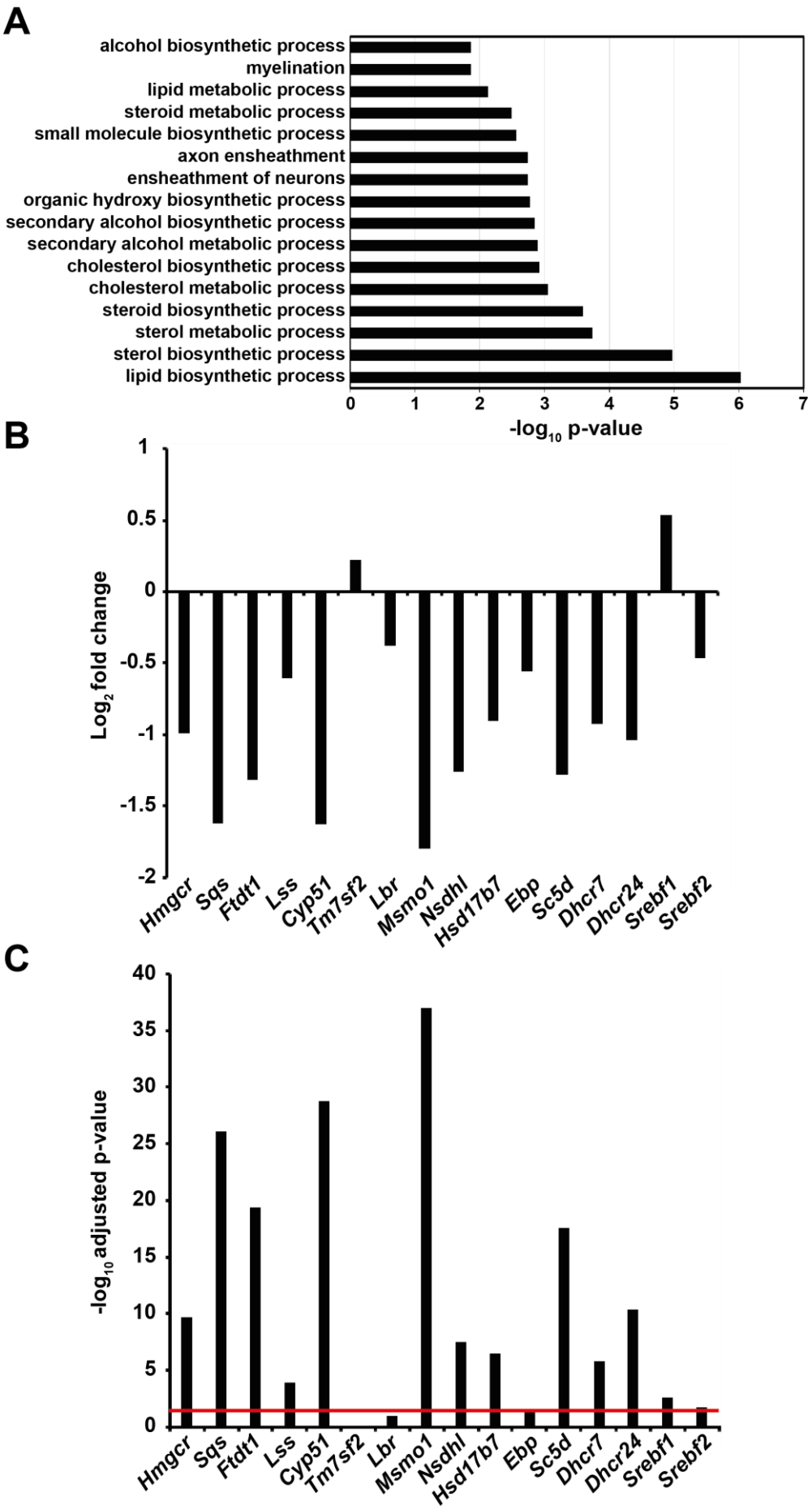
A
alcohol biosynthetic process
myelination
lipid metabolic process
steroid metabolic process
small molecule biosynthetic process
axon ensheathment
ensheathment of neurons
organic hydroxy biosynthetic process
secondary alcohol biosynthetic process
secondary alcohol metabolic process
cholesterol biosynthetic process
cholesterol metabolic process
steroid biosynthetic process
sterol metabolic process
sterol biosynthetic process
lipid biosynthetic process
0 1 2 3 4 5 6 7
-log10 p-value
B
Log2 fold change
1 0.5 0 -0.5 -1 -1.5 -2
Hmgcr Sqs Ftdt1 Lss Cyp51 Tm7sf2 Lbr Msmo1 Nsdhl Hsd17b7 Ebp Sc5d Dhcr7 Dhcr24 Srebf1 Srebf2
C
-log10 adjusted p-value
40 35 30 25 20 15 10 5 0
Hmgcr Sqs Ftdt1 Lss Cyp51 Tm7sf2 Lbr Msmo1 Nsdhl Hsd17b7 Ebp Sc5d Dhcr7 Dhcr24 Srebf1 Srebf2

Figure 6-5 Cholesterol biosynthetic genes are almost uniformly under-expressed in *Lsh$^{off/off}$* optic nerve

A) Gene ontology analysis by G:profiler of under-expressed genes in *Lsh$^{off/off}$* in comparison to *Lsh$^{+/off}$*.
B) Fold change in *Lsh$^{off/off}$* relative to *Lsh$^{+/off}$* transcripts for enzymes involved in sterol biosynthesis defined in Hubler et al. and the sterol regulatory element binding transcription factors *Srebf1 and Srebf2*.
C) Adjusted p-value for the genes shown in B, the red line indicates the P=<0.5 threshold for significance.

6.1.5 *Lsh$^{off/off}$* primarily fails to silence genes involved in protein synthesis and those not normally expressed in optic nerve

OPC and non-OL lineage CNS cell type specific genes are not over-expressed in *Lsh$^{off/off}$*, but most significant expression changes in *Lsh$^{off/off}$* are over-expressed compared to *Lsh$^{+/off}$*. In previous *Lsh* knock-outs, there is significant over-expression of genes present in constitutive heterochromatin, such as intracisternal A-particle (IAP) retrotransposons, along with other repetitive elements (Muegge 2005). This leads to the hypothesis that the over-expressed genes in *Lsh$^{off/off}$* optic nerve are mainly composed of such elements and genes that are not expressed in *Lsh$^{+/off}$* optic nerve.

To test this, I performed similar gene ontology analysis as previously but including genes overexpressed greater than 2-fold reveals the most significantly over-represented processes are related to general protein synthesis (Fig. 6.6A). This is surprising given the obvious essential role for these proteins in all cell-types. In addition, the number of genes associated with a significant term were much lower for over-expressed genes compared to under-expressed despite more genes being over-expressed overall. I reasoned that if most genes being over-expressed in *Lsh$^{off/off}$* are associated with heterochromatic regions in OLs, it might be expected that they are associated with disparate biological processes or are transposable elements that won't be associated with a GO-term. To see if the former was the case, I plotted expression level in *Lsh$^{+/off}$* as an indication of expression in a phenotypically normal optic nerve against $\log_2$ fold change in *Lsh$^{off/off}$*. This reveals that indeed many overexpressed genes are expressed to a very low level in *Lsh$^{+/off}$* despite low coverage making determination of significance for

these genes more challenging (Fig. 6.6B). It is conversely not the case that genes expressed at low levels in *Lsh*$^{off/off}$ are over-expressed in *Lsh*$^{+/off}$. To test if these genes included transposable elements, we plotted reads mapping to IAP features across libraries. This revealed there was a significant overexpression of these elements in *Lsh*$^{off/off}$ however fold changes are not comparable to even conditional gene knock-outs where IAP element repression is ablated (Fig.6.6C)(Ramesh et al. 2016). To see if any link between IAP overexpression and the severity of the OL differentiation phenotype was apparent, I performed qPCR on cDNA reverse transcribed from mRNA isolated from P14 optic nerve, P90 optic nerve and P90 spinal cord. I reasoned that if IAP overexpression prevented OL differentiation, I would expect to see a larger magnitude increase in optic nerve, where phenotype is more severe, than spinal cord, where OPCs can differentiation to a later stage. This was not the case, with comparable fold-changes between P90 tissues (Fig 6.6D). It is conceivable that the over-expression of translation associated genes is linked to the de-repression of repetitive elements in *Lsh*$^{off/off}$, as expression of viral mRNA has previously been associated with modulation of translational machinery expression (Le Sage et al. 2016). Also, retroviral element overexpression may explain the over-representation of the anti-microbial humoral immune response (Chernyavskaya et al. 2017, Grow et al. 2015). The overexpression non-optic nerve associated genes, retroviral elements and the associated responses to this over expression could conceivably perturb OL differentiation.

Figure 6-6 Overexpressed genes in *Lsh*$^{off/off}$ optic nerve are from divergent biological processes and generally expressed to a low level in *Lsh*$^{+/off}$

A) Gene ontology analysis by G:profiler of overexpressed genes in *Lsh*$^{off/off}$ in comparison to *Lsh*$^{+/off}$
B) Fold change of genes in *Lsh*$^{off/off}$ relative to *Lsh*$^{+/off}$ plotted against expression in *Lsh*$^{+/off}$ and colour coded to expression in *Lsh*$^{off/off}$. There is a tendency in low expression genes in *Lsh*$^{+/off}$ to be more overexpressed in *Lsh*$^{off/off}$ than the reverse comparison, although the colour coding reveals, despite high fold changes the contribution of their genes do not represent a large number of transcripts in *Lsh*$^{off/off}$ optic nerve,
C) Sum of normalised read counts mapping to IAP elements across libraries sequenced.
D) qPCR using IAP element specific primers on cDNA from CNS tissues in *Lsh*$^{+/off}$ and *Lsh*$^{off/off}$. Error bars represent standard deviation and bars mean of 2 biological replicates (see materials and methods).

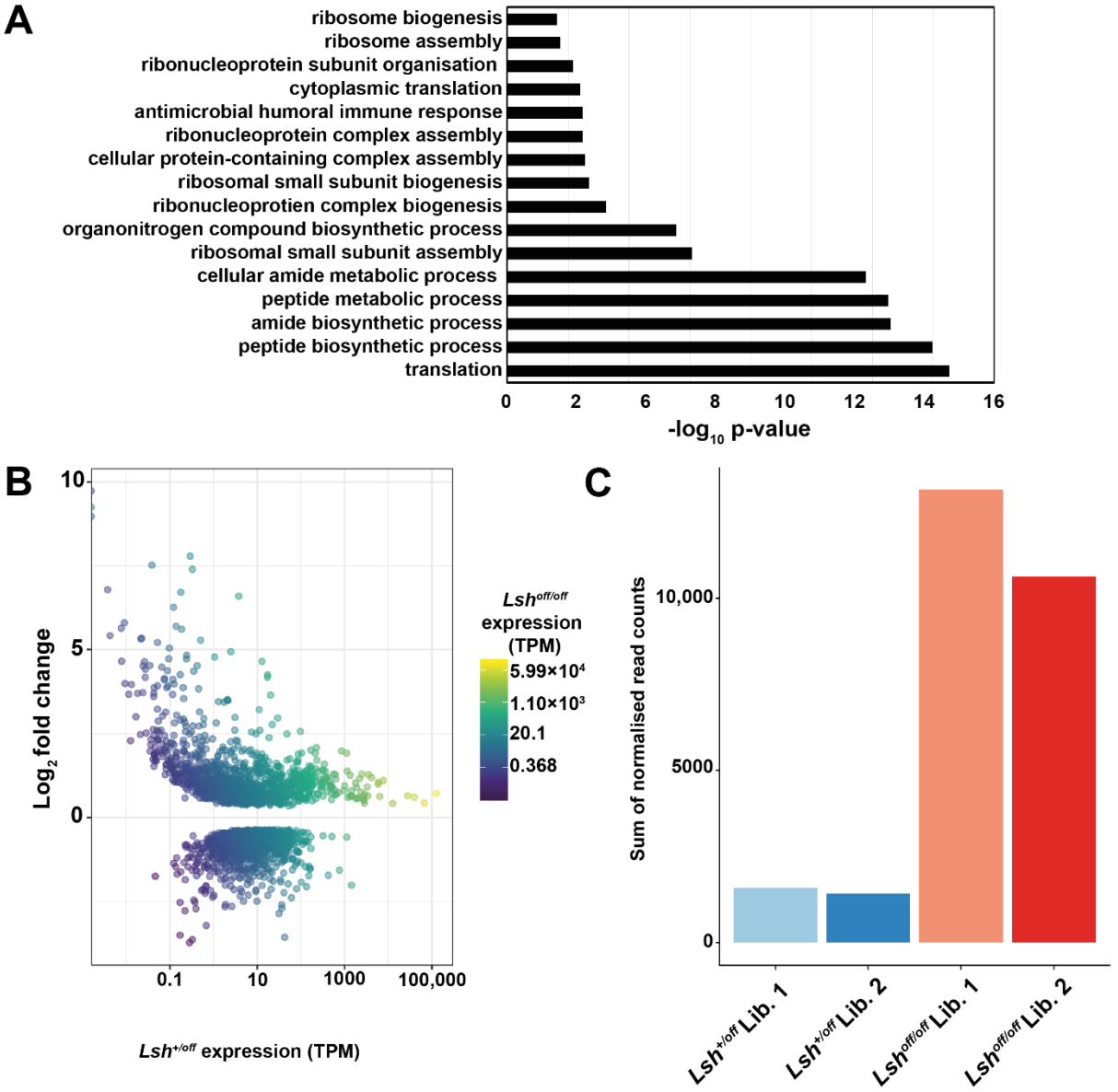
A
ribosome biogenesis
ribosome assembly
ribonucleoprotein subunit organisation
cytoplasmic translation
antimicrobial humoral immune response
ribonucleoprotein complex assembly
cellular protein-containing complex assembly
ribosomal small subunit biogenesis
ribonucleoprotien complex biogenesis
organonitrogen compound biosynthetic process
ribosomal small subunit assembly
cellular amide metabolic process
peptide metabolic process
amide biosynthetic process
peptide biosynthetic process
translation
0 2 6 8 10 12 14 16
-log10 p-value
B
10
5
0
Log2 fold change
0.1 10 1000 100,000
Lsh+/off expression (TPM)
Lshoff/off expression (TPM)
5.99×10⁴
1.10×10³
20.1
0.368
C
10,000
5000
0
Sum of normalised read counts
Lsh+/off Lib. 1
Lsh+/off Lib. 2
Lshoff/off Lib. 1
Lshoff/off Lib. 2
D
25
20
15
10
5
0
Fold change in expression relative to Lsh+/off normalised to Gapdh
P14 Lshoff/off optic nerve
P90 Lshoff/off optic nerve
P90 Lshoff/off spinal cord

6.2 There is genome wide DNA hypomethylation in *Lsh*$^{off/off}$ OPCs, but these patterns are largely unchanged on rescue of LSH expression

6.2.1 Introduction

The RNA-seq on P90 optic nerve identifies several potentially causal factors for the OL differentiation defect, the failure to upregulate genes involved in cholesterol biosynthesis and the overexpression of genes that are non-CNS lineage specific along with endogenous transposable elements and genes involved in translation. It is possible that any or all of these changes in gene expression are not causal, but either a secondary effect of inability to differentiate, in the case of cholesterol biosynthesis genes, or do not affect OLs ability to differentiate, which may be the case with the relatively low total expression levels of IAPs and non-CNS specific genes.

To shed light on what aspect of LSH's molecular function is required for its essential role in OL differentiation, I need to distinguish which of these observed changes in expression are causal of the OL differentiation defect. In order to attempt this, I need to interrogate a system in which the secondary effects of a failure to differentiate, such as potentially the lack of late stage gene upregulation, are not apparent, but where the molecular cause of failure to differentiate has already been established. Previous experiments exploiting the conditionally reversable nature of the *Lsh*^{off} allele reveal that LSH expression in OPCs and late in the lineage can rescue the OL differentiation defect (Fig 5.3). In addition, OPC specific knock-out of LSH causes no myelination or OL differentiation phenotype. I reasoned therefor that the molecular cause of the *Lsh*$^{off/off}$ phenotype must be present in *Lsh*$^{off/off}$ OPCs before they differentiate to mOLs. I also reasoned if I could interrogate OPCs that have not yet initiated differentiation in *Lsh*$^{off/off}$ and control genotypes, then any secondary effects of a failure to differentiate will not have arisen.

To address if changes in gene expression revealed in the RNA-seq are compatible with OL differentiation, especially conceivable in the case of non-CNS genes and IAPs, I needed to interrogate a system in which only a subset of the LSH's activity was recapitulated, but OLs could still differentiate. This would enable me to rule out non-essential aspects of LSH's molecular function, as presumably non-essential molecular differences from control genotypes seen in *Lsh*$^{off/off}$ animals would still be present in the partial LSH rescue. I reasoned that because *Lsh*$^{off/off}$*;Pdgfrα-Cre* animals still possess some phenotypes of *Lsh*$^{off/off}$, their progenitors of OPCs lack LSH throughout early development before the specification of OL lineage cells and their OPCs are still ultimately able to differentiate and form myelin, they might fit the criteria needed. Whether they do depends on if the *Lsh*$^{off/off}$*;Pdgfrα-Cre* OPCs completely rescue all molecular defects seen in *Lsh*$^{off/off}$, even those not essential for differentiation, but this itself could not be seen without some interrogation of their molecular phenotype.

In addition to which cells to interrogate, I also needed to decide what aspect of LSH's known molecular function to investigate. I hypothesised that as changes in DNA methylation are observable in every hypomorphic or *Lsh* knock-out line and the modification recently has been implicated in OL differentiation, though using an approach that makes identification of loci requiring methylation for OPCs to differentiate difficult (Moyon et al. 2016), that changes in DNA methylation as specific loci in *Lsh*$^{off/off}$ OPCs prior to differentiation were responsible for the differentiation defect.

6.2.2 *Lsh*$^{off/off}$*;Pdgfrα-Cre* OPCs have only a slight rescue in total mCpG levels, which is evenly distributed across genomic features

To test the hypothesis that rescue in phenotype is accompanied by rescue in DNA methylation at regulatory regions of specific genes, I performed whole-genome bisulphite sequencing of DNA from OPCs isolated from *Lsh*$^{+/off}$*;Pdgfra-Cre, Lsh*$^{off/off}$*;Pdgfrα-Cre* and *Lsh*$^{off/off}$ P7 cortexes. Fold coverage averaged ~6 across CpGs in libraries for each

condition, however ~58% of CpGs were covered by <3 reads, with some regions being covered far more than others. I decided to use low coverage initially due to cost constraints, and the conceivable possibility that DNA methylation is not restored in the rescued OPCs, as previous experiments in the Stancheva lab showed this was the case for LSH regulated loci in *in vitro* rescued MEF cell lines (work by Natalia Torrea). Comparison of total methyl CpG levels between genotypes revealed that indeed methylation was not restored in rescued OPCs to a significantly above that of *Lsh*$^{off/off}$ (Fig. 6.7A). I reasoned that it was conceivable that differences in the distribution of methylation in the genome could still be an important molecular signature for differentiation essential LSH activity. To test this possibility, I decided to map percent changes in CpG methylation in 1 Kb windows across genotypes reasoning that skewed rescue of methylation in *Lsh*$^{off/off}$*;Pdgfrα-Cre* to a particular features supports a functional impact related to the generalised function of methylation at that feature. For example, DNA methylation in promoters is negatively correlated with gene expression (Discussed in chapter 1). This analysis revealed no more apparent rescue of CpG methylation in any region based on median percentage CpG methylation (Fig. 6.7B). This analysis therefore rules out a generalised rescue at methylation in promoters or gene body regions, where correlation between gene expression and DNA methylation is more well studied. The median value in such the window analysis is heavily skewed by low coverage regions giving a binary output for methylation percentage. Coverage however is grossly similar across features between genotypes, presumably limiting the effect of this skew in comparative analysis (Fig.6.7C), low coverage in certain regions, for example distal intergenic, could be an explanation for lack of changes detected in rescue in *Lsh*$^{off/off}$*;Pdgfrα-Cre*. Due to a lack of statistical significance testing in this analysis, average CpG methylation changes at a locus cannot be determined to be greater than those expected by chance. This leads to an inability to detect changes at specific features that may have a disproportionate impact on the OL differentiation phenotype. There is also no way of telling from this analysis if features methylated to a greater extent in *Lsh*$^{off/off}$*;Pdgfrα-Cre* are hypomethylated in *Lsh*$^{off/off}$.

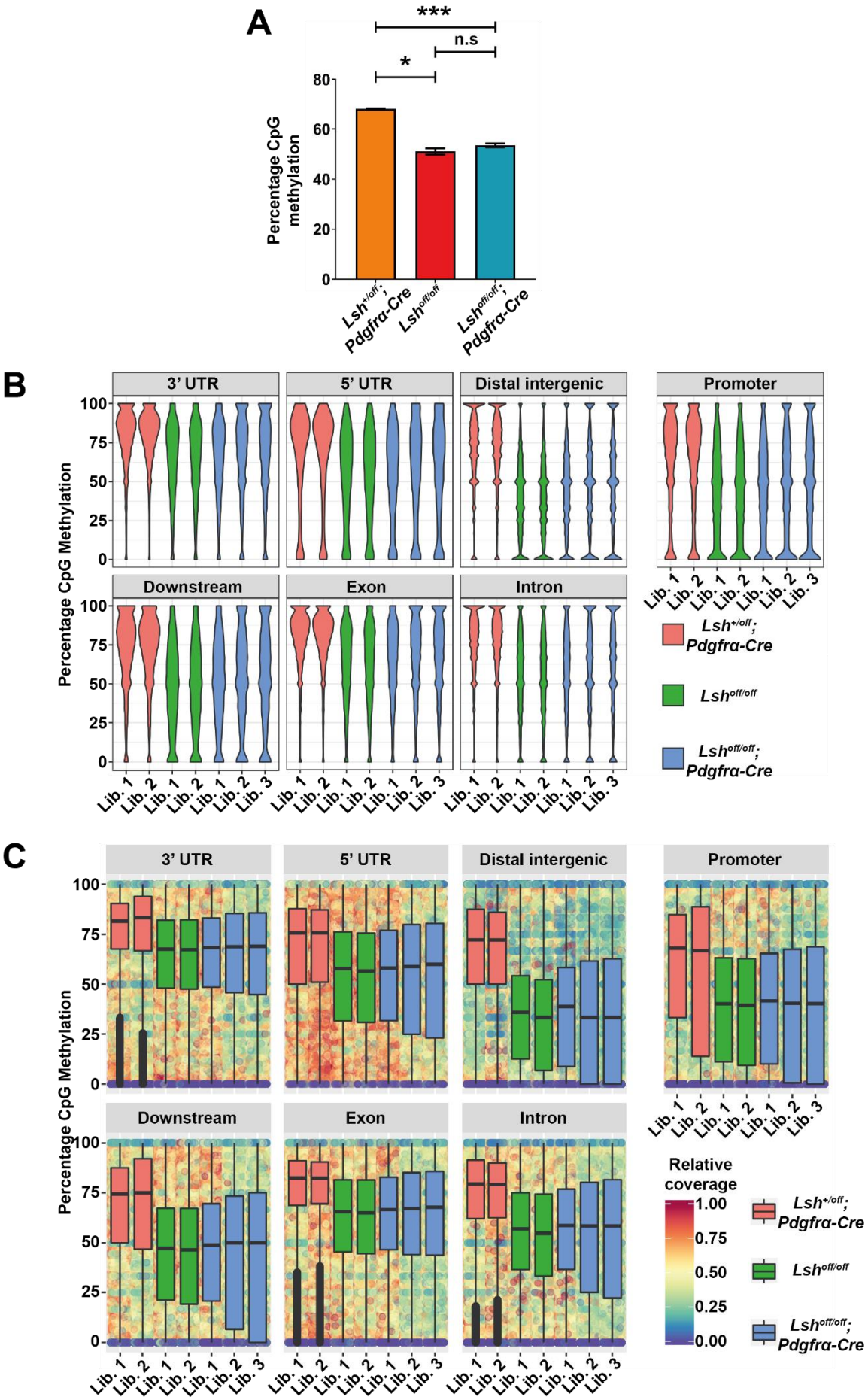
A
***
n.s
*
Percentage CpG methylation
80
60
40
20
0
Lsh+/off; Pdgfrα-Cre
Lshoff/off
Lshoff/off; Pdgfrα-Cre
B
3' UTR
5' UTR
Distal intergenic
Promoter
Downstream
Exon
Intron
Percentage CpG Methylation
100
75
50
25
0
Lib. 1
Lib. 2
Lib. 3
Lsh+/off; Pdgfrα-Cre
Lshoff/off
Lshoff/off; Pdgfrα-Cre
C
3' UTR
5' UTR
Distal intergenic
Promoter
Downstream
Exon
Intron
Percentage CpG Methylation
Relative coverage
1.00
0.75
0.50
0.25
0.00
Lsh+/off; Pdgfrα-Cre
Lshoff/off
Lshoff/off; Pdgfrα-Cre

Figure 6-7 DNA methylation levels are largely unchanged on rescue of LSH expression in the oligodendrocyte lineage

A) Percentage CpG methylation detected in bisulphite sequencing of libraries across genotypes. Error bars represent standard deviation between the percentage values given, unpaired t-tests were used to calculate statistical significance. *=P<0.05. ***=P<0.0005
B) Violin plots of percentage methylation for 1kb windows of the genome stratified by contents of genomic features.
C) The same data as B plotted as boxplots with points colour coded according to coverage, with each point representing a 1kb window and 1 relative coverage being the most covered window in the genome and 0 the least.

6.2.3 Differentially methylated regions overlap extensively between *Lsh$^{off/off}$* and rescue.

To try and address these caveats, I decided to see if a skew towards a feature was present in statistically significant differentially methylated regions (DMRs) derived from pair-wise comparisons between genotypes. Analysis reveals 8107 DMRs in comparison *Lsh$^{off/off}$* vs *Lsh$^{+/off}$;Pdgfrα-Cre,* 7643 in *Lsh$^{off/off}$;Pdgfrα-Cre* vs *Lsh$^{+/off}$;Pdgfrα-Cre* and 1688 in *Lsh$^{off/off}$* vs *Lsh$^{off/off}$;Pdgfrα-Cre* (Fig.6.8A). The similar number of DMRs in *Lsh$^{off/off}$* vs *Lsh$^{+/off}$;Pdgfrα-Cre* and *Lsh$^{off/off}$;Pdgfrα-Cre* vs *Lsh$^{+/off}$;Pdgfrα-Cre* supports the conclusion of previous analysis that the 2 conditions where LSH has been absent during the early stage of development, when most DNA methylation is established (Reik 2007), are comparably different from *Lsh$^{+/off}$;Pdgfrα-Cre*. Comparison of the genomic feature annotation for these comparisons interestingly shows that the largest single feature represent in the DMRs between *Lsh$^{off/off}$* vs *Lsh$^{+/off}$;Pdgfrα-Cre* fall within <=1Kb of a promotor region (Fig.6.8B). This is surprising as LSH has previously been characterised to have most impact in regions of heterochromatin. This promoter overrepresentation is also present in the *Lsh$^{off/off}$;Pdgfrα-Cre* vs *Lsh$^{+/off}$;Pdgfrα-Cre* DMRs, which share a similar distribution in DMR features to *Lsh$^{off/off}$* vs *Lsh$^{+/off}$;Pdgfrα-Cre*, though with a lower proportion of promoters differentially methylated in favour for more DMRs in distal intergenic regions (Fig. 6.8C). This proportion of distal intergenic regions represented in DMRs is highest in the *Lsh$^{off/off}$* vs *Lsh$^{off/off}$;Pdgfrα-Cre* DMR feature analysis (Fig. 6.8D).

Despite the *Lsh*$^{off/off}$ vs *Lsh*$^{off/off}$*;Pdgfrα-Cre* comparison revealing by far the least number of DMRs, this was still more than the overall CpG methylation levels in the genotype would suggest. This implies that methylation is going both up and down in the DMRs, with the average total CpG methylation remaining similar. To gain insight into what extent these DMRs represent a return to *Lsh*$^{+/off}$*;Pdgfrα-Cre* DNA methylation patterns, and if those returns in methylation could be present in regulatory regions of genes that are conceivably related to the OL differentiation phenotype I set out to analyse the overlaps between DMRs in the different comparisons. As expected, the greatest overlap between comparisons is between *Lsh*$^{off/off}$ vs *Lsh*$^{+/off}$*;Pdgfrα-Cre* and *Lsh*$^{off/off}$*;Pdgfrα-Cre* vs *Lsh*$^{+/off}$*;Pdgfrα-Cre* with 5652 regions overlapping (Fig. 6.8E). These follow a similar feature distribution to the previous comparisons of *Lsh*$^{off/off}$ or *Lsh*$^{off/off}$*;Pdgfrα-Cre* to *Lsh*$^{+/off}$*;Pdgfrα-Cre* but with an increased proportion of promoters represented, supporting the conclusions earlier that these are the regions LSH acts on following rescue (Fig. 6.8F). The second biggest overlap is between all 3 comparisons, representing 1651, 98% of all DMRs present between *Lsh*$^{off/off}$ vs *Lsh*$^{off/off}$*;Pdgfrα-Cre*, meaning that nearly all of the DMRs between *Lsh*$^{off/off}$ vs *Lsh*$^{off/off}$*;Pdgfrα-Cre* are also present in *Lsh*$^{off/off}$*;Pdgfrα-Cre* vs *Lsh*$^{+/off}$*;Pdgfrα-Cre*, and so do not represent a return to usual patterns required for OL differentiation (Fig.6.8E). Strikingly only 7 DMRs fit this criteria, being different between both *Lsh*$^{off/off}$ vs *Lsh*$^{+/off}$*;Pdgfrα-Cre* and *Lsh*$^{off/off}$ vs *Lsh*$^{off/off}$*;Pdgfrα-Cre* (Fig.6.8E). Only 1 of these is present in the of promoter region of a protein coding gene, and 1 a microRNA. Remaining DMRs are equally distributed between remaining features (Fig.6.8G). Taken together the bisulphite analysis rejects the hypothesis that DNA methylation in OPCs is the causal factor in the *Lsh*$^{off/off}$ differentiation defect.

Figure 6-8 DMR analysis supports a lack of change in DNA methylation in rescued OPCs

A) The number of DMRs called across pairwise comparisons between genotypes.
B-D) Distribution of genomic features within DMRs called for pairwise comparisons between genotypes.
E) Bar graph showing the extent of shared DMRs between different comparisons, a filled in black dot for a comparison indicates the bar above includes all the DMRs that are shared with other black dot comparisons in the column, and not within any of the unfilled dots.
F-G) Distribution of genomic features within DMRs called as shared and unique between multiple pairwise comparisons between genotypes.

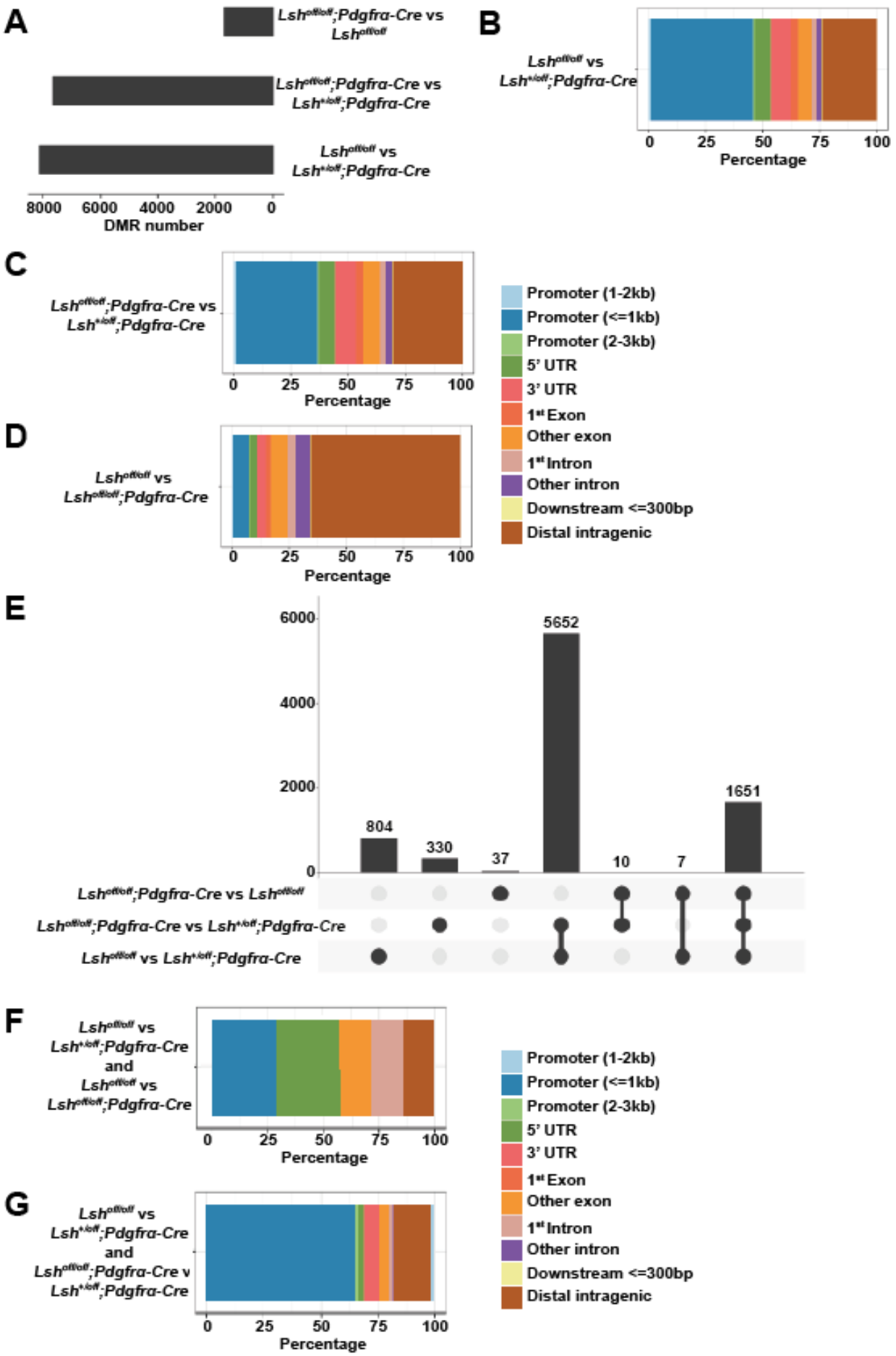
A
Lsh^off/off;Pdgfra-Cre vs Lsh^off/off
Lsh^off/off;Pdgfra-Cre vs Lsh^+/off;Pdgfra-Cre
Lsh^off/off vs Lsh^+/off;Pdgfra-Cre
8000 6000 4000 2000 0
DMR number
B
Lsh^off/off vs Lsh^+/off;Pdgfra-Cre
0 25 50 75 100
Percentage
C
Lsh^off/off;Pdgfra-Cre vs Lsh^+/off;Pdgfra-Cre
0 25 50 75 100
Percentage
D
Lsh^off/off vs Lsh^off/off;Pdgfra-Cre
0 25 50 75 100
Percentage
Promoter (1-2kb)
Promoter (<=1kb)
Promoter (2-3kb)
5' UTR
3' UTR
1st Exon
Other exon
1st Intron
Other intron
Downstream <=300bp
Distal intragenic
E
6000
4000
2000
0
804
330
37
5652
10
7
1651
Lsh^off/off;Pdgfra-Cre vs Lsh^off/off
Lsh^off/off;Pdgfra-Cre vs Lsh^+/off;Pdgfra-Cre
Lsh^off/off vs Lsh^+/off;Pdgfra-Cre
F
Lsh^off/off vs Lsh^+/off;Pdgfra-Cre and Lsh^off/off vs Lsh^off/off;Pdgfra-Cre
0 25 50 75 100
Percentage
G
Lsh^off/off vs Lsh^+/off;Pdgfra-Cre and Lsh^off/off;Pdgfra-Cre v Lsh^+/off;Pdgfra-Cre
0 25 50 75 100
Percentage
Promoter (1-2kb)
Promoter (<=1kb)
Promoter (2-3kb)
5' UTR
3' UTR
1st Exon
Other exon
1st Intron
Other intron
Downstream <=300bp
Distal intragenic

6.3 Summary

Differential expression analysis of *Lsh*$^{off/off}$ and *Lsh*$^{+/off}$ optic nerve RNA-seq and comparison to the Barres database reveals that the differentiation defect in *Lsh*$^{off/off}$ mainly results in a under expression of mOL genes, with other CNS cell types at least not being effected in a way that alters their differentiation from progenitors or cell fate choice in the optic nerve (as would be indicated by a large under-expression or overexpression in genes particular to that cell type). Comparison to gene sets defined as changing during OL differentiation highlights that the under-expression of mature genes is not generic to all such genes, with some genes upregulated late during differentiation being overexpressed in *Lsh*$^{off/off}$. The comparison to *in vivo* single cell RNA-seq derived definitions of OL cell types supports both these conclusions, with mature genes again being under-expressed but not genes expressed in myelin forming OLs or a selection of OL subtypes. However, it cannot be ruled out that this is the result of those subtypes not being present in either genotype as they represent a character of OL from a different anatomical location or developmental timepoint.

Gene ontology analysis reveals a strong enrichment for cholesterol biosynthesis genes being under expressed in *Lsh*$^{off/off}$ which could conceivably be a route cause for failure to differentiate. However, this could be a secondary effect on expression caused by failure to differentiate, rather than mis-regulation of gene expression due to LSH need to be ruled out.

Attempts to do this by looking at one aspect of chromatin state (DNA methylation) in OPCs, a stage we know there is likely to be a defect caused by LSH deficiency, due to the ability of cells that lose LSH past this point to differentiate normally, failed to find any significant differences between cells unable to differentiate and those that are phenotypically rescued. This indicates that some other aspect of LSH function could be responsible for establishing a failure to differentiate in OPCs early in life.

Chapter Seven- Discussion

Many unanswered questions remain about LSH's potential function in OL differentiation and during this PhD I have only really been successful in characterising that a cell autonomous defect in differentiation exists when LSH is absent in OPCs. I will briefly discuss here the progress on achieving my project aims, with a view to what future work might be fruitful in expanding upon what I have been able to achieve in my PhD.

7.1 Is *Lsh*$^{off/off}$ a complete knock-out of LSH expression? What phenotypic defect(s) is/are present in the *Lsh*$^{off/off}$ mouse?

In relation to the first aspect of the aim, I have been successful in quantifying at least a 97% knock out in LSH protein through a western blotting approach. However, there are several caveats in using this technique to measure extent of knock-out. For example, the less efficient transfer of higher molecular weight proteins means it is possible that a fusion protein of LSHGFPneo (around 170kDa) exists in these cells, and the difficulty in detecting either GFP or LSH via techniques such as immunofluorescence has frustrated attempts to overcome this problem. Previously in the Stancheva lab, a mass spectroscopy-based attempt of quantifying LSH peptides between *Lsh*$^{+/+}$ and *Lsh*$^{off/off}$ was attempted, but insufficient peptide numbers in *Lsh*$^{+/+}$ cells made any quantitative comparison impossible. In the light of this I think it's practical to adopt an approach that recognises the possibility of hypomorphic mutation in the *Lsh*$^{off/off}$ allele. So what I have chosen to focus on during my project is the phenotype of the *Lsh*$^{off/off}$ mice.

Through extensive characterisation of myelination and OPC gene marker expression I have successfully characterised a cell autonomous OL differentiation defect, uncovering a new role for LSH in this lineage. But this is not the only potentially interesting phenotype these mice possess. Small spleen and preliminary data from a previous post-doc Anuj Sengal also

hint at a B-cell maturation defect in these mice. A potential function of LSH in immune cells has long been recognised (Geiman and Muegge 2000). This also provides a link with the pathophysiology of ICF syndrome, which is recognised to be caused by mutations in *Lsh (Thijssen et al. 2016).* Indeed, several ICF patients have present with corpus callosum hypoplasia (Hagleitner et al. 2008)which could conceivably be linked to an as yet unrecognised myelination defect. The extent to which this mouse could be used as a disease model for therefor ICF warrants further investigation.

7.2 In what cell type(s) and at what stage in development is LSH required?

Again, progress has been made on this aim through the *Pdgfrα-Cre* driver experiments showing that LSH is specifically required in OPCs and not later in development. A problem however is again verifying that the second conversion necessary to convert to Lsh^{off2} in the OPC specific knock-out actually abolishes expression of the protein. Due to LSH's relatively low level of expression and difficulty of detection, an experiment in a cell type that expresses LSH highly is required, such as $Lsh^{on/on}$ MEFs or ESCs with an inducible Cre.

Another important question however is can restoration of LSH in adult $Lsh^{off/off}$ CNS rescue the phenotype. This experiment is currently in progress using a tamoxifen inducible Cre line crossed into Lsh^{off}. Interesting preliminary observations indicate that although the growth and weightless phenotype is largely rescued in these animals, they are still ataxic. If it is the case that this ataxia is due to inability of OPCs to differentiate even when LSH expression is restored, it strongly supports the conclusions of this thesis that early life expression of LSH is the essential aspect. If this is the case $Lsh^{off/off}$ could provide a good system in which to study the early life chromatin events that are essential for subsequent differentiation.

7.3 What is the molecular mechanism of any *Lsh*$^{off/off}$ phenotype?

This is probably the most unexplored aim of the thesis, despite extensive focus placed on it. The result that DNA methylation is not rescued in OPCs rescued for LSH expression prompts several possibilities. Does DNA methylation become restored later in life closer to differentiation? Is chromatin state at all altered in *Lsh*$^{off/off}$ OPCs? To address these a more thorough exploration of the OPC phenotype is required.

For example, RNA-seq in OPCs would reveal the loci that become affected before secondary effects of failure to differentiate arise, a key caveat of the optic nerve RNA-seq experiment. Low in-put ChIP methods are now available that would enable interrogation of LSH or histone modifications, such as H3K9me2 and H3K9me3, to see if LSH's previously characterised association with G9a is the crucial effector on chromatin that is important for OL differentiation (Brind'Amour et al. 2015).

A simple experiment that would support the possibility raised by optic nerve RNA-seq that cholesterol biosynthesis is the key factor in the *Lsh*$^{off/off}$ OPC phenotype would be isolation and culture of *Lsh*$^{off/off}$ OPCs supplemented with increased cholesterol or statins, this has proven successful in other mouse models deficient in this pathway (Lin et al. 2017).

An intriguing possibility is that LSH does not act on any particular gene that is important for the myelination process, but instead the depletion of heterochromatin caused by its knock-out leads to a deficit of activating histone modifications and or trans activations of transcription. Evidence for this could be the spurious overexpression of normally silent genes we see in *Lsh*$^{off/off}$ optic nerve. With seemingly litter changed in DNA methylation in the rescue, it could be that later in development LSH has a DNA methylation independent silencing function that can rescue this phenotype. To investigate this a technique such as ATAC-seq that interrogates accessibility of chromatin rather than a particular mark.

7.4 Final summary

I have been able to make progress in all aims in this project, uncovering a new role for LSH in a postnatal *in vivo* developmental process and showing that LSH is required early in OPC differentiation to mOLs, but not late. Efforts to look into potential mechanisms reveal that rescue in phenotype is not accompanied by rescue of DNA methylation early in the lineage, opening the possibility that there are previously unknown waves of establishment for *de* novo DNA methylation later in OL lineage, or that LSH in fact possesses DNA-methylation independent gene regulatory activity.

Appendix

8.1 Video 1

This is an example of a mild ataxia and tremor phenotype in a P80 *Lsh*$^{off/off}$ animal (top of cage on start) and a healthy *Lsh*$^{+/of}$ littermate.

8.2 Video 2

This is an example of a mild ataxia phenotype in a P94 *Lsh*$^{off/off}$ animal (top of cage at start) and 2 healthy *Lsh*$^{+/off}$ littermates.

8.3 Video 3

This is an example of a moderate ataxia and tremor phenotype in an P91 *Lsh*$^{off/off}$ animal (middle of the 3 at start) and 2 healthy *Lsh*$^{+/off}$ littermates, Increased huntching of back and reduced movement are the main contributors to higher score than video 1 or 2.

8.4 Video 4

This is an example of severe ataxia and tremor in a P100 *Lsh*$^{off/off}$ animal.

8.5 Video 5

This is a healthy P72 *Lsh*$^{off/off}$*;Pdgfrα-Cre* animal.

8.6 Video 6

These are all healthy *Lsh*$^{on/on}$ P97 littermates.

References

Allis, C. D. and Jenuwein, T. (2016) 'The molecular hallmarks of epigenetic control', *Nat Rev Genet,* 17(8), 487-500.

Almeida, R. G., Czopka, T., Ffrench-Constant, C. and Lyons, D. A. (2011) 'Individual axons regulate the myelinating potential of single oligodendrocytes in vivo', *Development,* 138(20), 4443-50.

Amabile, A., Migliara, A., Capasso, P., Biffi, M., Cittaro, D., Naldini, L. and Lombardo, A. (2016) 'Inheritable Silencing of Endogenous Genes by Hit-and-Run Targeted Epigenetic Editing', *Cell,* 167(1), 219-232.e14.

Andrae, J., Gouveia, L., He, L. and Betsholtz, C. (2014) 'Characterization of platelet-derived growth factor-A expression in mouse tissues using a lacZ knock-in approach', *PLoS One,* 9(8), e105477.

Antequera, F. and Bird, A. (1993) 'Number of CpG islands and genes in human and mouse', *Proc Natl Acad Sci U S A,* 90(24), 11995-9.

Bachman, M., Uribe-Lewis, S., Yang, X., Williams, M., Murrell, A. and Balasubramanian, S. (2014) '5-Hydroxymethylcytosine is a predominantly stable DNA modification', *Nat Chem,* 6(12), 1049-55.

Barski, A., Cuddapah, S., Cui, K., Roh, T. Y., Schones, D. E., Wang, Z., Wei, G., Chepelev, I. and Zhao, K. (2007) 'High-resolution profiling of histone methylations in the human genome', *Cell,* 129(4), 823-37.

Berger, S. L., Kouzarides, T., Shiekhattar, R. and Shilatifard, A. (2009) 'An operational definition of epigenetics', *Genes Dev,* 23(7), 781-3.

Bird, A. (2002) 'DNA methylation patterns and epigenetic memory', *Genes Dev,* 16(1), 6-21.

Bird, A., Taggart, M., Frommer, M., Miller, O. J. and Macleod, D. (1985) 'A fraction of the mouse genome that is derived from islands of nonmethylated, CpG-rich DNA', *Cell,* 40(1), 91-9.

Bird, A. P. (1980) 'DNA methylation and the frequency of CpG in animal DNA', *Nucleic Acids Res,* 8(7), 1499-504.

Bischof, M., Weider, M., Küspert, M., Nave, K. A. and Wegner, M. (2015) 'Brg1-dependent chromatin remodelling is not essentially required during oligodendroglial differentiation', *J Neurosci,* 35(1), 21-35.

Bork, P. and Koonin, E. V. (1993) 'An expanding family of helicases within the 'DEAD/H' superfamily', *Nucleic Acids Res,* 21(3), 751-2.

Boulanger, J. J. and Messier, C. (2014) 'From precursors to myelinating oligodendrocytes: contribution of intrinsic and extrinsic factors to white matter plasticity in the adult brain', *Neuroscience,* 269, 343-66.

Boyer, L. A., Plath, K., Zeitlinger, J., Brambrink, T., Medeiros, L. A., Lee, T. I., Levine, S. S., Wernig, M., Tajonar, A., Ray, M. K., Bell, G. W., Otte, A. P., Vidal, M., Gifford, D. K., Young, R. A. and Jaenisch, R. (2006) 'Polycomb complexes repress developmental regulators in murine embryonic stem cells', *Nature,* 441(7091), 349-53.

Brind'Amour, J., Liu, S., Hudson, M., Chen, C., Karimi, M. M. and Lorincz, M. C. (2015) 'An ultra-low-input native ChIP-seq protocol for genome-wide profiling of rare cell populations', *Nat Commun,* 6, 6033.

Brinkman, A. B., Gu, H., Bartels, S. J., Zhang, Y., Matarese, F., Simmer, F., Marks, H., Bock, C., Gnirke, A., Meissner, A. and Stunnenberg, H. G. (2012) 'Sequential ChIP-bisulfite sequencing enables direct genome-scale investigation of chromatin and DNA methylation cross-talk', *Genome Res,* 22(6), 1128-38.

Briscoe, J., Pierani, A., Jessell, T. M. and Ericson, J. (2000) 'A homeodomain protein code specifies progenitor cell identity and neuronal fate in the ventral neural tube', *Cell,* 101(4), 435-45.

Brzeski, J. and Jerzmanowski, A. (2003) 'Deficient in DNA methylation 1 (DDM1) defines a novel family of chromatin-remodeling factors', *J Biol Chem,* 278(2), 823-8.

Burns, L. G. and Peterson, C. L. (1997) 'The yeast SWI-SNF complex facilitates binding of a transcriptional activator to nucleosomal sites in vivo', *Mol Cell Biol,* 17(8), 4811-9.

Cahoy, J. D., Emery, B., Kaushal, A., Foo, L. C., Zamanian, J. L., Christopherson, K. S., Xing, Y., Lubischer, J. L., Krieg, P. A., Krupenko, S. A., Thompson, W. J. and Barres, B. A. (2008) 'A transcriptome database for astrocytes, neurons, and oligodendrocytes: a new resource for understanding brain development and function', *J Neurosci,* 28(1), 264-78.

Chen, T. and Dent, S. Y. (2014) 'Chromatin modifiers and remodellers: regulators of cellular differentiation', *Nat Rev Genet,* 15(2), 93-106.

Chen, T., Hevi, S., Gay, F., Tsujimoto, N., He, T., Zhang, B., Ueda, Y. and Li, E. (2007) 'Complete inactivation of DNMT1 leads to mitotic catastrophe in human cancer cells', *Nat Genet,* 39(3), 391-6.

Chen, Y., Tian, D., Ku, L., Osterhout, D. J. and Feng, Y. (2007) 'The selective RNA-binding protein quaking I (QKI) is necessary and sufficient for promoting oligodendroglia differentiation', *J Biol Chem,* 282(32), 23553-60.

Chereji, R. V., Kan, T. W., Grudniewska, M. K., Romashchenko, A. V., Berezikov, E., Zhimulev, I. F., Guryev, V., Morozov, A. V. and Moshkin, Y. M. (2016) 'Genome-wide profiling of nucleosome sensitivity and chromatin accessibility in Drosophila melanogaster', *Nucleic Acids Res,* 44(3), 1036-51.

Chernyavskaya, Y., Mudbhary, R., Zhang, C., Tokarz, D., Jacob, V., Gopinath, S., Sun, X., Wang, S., Magnani, E., Madakashira, B. P., Yoder, J. A., Hoshida, Y. and Sadler, K. C. (2017) 'Loss of DNA methylation in zebrafish embryos activates retrotransposons to trigger antiviral signaling', *Development,* 144(16), 2925-2939.

Chi, T. H., Wan, M., Lee, P. P., Akashi, K., Metzger, D., Chambon, P., Wilson, C. B. and Crabtree, G. R. (2003) 'Sequential roles of Brg, the ATPase subunit of BAF chromatin remodeling complexes, in thymocyte development', *Immunity,* 19(2), 169-82.

Chi, T. H., Wan, M., Zhao, K., Taniuchi, I., Chen, L., Littman, D. R. and Crabtree, G. R. (2002) 'Reciprocal regulation of CD4/CD8 expression by SWI/SNF-like BAF complexes', *Nature,* 418(6894), 195-9.

Chomiak, T. and Hu, B. (2009) 'What is the optimal value of the g-ratio for myelinated fibers in the rat CNS? A theoretical approach', *PLoS One,* 4(11), e7754.

Chrast, R., Saher, G., Nave, K. A. and Verheijen, M. H. (2011) 'Lipid metabolism in myelinating glial cells: lessons from human inherited disorders and mouse models', *J Lipid Res,* 52(3), 419-34.

Cirillo, L. A., Lin, F. R., Cuesta, I., Friedman, D., Jarnik, M. and Zaret, K. S. (2002) 'Opening of compacted chromatin by early developmental transcription factors HNF3 (FoxA) and GATA-4', *Mol Cell,* 9(2), 279-89.

Clapier, C. R., Iwasa, J., Cairns, B. R. and Peterson, C. L. (2017) 'Mechanisms of action and regulation of ATP-dependent chromatin-remodelling complexes', *Nat Rev Mol Cell Biol,* 18(7), 407-422.

Cosma, M. P., Tanaka, T. and Nasmyth, K. (1999) 'Ordered recruitment of transcription and chromatin remodeling factors to a cell cycle- and developmentally regulated promoter', *Cell,* 97(3), 299-311.

Coulondre, C., Miller, J. H., Farabaugh, P. J. and Gilbert, W. (1978) 'Molecular basis of base substitution hotspots in Escherichia coli', *Nature,* 274(5673), 775-80.

Côté, J., Quinn, J., Workman, J. L. and Peterson, C. L. (1994) 'Stimulation of GAL4 derivative binding to nucleosomal DNA by the yeast SWI/SNF complex', *Science,* 265(5168), 53-60.

Dawson, M. R., Polito, A., Levine, J. M. and Reynolds, R. (2003) 'NG2-expressing glial progenitor cells: an abundant and widespread population of cycling cells in the adult rat CNS', *Mol Cell Neurosci,* 24(2), 476-88.

De Rubertis, F., Kadosh, D., Henchoz, S., Pauli, D., Reuter, G., Struhl, K. and Spierer, P. (1996) 'The histone deacetylase RPD3 counteracts genomic silencing in Drosophila and yeast', *Nature,* 384(6609), 589-91.

Dennis, K., Fan, T., Geiman, T., Yan, Q. and Muegge, K. (2001) 'Lsh, a member of the SNF2 family, is required for genome-wide methylation', *Genes Dev,* 15(22), 2940-4.

Dong, K. B., Maksakova, I. A., Mohn, F., Leung, D., Appanah, R., Lee, S., Yang, H. W., Lam, L. L., Mager, D. L., Schübeler, D., Tachibana, M., Shinkai, Y. and Lorincz, M. C. (2008) 'DNA methylation in ES cells requires the lysine methyltransferase G9a but not its catalytic activity', *EMBO J,* 27(20), 2691-701.

Dougherty, K. D., Dreyfus, C. F. and Black, I. B. (2000) 'Brain-derived neurotrophic factor in astrocytes, oligodendrocytes, and microglia/macrophages after spinal cord injury', *Neurobiol Dis,* 7(6 Pt B), 574-85.

Eisen, J. A., Sweder, K. S. and Hanawalt, P. C. (1995) 'Evolution of the SNF2 family of proteins: subfamilies with distinct sequences and functions', *Nucleic Acids Res,* 23(14), 2715-23.

Emery, B., Agalliu, D., Cahoy, J. D., Watkins, T. A., Dugas, J. C., Mulinyawe, S. B., Ibrahim, A., Ligon, K. L., Rowitch, D. H. and Barres, B. A. (2009) 'Myelin gene regulatory factor is a critical transcriptional regulator required for CNS myelination', *Cell,* 138(1), 172-85.

Emery, B. and Dugas, J. C. (2013) 'Purification of oligodendrocyte lineage cells from mouse cortices by immunopanning', *Cold Spring Harb Protoc,* 2013(9), 854-68.

Epsztejn-Litman, S., Feldman, N., Abu-Remaileh, M., Shufaro, Y., Gerson, A., Ueda, J., Deplus, R., Fuks, F., Shinkai, Y., Cedar, H. and Bergman, Y. (2008) 'De novo DNA methylation promoted by G9a prevents reprogramming of embryonically silenced genes', *Nat Struct Mol Biol,* 15(11), 1176-1183.

Fan, T., Yan, Q., Huang, J., Austin, S., Cho, E., Ferris, D. and Muegge, K. (2003) 'Lsh-deficient murine embryonal fibroblasts show reduced proliferation with signs of abnormal mitosis', *Cancer Res,* 63(15), 4677-83.

Feldman, N., Gerson, A., Fang, J., Li, E., Zhang, Y., Shinkai, Y., Cedar, H. and Bergman, Y. (2006) 'G9a-mediated irreversible epigenetic inactivation of Oct-3/4 during early embryogenesis', *Nat Cell Biol,* 8(2), 188-94.

Flaus, A., Martin, D. M., Barton, G. J. and Owen-Hughes, T. (2006) 'Identification of multiple distinct Snf2 subfamilies with conserved structural motifs', *Nucleic Acids Res,* 34(10), 2887-905.

Flores, A. I., Narayanan, S. P., Morse, E. N., Shick, H. E., Yin, X., Kidd, G., Avila, R. L., Kirschner, D. A. and Macklin, W. B. (2008) 'Constitutively active Akt induces enhanced myelination in the CNS', *J Neurosci,* 28(28), 7174-83.

Foran, D. R. and Peterson, A. C. (1992) 'Myelin acquisition in the central nervous system of the mouse revealed by an MBP-Lac Z transgene', *J Neurosci,* 12(12), 4890-7.

Fünfschilling, U., Supplie, L. M., Mahad, D., Boretius, S., Saab, A. S., Edgar, J., Brinkmann, B. G., Kassmann, C. M., Tzvetanova, I. D., Möbius, W., Diaz, F., Meijer, D., Suter, U., Hamprecht, B., Sereda, M. W., Moraes, C. T., Frahm, J., Goebbels, S. and Nave, K. A. (2012) 'Glycolytic oligodendrocytes maintain myelin and long-term axonal integrity', *Nature,* 485(7399), 517-21.

Gatto, S., Gagliardi, M., Franzese, M., Leppert, S., Papa, M., Cammisa, M., Grillo, G., Velasco, G., Francastel, C., Toubiana, S., D'Esposito, M., Angelini, C. and Matarazzo, M. R. (2017) 'ICF-specific DNMT3B dysfunction interferes with intragenic regulation of mRNA transcription and alternative splicing', *Nucleic Acids Res,* 45(10), 5739-5756.

Gautier, F., Bünemann, H. and Grotjahn, L. (1977) 'Analysis of calf-thymus satellite DNA: evidence for specific methylation of cytosine in C-G sequences', *Eur J Biochem,* 80(1), 175-83.

Geiman, T. M., Durum, S. K. and Muegge, K. (1998) 'Characterization of gene expression, genomic structure, and chromosomal localization of Hells (Lsh)', *Genomics,* 54(3), 477-83.

Geiman, T. M. and Muegge, K. (2000) 'Lsh, an SNF2/helicase family member, is required for proliferation of mature T lymphocytes', *Proc Natl Acad Sci U S A,* 97(9), 4772-7.

Geiman, T. M., Tessarollo, L., Anver, M. R., Kopp, J. B., Ward, J. M. and Muegge, K. (2001) 'Lsh, a SNF2 family member, is required for normal murine development', *Biochim Biophys Acta,* 1526(2), 211-20.

Goebbels, S., Oltrogge, J. H., Kemper, R., Heilmann, I., Bormuth, I., Wolfer, S., Wichert, S. P., Mobius, W., Liu, X., Lappe-Siefke, C., Rossner, M. J., Groszer, M., Suter, U., Frahm, J., Boretius, S. and Nave, K. A. (2010) 'Elevated phosphatidylinositol 3,4,5-trisphosphate in glia triggers cell-autonomous membrane wrapping and myelination', *J Neurosci,* 30(26), 8953-64.

Gorbalenya, A. E. and Koonin, E. V. (1993) 'Helicases: amino acid sequence comparisons and structure-function relationships', *Current Opinion in Structural Biology,* 3(3), 419-429.

Gorbalenya, A. E., Koonin, E. V., Donchenko, A. P. and Blinov, V. M. (1988) 'A novel superfamily of nucleoside triphosphate-binding motif containing proteins which are probably involved in duplex unwinding in DNA and RNA replication and recombination', *FEBS Lett,* 235(1-2), 16-24.

Grow, E. J., Flynn, R. A., Chavez, S. L., Bayless, N. L., Wossidlo, M., Wesche, D. J., Martin, L., Ware, C. B., Blish, C. A., Chang, H. Y., Pera, R. A. and Wysocka, J. (2015) 'Intrinsic retroviral reactivation in human preimplantation embryos and pluripotent cells', *Nature,* 522(7555), 221-5.

Hagleitner, M. M., Lankester, A., Maraschio, P., Hultén, M., Fryns, J. P., Schuetz, C., Gimelli, G., Davies, E. G., Gennery, A., Belohradsky, B. H., de Groot, R., Gerritsen, E. J., Mattina, T., Howard, P. J., Fasth, A., Reisli, I., Furthner, D., Slatter, M. A., Cant, A. J., Cazzola, G., van Dijken, P. J., van Deuren, M., de Greef, J. C., van der Maarel, S. M. and Weemaes, C. M. (2008) 'Clinical spectrum of immunodeficiency, centromeric instability and facial dysmorphism (ICF syndrome)', *J Med Genet,* 45(2), 93-9.

Han, Y., Ren, J., Lee, E., Xu, X., Yu, W. and Muegge, K. (2017) 'Lsh/HELLS regulates self-renewal/proliferation of neural stem/progenitor cells', *Sci Rep,* 7(1), 1136.

He, D., Marie, C., Zhao, C., Kim, B., Wang, J., Deng, Y., Clavairoly, A., Frah, M., Wang, H., He, X., Hmidan, H., Jones, B. V., Witte, D., Zalc, B., Zhou, X., Choo, D. I., Martin, D. M., Parras, C. and Lu, Q. R. (2016) 'Chd7 cooperates with Sox10 and regulates the onset of CNS myelination and remyelination', *Nat Neurosci,* 19(5), 678-689.

Heintzman, N. D., Stuart, R. K., Hon, G., Fu, Y., Ching, C. W., Hawkins, R. D., Barrera, L. O., Van Calcar, S., Qu, C., Ching, K. A., Wang, W., Weng, Z., Green, R. D., Crawford, G. E. and Ren, B. (2007) 'Distinct and predictive chromatin signatures of transcriptional promoters and enhancers in the human genome', *Nat Genet,* 39(3), 311-8.

Heitz, E. (1928) *Das Heterochromatin der Moose,* Bornträger.

Hildebrand, C., Remahl, S., Persson, H. and Bjartmar, C. (1993) 'Myelinated nerve fibres in the CNS', *Prog Neurobiol,* 40(3), 319-84.

Hill, R. A., Li, A. M. and Grutzendler, J. (2018) 'Lifelong cortical myelin plasticity and age-related degeneration in the live mammalian brain', *Nat Neurosci,* 21(5), 683-695.

Hirschhorn, J. N., Brown, S. A., Clark, C. D. and Winston, F. (1992) 'Evidence that SNF2/SWI2 and SNF5 activate transcription in yeast by altering chromatin structure', *Genes Dev,* 6(12A), 2288-98.

Ho, L. and Crabtree, G. R. (2010) 'Chromatin remodelling during development', *Nature,* 463(7280), 474-84.

Ho, L., Jothi, R., Ronan, J. L., Cui, K., Zhao, K. and Crabtree, G. R. (2009) 'An embryonic stem cell chromatin remodeling complex, esBAF, is an essential component of the core pluripotency transcriptional network', *Proc Natl Acad Sci U S A,* 106(13), 5187-91.

Holliday, R. and Pugh, J. E. (1975) 'DNA modification mechanisms and gene activity during development', *Science,* 187(4173), 226-32.

Hon, G. C., Song, C. X., Du, T., Jin, F., Selvaraj, S., Lee, A. Y., Yen, C. A., Ye, Z., Mao, S. Q., Wang, B. A., Kuan, S., Edsall, L. E., Zhao, B. S., Xu, G. L., He, C. and Ren, B. (2014) '5mC oxidation by Tet2 modulates enhancer activity and timing of transcriptome reprogramming during differentiation', *Mol Cell,* 56(2), 286-297.

Hsieh, J. and Gage, F. H. (2004) 'Epigenetic control of neural stem cell fate', *Curr Opin Genet Dev,* 14(5), 461-9.

Hsu, H. T., Chen, H. M., Yang, Z., Wang, J., Lee, N. K., Burger, A., Zaret, K., Liu, T., Levine, E. and Mango, S. E. (2015) 'TRANSCRIPTION. Recruitment of RNA polymerase II by the pioneer transcription factor PHA-4', *Science,* 348(6241), 1372-6.

Hubler, Z., Allimuthu, D., Bederman, I., Elitt, M. S., Madhavan, M., Allan, K. C., Shick, H. E., Garrison, E., T Karl, M., Factor, D. C., Nevin, Z. S., Sax, J. L., Thompson, M. A., Fedorov, Y., Jin, J., Wilson, W. K., Giera, M., Bracher, F., Miller, R. H., Tesar, P. J. and Adams, D. J. (2018) 'Accumulation of 8,9-unsaturated sterols drives oligodendrocyte formation and remyelination', *Nature,* 560(7718), 372-376.

Hughes, E. G., Kang, S. H., Fukaya, M. and Bergles, D. E. (2013) 'Oligodendrocyte progenitors balance growth with self-repulsion to achieve homeostasis in the adult brain', *Nat Neurosci,* 16(6), 668-76.

Jackson-Grusby, L., Beard, C., Possemato, R., Tudor, M., Fambrough, D., Csankovszki, G., Dausman, J., Lee, P., Wilson, C., Lander, E. and Jaenisch, R. (2001) 'Loss of genomic methylation causes p53-dependent apoptosis and epigenetic deregulation', *Nat Genet,* 27(1), 31-9.

Jarvis, C. D., Geiman, T., Vila-Storm, M. P., Osipovich, O., Akella, U., Candeias, S., Nathan, I., Durum, S. K. and Muegge, K. (1996) 'A novel putative helicase produced in early murine lymphocytes', *Gene,* 169(2), 203-7.

Jeddeloh, J. A., Stokes, T. L. and Richards, E. J. (1999) 'Maintenance of genomic methylation requires a SWI2/SNF2-like protein', *Nat Genet,* 22(1), 94-7.

Jenness, C., Giunta, S., Müller, M. M., Kimura, H., Muir, T. W. and Funabiki, H. (2018) 'HELLS and CDCA7 comprise a bipartite nucleosome remodeling complex defective in ICF syndrome', *Proc Natl Acad Sci U S A,* 115(5), E876-E885.

Jenuwein, T. and Allis, C. D. (2001) 'Translating the histone code', *Science,* 293(5532), 1074-80.

Jones, P. A. and Taylor, S. M. (1980) 'Cellular differentiation, cytidine analogs and DNA methylation', *Cell,* 20(1), 85-93.

Kakutani, T., Jeddeloh, J. A., Flowers, S. K., Munakata, K. and Richards, E. J. (1996) 'Developmental abnormalities and epimutations associated with DNA hypomethylation mutations', *Proc Natl Acad Sci U S A,* 93(22), 12406-11.

Kakutani, T., Jeddeloh, J. A. and Richards, E. J. (1995) 'Characterization of an Arabidopsis thaliana DNA hypomethylation mutant', *Nucleic Acids Res,* 23(1), 130-7.

Kalyani, A., Hobson, K. and Rao, M. S. (1997) 'Neuroepithelial stem cells from the embryonic spinal cord: isolation, characterization, and clonal analysis', *Dev Biol,* 186(2), 202-23.

Karimi, M. M., Goyal, P., Maksakova, I. A., Bilenky, M., Leung, D., Tang, J. X., Shinkai, Y., Mager, D. L., Jones, S., Hirst, M. and Lorincz, M. C. (2011) 'DNA methylation and SETDB1/H3K9me3 regulate predominantly distinct sets of genes, retroelements, and chimeric transcripts in mESCs', *Cell Stem Cell,* 8(6), 676-87.

Kessaris, N., Fogarty, M., Iannarelli, P., Grist, M., Wegner, M. and Richardson, W. D. (2006) 'Competing waves of oligodendrocytes in the forebrain and postnatal elimination of an embryonic lineage', *Nat Neurosci,* 9(2), 173-9.

Kornberg, R. D. (1974) 'Chromatin structure: a repeating unit of histones and DNA', *Science,* 184(4139), 868-71.

Kundaje, A., Kyriazopoulou-Panagiotopoulou, S., Libbrecht, M., Smith, C. L., Raha, D., Winters, E. E., Johnson, S. M., Snyder, M., Batzoglou, S. and Sidow, A. (2012) 'Ubiquitous heterogeneity and asymmetry of the chromatin environment at regulatory elements', *Genome Res,* 22(9), 1735-47.

Kwon, H., Imbalzano, A. N., Khavari, P. A., Kingston, R. E. and Green, M. R. (1994) 'Nucleosome disruption and enhancement of activator binding by a human SW1/SNF complex', *Nature,* 370(6489), 477-81.

Küspert, M., Hammer, A., Bösl, M. R. and Wegner, M. (2011) 'Olig2 regulates Sox10 expression in oligodendrocyte precursors through an evolutionary conserved distal enhancer', *Nucleic Acids Res,* 39(4), 1280-93.

Lappe-Siefke, C., Goebbels, S., Gravel, M., Nicksch, E., Lee, J., Braun, P. E., Griffiths, I. R. and Nave, K. A. (2003) 'Disruption of Cnp1 uncouples oligodendroglial functions in axonal support and myelination', *Nat Genet,* 33(3), 366-74.

Lara-Astiaso, D., Weiner, A., Lorenzo-Vivas, E., Zaretsky, I., Jaitin, D. A., David, E., Keren-Shaul, H., Mildner, A., Winter, D., Jung, S., Friedman, N. and Amit, I. (2014) 'Immunogenetics. Chromatin state dynamics during blood formation', *Science,* 345(6199), 943-9.

Larsen, F., Gundersen, G., Lopez, R. and Prydz, H. (1992) 'CpG islands as gene markers in the human genome', *Genomics,* 13(4), 1095-107.

Laurent, L., Wong, E., Li, G., Huynh, T., Tsirigos, A., Ong, C. T., Low, H. M., Kin Sung, K. W., Rigoutsos, I., Loring, J. and Wei, C. L. (2010) 'Dynamic changes in the human methylome during differentiation', *Genome Res,* 20(3), 320-31.

Le Sage, V., Cinti, A., Amorim, R. and Mouland, A. J. (2016) 'Adapting the Stress Response: Viral Subversion of the mTOR Signaling Pathway', *Viruses,* 8(6).

Lea, A. J., Vockley, C. M., Johnston, R. A., Del Carpio, C. A., Barreiro, L. B., Reddy, T. E. and Tung, J. (2018) 'Genome-wide quantification of the effects of DNA methylation on human gene regulation', *Elife,* 7.

Lee, W., Tillo, D., Bray, N., Morse, R. H., Davis, R. W., Hughes, T. R. and Nislow, C. (2007) 'A high-resolution atlas of nucleosome occupancy in yeast', *Nat Genet,* 39(10), 1235-44.

Lee, Y., Morrison, B. M., Li, Y., Lengacher, S., Farah, M. H., Hoffman, P. N., Liu, Y., Tsingalia, A., Jin, L., Zhang, P. W., Pellerin, L., Magistretti, P. J. and Rothstein, J. D. (2012) 'Oligodendroglia metabolically support axons and contribute to neurodegeneration', *Nature,* 487(7408), 443-8.

Lehnertz, B., Ueda, Y., Derijck, A. A., Braunschweig, U., Perez-Burgos, L., Kubicek, S., Chen, T., Li, E., Jenuwein, T. and Peters, A. H. (2003) 'Suv39h-mediated histone H3 lysine 9 methylation directs DNA methylation to major satellite repeats at pericentric heterochromatin', *Curr Biol,* 13(14), 1192-200.

Lessard, J., Wu, J. I., Ranish, J. A., Wan, M., Winslow, M. M., Staahl, B. T., Wu, H., Aebersold, R., Graef, I. A. and Crabtree, G. R. (2007) 'An essential switch in subunit composition of a chromatin remodeling complex during neural development', *Neuron,* 55(2), 201-15.

Levine, J. M., Stincone, F. and Lee, Y. S. (1993) 'Development and differentiation of glial precursor cells in the rat cerebellum', *Glia,* 7(4), 307-21.

Li, E., Bestor, T. H. and Jaenisch, R. (1992) 'Targeted mutation of the DNA methyltransferase gene results in embryonic lethality', *Cell,* 69(6), 915-26.

Li, H., Lu, Y., Smith, H. K. and Richardson, W. D. (2007) 'Olig1 and Sox10 interact synergistically to drive myelin basic protein transcription in oligodendrocytes', *J Neurosci,* 27(52), 14375-82.

Liang, G., Chan, M. F., Tomigahara, Y., Tsai, Y. C., Gonzales, F. A., Li, E., Laird, P. W. and Jones, P. A. (2002) 'Cooperativity between DNA methyltransferases in the maintenance methylation of repetitive elements', *Mol Cell Biol,* 22(2), 480-91.

Lin, J. P., Mironova, Y. A., Shrager, P. and Giger, R. J. (2017) 'LRP1 regulates peroxisome biogenesis and cholesterol homeostasis in oligodendrocytes and is required for proper CNS myelin development and repair', *Elife,* 6.

Lindroth, A. M., Park, Y. J., McLean, C. M., Dokshin, G. A., Persson, J. M., Herman, H., Pasini, D., Miró, X., Donohoe, M. E., Lee, J. T., Helin, K. and Soloway, P. D. (2008) 'Antagonism between DNA and H3K27 methylation at the imprinted Rasgrf1 locus', *PLoS Genet,* 4(8), e1000145.

Liu, A., Li, J., Marin-Husstege, M., Kageyama, R., Fan, Y., Gelinas, C. and Casaccia-Bonnefil, P. (2006) 'A molecular insight of Hes5-dependent inhibition of myelin gene expression: old partners and new players', *EMBO J,* 25(20), 4833-42.

Liu, J., Magri, L., Zhang, F., Marsh, N. O., Albrecht, S., Huynh, J. L., Kaur, J., Kuhlmann, T., Zhang, W., Slesinger, P. A. and Casaccia, P. (2015) 'Chromatin landscape defined by repressive histone methylation during oligodendrocyte differentiation', *J Neurosci,* 35(1), 352-65.

Liu, X. S., Wu, H., Ji, X., Stelzer, Y., Wu, X., Czauderna, S., Shu, J., Dadon, D., Young, R. A. and Jaenisch, R. (2016) 'Editing DNA Methylation in the Mammalian Genome', *Cell,* 167(1), 233-247.e17.

Lu, Q. R., Sun, T., Zhu, Z., Ma, N., Garcia, M., Stiles, C. D. and Rowitch, D. H. (2002) 'Common developmental requirement for Olig function indicates a motor neuron/oligodendrocyte connection', *Cell,* 109(1), 75-86.

Lu, Q. R., Yuk, D., Alberta, J. A., Zhu, Z., Pawlitzky, I., Chan, J., McMahon, A. P., Stiles, C. D. and Rowitch, D. H. (2000) 'Sonic hedgehog--regulated oligodendrocyte lineage genes encoding bHLH proteins in the mammalian central nervous system', *Neuron,* 25(2), 317-29.

Luger, K., Mader, A. W., Richmond, R. K., Sargent, D. F. and Richmond, T. J. (1997) 'Crystal structure of the nucleosome core particle at 2.8 A resolution', *Nature,* 389(6648), 251-60.

Luskin, M. B., Parnavelas, J. G. and Barfield, J. A. (1993) 'Neurons, astrocytes, and oligodendrocytes of the rat cerebral cortex originate from separate progenitor cells: an ultrastructural analysis of clonally related cells', *J Neurosci,* 13(4), 1730-50.

Lyons, D. B. and Zilberman, D. (2017) 'DDM1 and Lsh remodelers allow methylation of DNA wrapped in nucleosomes', *Elife,* 6.

Maeder, M. L., Angstman, J. F., Richardson, M. E., Linder, S. J., Cascio, V. M., Tsai, S. Q., Ho, Q. H., Sander, J. D., Reyon, D., Bernstein, B. E., Costello, J. F., Wilkinson, M. F. and Joung, J. K. (2013) 'Targeted DNA demethylation and activation of endogenous genes using programmable TALE-TET1 fusion proteins', *Nat Biotechnol,* 31(12), 1137-42.

Makinodan, M., Rosen, K. M., Ito, S. and Corfas, G. (2012) 'A critical period for social experience-dependent oligodendrocyte maturation and myelination', *Science,* 337(6100), 1357-60.

Mann, M. B. and Smith, H. O. (1977) 'Specificity of Hpa II and Hae III DNA methylases', *Nucleic Acids Res,* 4(12), 4211-21.

Margueron, R. and Reinberg, D. (2010) 'Chromatin structure and the inheritance of epigenetic information', *Nat Rev Genet,* 11(4), 285-96.

Marie, C., Clavairoly, A., Frah, M., Hmidan, H., Yan, J., Zhao, C., Van Steenwinckel, J., Daveau, R., Zalc, B., Hassan, B., Thomas, J. L., Gressens, P., Ravassard, P., Moszer, I., Martin, D. M., Lu, Q. R. and Parras, C. (2018) 'Oligodendrocyte precursor survival and differentiation requires chromatin remodeling by Chd7 and Chd8', *Proc Natl Acad Sci U S A,* 115(35), E8246-E8255.

Marques, S., Zeisel, A., Codeluppi, S., van Bruggen, D., Mendanha Falcão, A., Xiao, L., Li, H., Häring, M., Hochgerner, H., Romanov, R. A., Gyllborg, D., Muñoz Manchado, A., La Manno, G., Lönnerberg, P., Floriddia, E. M., Rezayee, F., Ernfors, P., Arenas, E., Hjerling-Leffler, J., Harkany, T., Richardson, W. D., Linnarsson, S. and Castelo-Branco, G. (2016) 'Oligodendrocyte heterogeneity in the mouse juvenile and adult central nervous system', *Science,* 352(6291), 1326-1329.

Martinez, S., Andreu, A., Mecklenburg, N. and Echevarria, D. (2013) 'Cellular and molecular basis of cerebellar development', *Front Neuroanat,* 7, 18.

Mavrich, T. N., Jiang, C., Ioshikhes, I. P., Li, X., Venters, B. J., Zanton, S. J., Tomsho, L. P., Qi, J., Glaser, R. L., Schuster, S. C., Gilmour, D. S., Albert, I. and Pugh, B. F. (2008) 'Nucleosome organization in the Drosophila genome', *Nature,* 453(7193), 358-62.

McClive, P., Pall, G., Newton, K., Lee, M., Mullins, J. and Forrester, L. (1998) 'Gene trap integrations expressed in the developing heart: insertion site affects splicing of the PT1-ATG vector', *Dev Dyn,* 212(2), 267-76.

McKnight, J. N., Tsukiyama, T. and Bowman, G. D. (2016) 'Sequence-targeted nucleosome sliding in vivo by a hybrid Chd1 chromatin remodeler', *Genome Res,* 26(5), 693-704.

Meehan, R. R., Pennings, S. and Stancheva, I. (2001) 'Lashings of DNA methylation, forkfuls of chromatin remodeling', *Genes Dev,* 15(24), 3231-6.

Mei, F., Wang, H., Liu, S., Niu, J., Wang, L., He, Y., Etxeberria, A., Chan, J. R. and Xiao, L. (2013) 'Stage-specific deletion of Olig2 conveys opposing functions on differentiation and maturation of oligodendrocytes', *J Neurosci,* 33(19), 8454-62.

Meissner, A., Mikkelsen, T. S., Gu, H., Wernig, M., Hanna, J., Sivachenko, A., Zhang, X., Bernstein, B. E., Nusbaum, C., Jaffe, D. B., Gnirke, A., Jaenisch, R. and Lander, E. S. (2008) 'Genome-scale DNA methylation maps of pluripotent and differentiated cells', *Nature,* 454(7205), 766-70.

Menn, B., Garcia-Verdugo, J. M., Yaschine, C., Gonzalez-Perez, O., Rowitch, D. and Alvarez-Buylla, A. (2006) 'Origin of oligodendrocytes in the subventricular zone of the adult brain', *J Neurosci,* 26(30), 7907-18.

Mensch, S., Baraban, M., Almeida, R., Czopka, T., Ausborn, J., El Manira, A. and Lyons, D. A. (2015) 'Synaptic vesicle release regulates myelin sheath number of individual oligodendrocytes in vivo', *Nat Neurosci,* 18(5), 628-30.

Mikkelsen, T. S., Ku, M., Jaffe, D. B., Issac, B., Lieberman, E., Giannoukos, G., Alvarez, P., Brockman, W., Kim, T. K., Koche, R. P., Lee, W., Mendenhall, E., O'Donovan, A., Presser, A., Russ, C., Xie, X., Meissner, A., Wernig, M., Jaenisch, R., Nusbaum, C., Lander, E. S. and Bernstein, B. E. (2007) 'Genome-wide maps of chromatin state in pluripotent and lineage-committed cells', *Nature,* 448(7153), 553-60.

Miller, R. H. (2002) 'Regulation of oligodendrocyte development in the vertebrate CNS', *Prog Neurobiol,* 67(6), 451-67.

Mittelsten Scheid, O., Afsar, K. and Paszkowski, J. (1998) 'Release of epigenetic gene silencing by trans-acting mutations in Arabidopsis', *Proc Natl Acad Sci U S A,* 95(2), 632-7.

Mount, C. W. and Monje, M. (2017) 'Wrapped to Adapt: Experience-Dependent Myelination', *Neuron,* 95(4), 743-756.

Moyon, S., Huynh, J. L., Dutta, D., Zhang, F., Ma, D., Yoo, S., Lawrence, R., Wegner, M., John, G. R., Emery, B., Lubetzki, C., Franklin, R. J. M., Fan, G., Zhu, J., Dupree, J. L. and Casaccia, P. (2016) 'Functional Characterization of DNA Methylation in the Oligodendrocyte Lineage', *Cell Rep,* 15(4), 748-760.

Muegge, K. (2005) 'Lsh, a guardian of heterochromatin at repeat elements', *Biochem Cell Biol,* 83(4), 548-54.

Mukouyama, Y. S., Deneen, B., Lukaszewicz, A., Novitch, B. G., Wichterle, H., Jessell, T. M. and Anderson, D. J. (2006) 'Olig2+ neuroepithelial motoneuron progenitors are not multipotent stem cells in vivo', *Proc Natl Acad Sci U S A,* 103(5), 1551-6.

Muller, H. J. (1930) 'Types of visible variations induced by X-rays in Drosophila', *Journal of Genetics,* 22(3), 299-334.

Musselman, C. A., Lalonde, M. E., Côté, J. and Kutateladze, T. G. (2012) 'Perceiving the epigenetic landscape through histone readers', *Nat Struct Mol Biol,* 19(12), 1218-27.

Myant, K. and Stancheva, I. (2008) 'LSH cooperates with DNA methyltransferases to repress transcription', *Mol Cell Biol,* 28(1), 215-26.

Myant, K., Termanis, A., Sundaram, A. Y., Boe, T., Li, C., Merusi, C., Burrage, J., de Las Heras, J. I. and Stancheva, I. (2011) 'LSH and G9a/GLP complex are required for developmentally programmed DNA methylation', *Genome Res,* 21(1), 83-94.

Nakatani, H., Martin, E., Hassani, H., Clavairoly, A., Maire, C. L., Viadieu, A., Kerninon, C., Delmasure, A., Frah, M., Weber, M., Nakafuku, M., Zalc, B., Thomas, J. L., Guillemot, F., Nait-Oumesmar, B. and Parras, C. (2013) 'Ascl1/Mash1 promotes brain oligodendrogenesis during myelination and remyelination', *J Neurosci,* 33(23), 9752-9768.

Neri, F., Rapelli, S., Krepelova, A., Incarnato, D., Parlato, C., Basile, G., Maldotti, M., Anselmi, F. and Oliviero, S. (2017) 'Intragenic DNA methylation prevents spurious transcription initiation', *Nature,* 543(7643), 72-77.

Nishiyama, A., Komitova, M., Suzuki, R. and Zhu, X. (2009) 'Polydendrocytes (NG2 cells): multifunctional cells with lineage plasticity', *Nat Rev Neurosci,* 10(1), 9-22.

Nishiyama, A., Watanabe, M., Yang, Z. and Bu, J. (2002) 'Identity, distribution, and development of polydendrocytes: NG2-expressing glial cells', *J Neurocytol,* 31(6-7), 437-55.

Noma, K., Allis, C. D. and Grewal, S. I. (2001) 'Transitions in distinct histone H3 methylation patterns at the heterochromatin domain boundaries', *Science,* 293(5532), 1150-5.

Okano, M., Bell, D. W., Haber, D. A. and Li, E. (1999) 'DNA methyltransferases Dnmt3a and Dnmt3b are essential for de novo methylation and mammalian development', *Cell,* 99(3), 247-57.

Orian, J. M., Mitchell, A. W., Marshman, W. E., Webb, G. C., Ayers, M. M., Grail, D., Ford, J. H., Kaye, A. H. and Gonzales, M. F. (1994) 'Insertional mutagenesis inducing hypomyelination in transgenic mice', *J Neurosci Res,* 39(5), 604-12.

Panning, B. and Jaenisch, R. (1996) 'DNA hypomethylation can activate Xist expression and silence X-linked genes', *Genes Dev,* 10(16), 1991-2002.

Pastor, W. A., Aravind, L. and Rao, A. (2013) 'TETonic shift: biological roles of TET proteins in DNA demethylation and transcription', *Nat Rev Mol Cell Biol,* 14(6), 341-56.

Pokholok, D. K., Harbison, C. T., Levine, S., Cole, M., Hannett, N. M., Lee, T. I., Bell, G. W., Walker, K., Rolfe, P. A., Herbolsheimer, E., Zeitlinger, J., Lewitter, F., Gifford, D. K. and Young, R. A. (2005) 'Genome-wide map of nucleosome acetylation and methylation in yeast', *Cell,* 122(4), 517-27.

Poliak, S. and Peles, E. (2003) 'The local differentiation of myelinated axons at nodes of Ranvier', *Nat Rev Neurosci,* 4(12), 968-80.

Pringle, N. P. and Richardson, W. D. (1993) 'A singularity of PDGF alpha-receptor expression in the dorsoventral axis of the neural tube may define the origin of the oligodendrocyte lineage', *Development,* 117(2), 525-33.

Qi, Y., Cai, J., Wu, Y., Wu, R., Lee, J., Fu, H., Rao, M., Sussel, L., Rubenstein, J. and Qiu, M. (2001) 'Control of oligodendrocyte differentiation by the Nkx2.2 homeodomain transcription factor', *Development,* 128(14), 2723-33.

Qian, X., Goderie, S. K., Shen, Q., Stern, J. H. and Temple, S. (1998) 'Intrinsic programs of patterned cell lineages in isolated vertebrate CNS ventricular zone cells', *Development,* 125(16), 3143-52.

Qian, X., Shen, Q., Goderie, S. K., He, W., Capela, A., Davis, A. A. and Temple, S. (2000) 'Timing of CNS cell generation: a programmed sequence of neuron and glial cell production from isolated murine cortical stem cells', *Neuron,* 28(1), 69-80.

Raabe, E. H., Abdurrahman, L., Behbehani, G. and Arceci, R. J. (2001) 'An SNF2 factor involved in mammalian development and cellular proliferation', *Dev Dyn,* 221(1), 92-105.

Ramesh, V., Bayam, E., Cernilogar, F. M., Bonapace, I. M., Schulze, M., Riemenschneider, M. J., Schotta, G. and Götz, M. (2016) 'Loss of Uhrf1 in neural stem cells leads to activation of retroviral elements and delayed neurodegeneration', *Genes Dev,* 30(19), 2199-2212.

Ramsahoye, B. H., Biniszkiewicz, D., Lyko, F., Clark, V., Bird, A. P. and Jaenisch, R. (2000) 'Non-CpG methylation is prevalent in embryonic stem cells and may be mediated by DNA methyltransferase 3a', *Proc Natl Acad Sci U S A,* 97(10), 5237-42.

Rasmussen, K. D., Jia, G., Johansen, J. V., Pedersen, M. T., Rapin, N., Bagger, F. O., Porse, B. T., Bernard, O. A., Christensen, J. and Helin, K. (2015) 'Loss of TET2 in hematopoietic cells leads to DNA hypermethylation of active enhancers and induction of leukemogenesis', *Genes Dev,* 29(9), 910-22.

Ravanelli, A. M. and Appel, B. (2015) 'Motor neurons and oligodendrocytes arise from distinct cell lineages by progenitor recruitment', *Genes Dev,* 29(23), 2504-15.

Rea, S., Eisenhaber, F., O'Carroll, D., Strahl, B. D., Sun, Z. W., Schmid, M., Opravil, S., Mechtler, K., Ponting, C. P., Allis, C. D. and Jenuwein, T. (2000) 'Regulation of chromatin structure by site-specific histone H3 methyltransferases', *Nature,* 406(6796), 593-9.

Reik, W. (2007) 'Stability and flexibility of epigenetic gene regulation in mammalian development', *Nature,* 447(7143), 425-32.

Richardson, W. D., Kessaris, N. and Pringle, N. (2006) 'Oligodendrocyte wars', *Nat Rev Neurosci,* 7(1), 11-8.

Richmond, T. J. and Davey, C. A. (2003) 'The structure of DNA in the nucleosome core', *Nature,* 423(6936), 145-50.

Ritchie, J. M. (1984) 'Physiological Basis of Conduction in Myelinated Nerve Fibers' in Morell, P., ed. *Myelin*, Boston, MA: Springer US, 117-145.

Rowitch, D. H. (2004) 'Glial specification in the vertebrate neural tube', *Nat Rev Neurosci,* 5(5), 409-19.

Salzer, J. L. (1997) 'Clustering sodium channels at the node of Ranvier: close encounters of the axon-glia kind', *Neuron,* 18(6), 843-6.

Samanta, J. and Kessler, J. A. (2004) 'Interactions between ID and OLIG proteins mediate the inhibitory effects of BMP4 on oligodendroglial differentiation', *Development,* 131(17), 4131-42.

Saxonov, S., Berg, P. and Brutlag, D. L. (2006) 'A genome-wide analysis of CpG dinucleotides in the human genome distinguishes two distinct classes of promoters', *Proc Natl Acad Sci U S A,* 103(5), 1412-7.

Schones, D. E., Cui, K., Cuddapah, S., Roh, T. Y., Barski, A., Wang, Z., Wei, G. and Zhao, K. (2008) 'Dynamic regulation of nucleosome positioning in the human genome', *Cell,* 132(5), 887-98.

Schubert, H. L., Wittmeyer, J., Kasten, M. M., Hinata, K., Rawling, D. C., Héroux, A., Cairns, B. R. and Hill, C. P. (2013) 'Structure of an actin-related subcomplex of the SWI/SNF chromatin remodeler', *Proc Natl Acad Sci U S A,* 110(9), 3345-50.

Scruggs, B. S., Gilchrist, D. A., Nechaev, S., Muse, G. W., Burkholder, A., Fargo, D. C. and Adelman, K. (2015) 'Bidirectional Transcription Arises from Two Distinct Hubs of Transcription Factor Binding and Active Chromatin', *Mol Cell,* 58(6), 1101-12.

Shen, S., Li, J. and Casaccia-Bonnefil, P. (2005) 'Histone modifications affect timing of oligodendrocyte progenitor differentiation in the developing rat brain', *J Cell Biol,* 169(4), 577-89.

Shen, S., Sandoval, J., Swiss, V. A., Li, J., Dupree, J., Franklin, R. J. and Casaccia-Bonnefil, P. (2008) 'Age-dependent epigenetic control of differentiation inhibitors is critical for remyelination efficiency', *Nat Neurosci,* 11(9), 1024-34.

Shen, X., Mizuguchi, G., Hamiche, A. and Wu, C. (2000) 'A chromatin remodelling complex involved in transcription and DNA processing', *Nature,* 406(6795), 541-4.

Shivaswamy, S., Bhinge, A., Zhao, Y., Jones, S., Hirst, M. and Iyer, V. R. (2008) 'Dynamic remodeling of individual nucleosomes across a eukaryotic genome in response to transcriptional perturbation', *PLoS Biol,* 6(3), e65.

Sim, F. J., McClain, C. R., Schanz, S. J., Protack, T. L., Windrem, M. S. and Goldman, S. A. (2011) 'CD140a identifies a population of highly myelinogenic, migration-competent and efficiently engrafting human oligodendrocyte progenitor cells', *Nat Biotechnol,* 29(10), 934-41.

Smith, C. D., Shu, S., Mungall, C. J. and Karpen, G. H. (2007) 'The Release 5.1 annotation of Drosophila melanogaster heterochromatin', *Science,* 316(5831), 1586-91.

Smith, Z. D., Chan, M. M., Mikkelsen, T. S., Gu, H., Gnirke, A., Regev, A. and Meissner, A. (2012) 'A unique regulatory phase of DNA methylation in the early mammalian embryo', *Nature,* 484(7394), 339-44.

Stedman, E. and Stedman, E. (1950) 'Cell Specificity of Histones', *Nature,* 166, 780.

Stepper, P., Kungulovski, G., Jurkowska, R. Z., Chandra, T., Krueger, F., Reinhardt, R., Reik, W., Jeltsch, A. and Jurkowski, T. P. (2017) 'Efficient targeted DNA methylation with chimeric dCas9-Dnmt3a-Dnmt3L methyltransferase', *Nucleic Acids Res,* 45(4), 1703-1713.

Stolt, C. C., Rehberg, S., Ader, M., Lommes, P., Riethmacher, D., Schachner, M., Bartsch, U. and Wegner, M. (2002) 'Terminal differentiation of myelin-forming oligodendrocytes depends on the transcription factor Sox10', *Genes Dev,* 16(2), 165-70.

Stunkel, W., Kober, I. and Seifart, K. H. (1997) 'A nucleosome positioned in the distal promoter region activates transcription of the human U6 gene', *Mol Cell Biol,* 17(8), 4397-405.

Sun, L. Q., Lee, D. W., Zhang, Q., Xiao, W., Raabe, E. H., Meeker, A., Miao, D., Huso, D. L. and Arceci, R. J. (2004) 'Growth retardation and premature aging phenotypes in mice with disruption of the SNF2-like gene, PASG', *Genes Dev,* 18(9), 1035-46.

Swiss, V. A., Nguyen, T., Dugas, J., Ibrahim, A., Barres, B., Androulakis, I. P. and Casaccia, P. (2011) 'Identification of a gene regulatory network necessary for the initiation of oligodendrocyte differentiation', *PLoS One,* 6(4), e18088.

Tasaki, I. (1982) *5. - Conduction of Impulses in Myelinated Nerve Fibers, Physiology and Electrochemistry of Nerve Fibers,* Academic Press.

Termanis, A., Torrea, N., Culley, J., Kerr, A., Ramsahoye, B. and Stancheva, I. (2016) 'The SNF2 family ATPase LSH promotes cell-autonomous de novo DNA methylation in somatic cells', *Nucleic Acids Res,* 44(16), 7592-604.

Thijssen, P. E., Ito, Y., Grillo, G., Wang, J., Velasco, G., Nitta, H., Unoki, M., Yoshihara, M., Suyama, M., Sun, Y., Lemmers, R. J., de Greef, J. C., Gennery, A., Picco, P., Kloeckener-Gruissem, B., Güngör, T., Reisli, I., Picard, C., Kebaili, K., Roquelaure, B., Iwai, T., Kondo, I., Kubota, T., van Ostaijen-Ten Dam, M. M., van Tol, M. J., Weemaes, C., Francastel, C., van der Maarel, S. M. and Sasaki, H. (2016) 'Corrigendum: Mutations in CDCA7 and HELLS cause immunodeficiency-centromeric instability-facial anomalies syndrome', *Nat Commun,* 7, 12003.

Tran, H. G., Steger, D. J., Iyer, V. R. and Johnson, A. D. (2000) 'The chromo domain protein chd1p from budding yeast is an ATP-dependent chromatin-modifying factor', *EMBO J,* 19(10), 2323-31.

Tsukiyama, T. and Wu, C. (1995) 'Purification and properties of an ATP-dependent nucleosome remodeling factor', *Cell,* 83(6), 1011-20.

Unterberger, A., Andrews, S. D., Weaver, I. C. and Szyf, M. (2006) 'DNA methyltransferase 1 knockdown activates a replication stress checkpoint', *Mol Cell Biol,* 26(20), 7575-86.

Vetter, M. (2001) 'A turn of the helix: preventing the glial fate', *Neuron,* 29(3), 559-62.

Vojta, A., Dobrinić, P., Tadić, V., Bočkor, L., Korać, P., Julg, B., Klasić, M. and Zoldoš, V. (2016) 'Repurposing the CRISPR-Cas9 system for targeted DNA methylation', *Nucleic Acids Res,* 44(12), 5615-28.

Vongs, A., Kakutani, T., Martienssen, R. A. and Richards, E. J. (1993) 'Arabidopsis thaliana DNA methylation mutants', *Science,* 260(5116), 1926-8.

Voss, A. K., Thomas, T. and Gruss, P. (1998) 'Compensation for a gene trap mutation in the murine microtubule-associated protein 4 locus by alternative polyadenylation and alternative splicing', *Dev Dyn,* 212(2), 258-66.

Wallrath, L. L. (1998) 'Unfolding the mysteries of heterochromatin', *Curr Opin Genet Dev,* 8(2), 147-53.

Walsh, C. P. and Bestor, T. H. (1999) 'Cytosine methylation and mammalian development', *Genes Dev,* 13(1), 26-34.

Walsh, C. P., Chaillet, J. R. and Bestor, T. H. (1998) 'Transcription of IAP endogenous retroviruses is constrained by cytosine methylation', *Nat Genet,* 20(2), 116-7.

Wan, M., Zhang, J., Lai, D., Jani, A., Prestone-Hurlburt, P., Zhao, L., Ramachandran, A., Schnitzler, G. R. and Chi, T. (2009) 'Molecular basis of CD4 repression by the Swi/Snf-like BAF chromatin remodeling complex', *Eur J Immunol,* 39(2), 580-8.

Wang, L., Ozark, P. A., Smith, E. R., Zhao, Z., Marshall, S. A., Rendleman, E. J., Piunti, A., Ryan, C., Whelan, A. L., Helmin, K. A., Morgan, M. A., Zou, L., Singer, B. D. and Shilatifard, A. (2018) 'TET2 coactivates gene expression through demethylation of enhancers', *Sci Adv,* 4(11), eaau6986.

Waterston, R. H., Lindblad-Toh, K., Birney, E., Rogers, J., Abril, J. F., Agarwal, P., Agarwala, R., Ainscough, R., Alexandersson, M., An, P., Antonarakis, S. E., Attwood, J., Baertsch, R., Bailey, J., Barlow, K., Beck, S., Berry, E., Birren, B., Bloom, T., Bork, P., Botcherby, M., Bray, N., Brent, M. R., Brown, D. G., Brown, S. D., Bult, C., Burton, J., Butler, J., Campbell, R. D., Carninci, P., Cawley, S., Chiaromonte, F., Chinwalla, A. T., Church, D. M., Clamp, M., Clee, C., Collins, F. S., Cook, L. L., Copley, R. R., Coulson, A., Couronne, O., Cuff, J., Curwen, V., Cutts, T., Daly, M., David, R., Davies, J., Delehaunty, K. D., Deri, J., Dermitzakis, E. T., Dewey, C., Dickens, N. J., Diekhans, M., Dodge, S., Dubchak, I., Dunn, D. M., Eddy, S. R., Elnitski, L., Emes, R. D., Eswara, P., Eyras, E., Felsenfeld, A., Fewell, G.

A., Flicek, P., Foley, K., Frankel, W. N., Fulton, L. A., Fulton, R. S., Furey, T. S., Gage, D., Gibbs, R. A., Glusman, G., Gnerre, S., Goldman, N., Goodstadt, L., Grafham, D., Graves, T. A., Green, E. D., Gregory, S., Guigó, R., Guyer, M., Hardison, R. C., Haussler, D., Hayashizaki, Y., Hillier, L. W., Hinrichs, A., Hlavina, W., Holzer, T., Hsu, F., Hua, A., Hubbard, T., Hunt, A., Jackson, I., Jaffe, D. B., Johnson, L. S., Jones, M., Jones, T. A., Joy, A., Kamal, M., Karlsson, E. K., et al. (2002) 'Initial sequencing and comparative analysis of the mouse genome', *Nature,* 420(6915), 520-62.

Weber, C. M., Ramachandran, S. and Henikoff, S. (2014) 'Nucleosomes are context-specific, H2A.Z-modulated barriers to RNA polymerase', *Mol Cell,* 53(5), 819-30.

Weiler, K. S. and Wakimoto, B. T. (1995) 'Heterochromatin and gene expression in Drosophila', *Annu Rev Genet,* 29, 577-605.

Weiner, A., Hughes, A., Yassour, M., Rando, O. J. and Friedman, N. (2010) 'High-resolution nucleosome mapping reveals transcription-dependent promoter packaging', *Genome Res,* 20(1), 90-100.

Wilkins, A., Chandran, S. and Compston, A. (2001) 'A role for oligodendrocyte-derived IGF-1 in trophic support of cortical neurons', *Glia,* 36(1), 48-57.

Wilkins, A., Majed, H., Layfield, R., Compston, A. and Chandran, S. (2003) 'Oligodendrocytes promote neuronal survival and axonal length by distinct intracellular mechanisms: a novel role for oligodendrocyte-derived glial cell line-derived neurotrophic factor', *J Neurosci,* 23(12), 4967-74.

Wu, J. I., Lessard, J., Olave, I. A., Qiu, Z., Ghosh, A., Graef, I. A. and Crabtree, G. R. (2007) 'Regulation of dendritic development by neuron-specific chromatin remodeling complexes', *Neuron,* 56(1), 94-108.

Wu, S., Wu, Y. and Capecchi, M. R. (2006) 'Motoneurons and oligodendrocytes are sequentially generated from neural stem cells but do not appear to share common lineage-restricted progenitors in vivo', *Development,* 133(4), 581-90.

Xin, B. and Rohs, R. (2018) 'Relationship between histone modifications and transcription factor binding is protein family specific', *Genome Res*.

Xin, M., Yue, T., Ma, Z., Wu, F. F., Gow, A. and Lu, Q. R. (2005) 'Myelinogenesis and axonal recognition by oligodendrocytes in brain are uncoupled in Olig1-null mice', *J Neurosci,* 25(6), 1354-65.

Xu, G. L., Bestor, T. H., Bourc'his, D., Hsieh, C. L., Tommerup, N., Bugge, M., Hulten, M., Qu, X., Russo, J. J. and Viegas-Péquignot, E. (1999) 'Chromosome instability and immunodeficiency syndrome caused by mutations in a DNA methyltransferase gene', *Nature,* 402(6758), 187-91.

Yang, X., Noushmehr, H., Han, H., Andreu-Vieyra, C., Liang, G. and Jones, P. A. (2012) 'Gene reactivation by 5-aza-2'-deoxycytidine-induced demethylation requires SRCAP-mediated H2A.Z insertion to establish nucleosome depleted regions', *PLoS Genet,* 8(3), e1002604.

Ye, F., Chen, Y., Hoang, T., Montgomery, R. L., Zhao, X. H., Bu, H., Hu, T., Taketo, M. M., van Es, J. H., Clevers, H., Hsieh, J., Bassel-Duby, R., Olson, E. N. and Lu, Q. R. (2009) 'HDAC1 and HDAC2 regulate oligodendrocyte differentiation by disrupting the beta-catenin-TCF interaction', *Nat Neurosci,* 12(7), 829-38.

Yoder, J. A., Walsh, C. P. and Bestor, T. H. (1997) 'Cytosine methylation and the ecology of intragenomic parasites', *Trends Genet,* 13(8), 335-40.

Young, K. M., Psachoulia, K., Tripathi, R. B., Dunn, S. J., Cossell, L., Attwell, D., Tohyama, K. and Richardson, W. D. (2013) 'Oligodendrocyte dynamics in the healthy adult CNS: evidence for myelin remodeling', *Neuron,* 77(5), 873-85.

Yu, W., McIntosh, C., Lister, R., Zhu, I., Han, Y., Ren, J., Landsman, D., Lee, E., Briones, V., Terashima, M., Leighty, R., Ecker, J. R. and Muegge, K. (2014) 'Genome-wide DNA methylation patterns in LSH mutant reveals de-repression of repeat elements and redundant epigenetic silencing pathways', *Genome Res,* 24(10), 1613-23.

Yu, Y., Chen, Y., Kim, B., Wang, H., Zhao, C., He, X., Liu, L., Liu, W., Wu, L. M., Mao, M., Chan, J. R., Wu, J. and Lu, Q. R. (2013) 'Olig2 targets chromatin remodelers to enhancers to initiate oligodendrocyte differentiation', *Cell,* 152(1-2), 248-61.

Zhang, Y., Chen, K., Sloan, S. A., Bennett, M. L., Scholze, A. R., O'Keeffe, S., Phatnani, H. P., Guarnieri, P., Caneda, C., Ruderisch, N., Deng, S., Liddelow, S. A., Zhang, C., Daneman, R., Maniatis, T., Barres, B. A. and Wu, J. Q. (2014) 'An RNA-sequencing

transcriptome and splicing database of glia, neurons, and vascular cells of the cerebral cortex', *J Neurosci,* 34(36), 11929-47.

Zhao, X., Pendergrast, P. S. and Hernandez, N. (2001) 'A positioned nucleosome on the human U6 promoter allows recruitment of SNAPc by the Oct-1 POU domain', *Mol Cell,* 7(3), 539-49.

Zhou, Q. and Anderson, D. J. (2002) 'The bHLH transcription factors OLIG2 and OLIG1 couple neuronal and glial subtype specification', *Cell,* 109(1), 61-73.

Zhou, Q., Choi, G. and Anderson, D. J. (2001) 'The bHLH transcription factor Olig2 promotes oligodendrocyte differentiation in collaboration with Nkx2.2', *Neuron,* 31(5), 791-807.

Zhou, Q., Wang, S. and Anderson, D. J. (2000) 'Identification of a novel family of oligodendrocyte lineage-specific basic helix-loop-helix transcription factors', *Neuron,* 25(2), 331-43.

Zhu, X., Bergles, D. E. and Nishiyama, A. (2008) 'NG2 cells generate both oligodendrocytes and gray matter astrocytes', *Development,* 135(1), 145-57.